

# Florida State University Libraries

---

Electronic Theses, Treatises and Dissertations

The Graduate School

---

2009

## Evaluation of Polar-Embedded Reversed-Phase Liquid Chromatography Columns and the Temperature Dependence of the Phase Ratio

Van Quach



FLORIDA STATE UNIVERSITY  
COLLEGE OF ARTS AND SCIENCES

EVALUATION OF POLAR-EMBEDDED REVERSED-PHASE LIQUID  
CHROMATOGRAPHY COLUMNS AND THE TEMPERATURE DEPENDENCE OF THE  
PHASE RATIO

By

VAN QUACH

A Dissertation submitted to the  
Department of Chemistry and Biochemistry  
in partial fulfillment of the  
requirements for the degree of  
Doctor of Philosophy

Degree Awarded:  
Fall Semester, 2009

The members of the committee approve the dissertation of Van Quach defended on August 6, 2009.

---

John G. Dorsey  
Professor Directing Dissertation

---

Michael Blaber  
Outside Committee Member

---

William T. Cooper  
Committee Member

---

Michael G. Roper  
Committee Member

---

Sanford A. Safron  
Committee Member

Approved:

---

Joseph B. Schlenoff, Chair, Department of Chemistry and Biochemistry

The Graduate School has verified and approved the above-named committee members.

## TABLE OF CONTENTS

List of Tables	v
List of Figures	vi
Abstract	ix
1. Reversed-phase liquid chromatography	1
1.1 Introduction	1
1.2 Stationary phase	2
1.2.1 Bonding reaction	3
1.2.2 Silica based stationary phases	5
1.2.3 Other types of stationary phases	7
1.3 Peak asymmetry	8
1.3.1 Descriptors for column efficiency	8
1.3.2 Silanols	12
1.3.3 Methods to reduce silanol activity	15
1.4 Research goals	17
2. Methods of stationary phase characterization	20
2.1 Introduction	20
2.2 Spectroscopy	21
2.3 Non-linear chromatography	24
2.4 Modeling	28
2.5 Chromatographic	34
3. van't Hoff analysis	38
3.1 Introduction	38
3.2 Phase ratio	41
3.2.1 Mobile phase volume	42
3.2.2 Stationary phase volume	44

3.3	Research goals	46
4.	Polar-embedded columns	50
4.1	Introduction	50
4.2	Instrumentation	51
4.3	Columns	51
4.4	Experimental	52
4.5	Results and discussion	54
4.5.1	Selectivity studies	54
4.5.2	van't Hoff studies	61
4.5.3	Methylene selectivity	69
5.	The phase ratio	74
5.1	Introduction	74
5.2	Instrumentation	75
5.3	Columns	75
5.4	Experimental	75
5.5	Results and discussion	76
6.	Summary and conclusions	83
	References	89
	Biographical sketch	99

## LIST OF TABLES

Table 4-1.	Columns and their physical properties.	50
Table 4-2.	Selectivity data for adjacent peaks in mixture 2.	57
Table 4-3.	Molar enthalpies of transfer and $\Delta S^\circ / R + \ln \phi$ values from van't Hoff plots. Mobile phase: 50/50 ACN/10 mM phosphate buffer, pH 3.0.	66
Table 4-4.	Thermodynamic values for methylene selectivity.	70

## LIST OF FIGURES

Figure 1-1.	Typical synthesis reaction for bonded phases.	3
Figure 1-2.	Monomeric versus polymeric stationary phase.	4
Figure 1-3.	Asymmetric peak used for calculating plate count.	9
Figure 1-4.	Three types of silanols on the silica surface.	12
Figure 1-5.	Stationary phase of conventional alkyl ligand compared to polar-embedded group.	17
Figure 2-1.	Break through curve using frontal analysis.	25
Figure 2-2.	Concentration profile using frontal analysis and frontal analysis by characteristic point. $C_a$ and $C_b$ are the initial and final solute concentrations, $V_D$ is the system dead volume, $V_F$ is the retention volume of the front.	27
Figure 3-1.	The hypothetical change in the phase ratio as a function of temperature when $\Delta H^\circ$ and $\Delta S^\circ$ are constant.	46
Figure 4-1.	Analytes used for selectivity and retention studies.	52
Figure 4-2.	Chromatograms for test mixture 1, pH 3.0. A. Synergi Fusion RP; B. Synergi Max; C. Polaris C8-Ether; D. Polaris C8-A; E. Symmetry Shield; F. Zorbax Bonus RP; G. Discovery Amide; H. Dionex Acclaim. Test mixture 1: 1. thiourea, 2. amitriptyline, 3. benzonitrile, 4. 4- <i>n</i> -butylbenzoic acid, 5. <i>trans</i> -chalcone.	54
Figure 4-3.	Chromatograms for test mixture 1, pH 7.0. A. Synergi Fusion RP; B. Synergi Max; C. Polaris C8-Ether; D. Polaris C8-A; E. Symmetry Shield; F. Zorbax Bonus RP; G. Discovery Amide; H. Dionex Acclaim. Test mixture 1: 1. thiourea, 2. amitriptyline, 3. benzonitrile, 4. 4- <i>n</i> -butylbenzoic acid, 5. <i>trans</i> -chalcone.	56

Figure 4-4.	Log-log plots for selectivity values at pH 3.0. Reference analyte was ethylbenzene.	58
Figure 4-5.	Log-log plots for selectivity values at pH 7.0. Reference analyte was ethylbenzene.	59
Figure 4-6.	van't Hoff plots for 4- <i>n</i> -propylbenzoic acid and 4- <i>n</i> -butylbenzoic acid. Mobile phase: 50/50 CAN/10 mM phosphate buffer, pH 3.0.	61
Figure 4-7.	van't Hoff plots for benzonitrile and phenylacetoneitrile. Mobile phase: 50/50 CAN/10 mM phosphate buffer, pH 3.0.	62
Figure 4-8.	van't Hoff plots for toluene and ethylbenzene. Mobile phase: 50/50 ACN/10 mM phosphate buffer, pH 3.0.	63
Figure 4-9.	van't Hoff plots for 4-pentylaniline and 4-hexylaniline. Mobile phase: 50/50 CAN/10 mM phosphate buffer, pH 3.0.	64
Figure 4-10.	van't Hoff plot of the anilines for temperatures of 5°C-85°C. Mobile phase: 50/50 ACN/10 mM phosphate buffer, pH 3.0.	65
Figure 4-11.	Methylene selectivity plots for 4- <i>n</i> -propyl benzoic acid and 4- <i>n</i> -butylbenzoic acid.	66
Figure 4-12.	Methylene selectivity plots for benzonitrile and phenylacetoneitrile.	69
Figure 4-13.	Methylene selectivity plots for 4-pentylaniline and 4-hexylaniline.	69
Figure 4-14.	Methylene selectivity plots for toluene and ethylbenzene.	71
Figure 5-1.	van't Hoff plots for benzene using the Synergi Hydro-RP (C <sub>18</sub> ) and Zorbax TMS (C <sub>1</sub> ) columns, mobile phase 30/70 ACN/H <sub>2</sub> O (v/v).	75
Figure 5-2.	van't Hoff plots using the Synergi Hydro-RP (C <sub>18</sub> ) and Spherisorb (C <sub>1</sub> ) columns, mobile phase 30/70 ACN/H <sub>2</sub> O (v/v) with 3% 1-PrOH.	77



- Figure 5-3. van't Hoff plots for benzene and toluene using the Synergi Hydro-RP (C<sub>18</sub>) column, mobile phase 5/95 1-PrOH/H<sub>2</sub>O (v/v). 79
- Figure 5-4. van't Hoff plots for benzene, toluene, and 4-hexylaniline using the Spherisorb (C<sub>1</sub>) column, mobile phase 5/95 1-PrOH/H<sub>2</sub>O (v/v). 79

## ABSTRACT

The most commonly used analytical separation technique, reversed-phase liquid chromatography (RPLC), can suffer from irreproducible retention times and asymmetric peaks when analyzing basic compounds. This has been of considerable concern especially in the pharmaceutical industry where many drug analytes contain basic amine groups. Though the fundamental basis for peak asymmetry is debatable, the conventional thought is that it arises from residual silanols on the stationary phase surface that interact with the analyte through hydrogen bonding and electrostatic interactions. Column manufacturers have invested heavily into column technologies to eliminate this insidious effect. The introduction of polar-embedded columns has offered one possible solution to improving the chromatography. However, due to their novelty, little is known about these types of columns.

This study investigated the character of seven polar-embedded columns along with one conventional column as a comparison. Using a variety of test analytes including acids, bases and neutral analytes, selectivity studies demonstrated that these columns offer unique chromatographic properties. The polar-embedded columns showed improved peak shape for basic compounds, especially at low pH. However, one column exhibited decreased efficiency for 4-*n*-butylbenzoic acid which was attributed to the manufacturing process. Different manufacturing processes were also responsible for the differences seen in columns with identical polar-embedded groups. In addition, log-log selectivity plots revealed similarities between columns with different bonded phases. Interestingly, the two column pairs that demonstrated the most similarity based on log-log plots were from the same manufacturer.

van't Hoff analysis was used to calculate the transfer enthalpies for four classes of compounds. Enthalpy values for the columns were compared to values reported for conventional alkyl columns and were in agreement. The selection of homologous analyte pairs also allowed for the calculation of  $\Delta\Delta H^\circ$  and  $\Delta\Delta S^\circ$  of methylene transfer. The thermodynamic values for methylene selectivity were found to depend significantly on the class of analytes used.

The last portion of this research investigated the role of the phase ratio in van't Hoff plots. Typically, plots of  $\ln k'$  vs  $1/T$  result in a linear relationship. However, the existence of non-linear van't Hoff plots raises the possibility that a change in the phase ratio with respect to

temperature may be the reason. Historically, non-linear van't Hoff plots were attributed to a change in the thermodynamics of retention, i.e., a change in the retention mechanism. Assessments of experimental van't Hoff plots using a C<sub>18</sub> and C<sub>1</sub> phase confirmed the conventional interpretation and showed that the phase ratio is temperature independent. Specifically, non-linear van't Hoff plots using a C<sub>1</sub> phase were observed. Since C<sub>1</sub> phases cannot experience changes in the stationary phase volume, the resulting non-linear plot was attributed to a change in the thermodynamics of retention. Further corroboration of this conclusion was established when non-linear methylene selectivity plots were obtained.

## CHAPTER ONE

### REVERSED-PHASE LIQUID CHROMATOGRAPHY

#### 1.1. Introduction

The practice of chromatography dates back to the early 1900's, when Russian botanist Mikhail Tswett separated plant pigments on a column containing calcium carbonate. However, it was not for another four decades until the theory of chromatography was developed. In their 1941 landmark paper, Martin and Synge published the first theoretical basis for the separation process [1]. Since then, numerous advances have led to the development of various separation techniques including liquid chromatography, gas chromatography, ion exchange, size exclusion, and supercritical fluid chromatography, just to name a few.

Liquid chromatography (LC) is the most widely used chromatographic technique. In LC, the mobile phase is a liquid that is passed through a stationary phase. The separation of analytes is based on differing affinities for the stationary phase. Unlike gas chromatography, in which the mobile phase only serves to transport the analytes through the column, the mobile phase composition can drastically change the separation in LC. Of the various LC modes, such as normal phase (NPLC), size exclusion (SEC), and ion-exchange (IE), reversed-phase (RPLC) is the most widely used mode comprising an estimated 75% of the liquid chromatographic separation [2]. Strictly speaking, reversed-phase LC is differentiated from normal phase in that the mobile phase is more polar than the stationary phase. In the 1970's, advances in the instrumentation, which allowed for operating at higher pressures, as well as the availability of higher quality silica, led to increased efficiency of separations via LC. These advances in technique and technology have led to modern LC, what is term High Performance Liquid Chromatography (HPLC).

High Performance Liquid Chromatography is the most widely used analytical technique for the separation of samples in solution, and comprises a multi-billion dollar industry. HPLC has been an indispensable tool for the routine separation and analysis of complex mixtures in pharmaceutical, food, and biotechnology industries. In addition to providing relatively fast

analysis, this technique's sample compatibility, versatility, and the ability for automation have made it the analytical technique of choice for the separation of complex mixtures. From analysis of environmental samples to drug research and development, HPLC instruments have found their way onto countless laboratory benches.

The popularity of RPLC can be attributed to the availability of high quality columns. The most common stationary phases are silica-based, though organometallic supports such as zirconia, alumina, and titania, are also commercially available. In addition, the variety of bonded ligands seems limitless. World-wide, over 600 different brands of stationary phases are available, each having unique chromatographic properties [2]. Over the last 40 years, the derivatization process in which the silica surface is chemically modified has been improved. Though the specifics of the synthesis reaction vary among manufacturers, the general reaction involves chemically grafting a suitable ligand to silanols and siloxanes on the silica surface.

## **1.2. Stationary phases**

In RPLC, the stationary phase plays an important role in the separation process. When HPLC was first developed, the stationary phase consisted of inert supports coated with a viscous liquid [3]. This proved to be inefficient and limiting, as it was difficult to maintain the liquid coating in the presence of a flowing mobile phase. The development of bonded stationary phases eliminated this issue, and is arguably the advancement that has led to modern LC. In bonded phase chromatography, the stationary phase ligand is covalently bonded to the solid support via silyl ether bonds (-Si-O-Si-). Bonded phases with various functionalities are commercially available leading to the versatility of this platform. However, the method of chemical bonding and the surface chemistry of the solid support can also affect the separation process. Realizing this importance, many manufacturers develop their own silica [3].

Ideally, the stationary phase should possess various characteristics. First, the support material should have an energetically homogenous surface as well as be susceptible to chemical modifications. It should also be chemically and thermally stable, having long-term stability at pH extremes. In addition, it should have high mechanical stability to withstand the high operating pressure common in HPLC. To be commercially viable, the manufacturing process

should be extremely reproducible, with the supports having narrow size distribution and desirable porosities, surface area, and pore diameters. Most importantly, the stationary phases must provide the needed retentivity, sample capacity, and selectivity required for the separation [4].

### 1.2.1 Bonding reaction

Though the specifics of the synthesis reaction vary among the manufacturers, the general reaction involves chemically bonding a suitable ligand to silanols (Si-OH) or siloxanes (Si-O-Si) on the silica support. It is generally accepted that the siloxanes have low activity, therefore are not consequential in the bonding process. The silanols therefore serve as the primary attachment point for the bonded phase. Figure 1-1 shows a schematic of a typical bonding process [5]. Coverage of the ligand on the silica surface is limited to the reactive silanols, which have a surface concentration of approximately  $8 \mu\text{mol}/\text{m}^2$ . However, incomplete reaction and steric hindrance results in bonding of no more than half of the available sites [6].

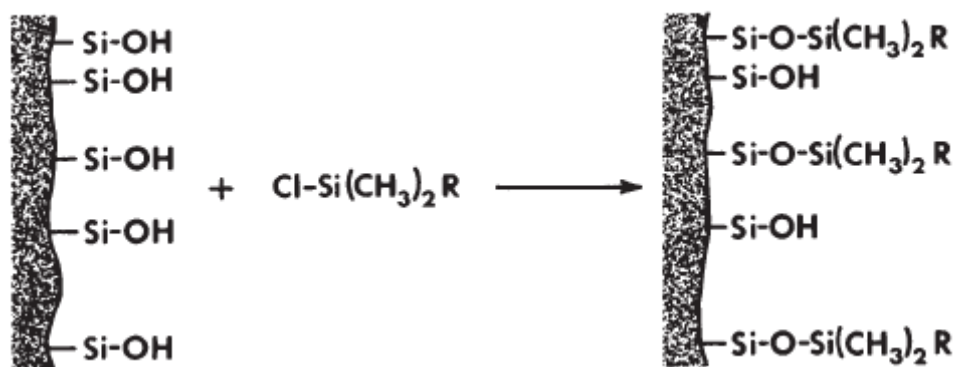


Figure 1-1. Typical synthesis reaction for bonded phases [5].

The process by which the bonded phase is attached to the support may potentially affect the characteristic of the resulting stationary phase. The most widely used preparation involves the reaction of the silanol group with a monofunctional organosilane reagent. This organosilane reagent typically contains a chloro or alkoxy functional group that serves as the leaving group. Reactions using monofunctional organosilanes are called monomeric stationary phase because of the resulting single-bond attachment between the organosilane ligand and the silica [7]. If a di- or trifunctional organosilane reagent is used, a more complex bonded phase results. The silane may bond in a single layer similar to the monomeric stationary phase. More often though, the extra functional sites of the organosilane hydrolyze, providing additional reactive sites to which more ligands may attach. This results in a polymeric network that can extend out from the silica surface. Depending on the sequence of reaction, the polymeric network can be formed prior to the reaction with the silica or it can occur at the silica surface. The former method is termed solution polymerized and the latter is termed surface polymerized; both forming what is known as polymeric stationary phases [7, 8].

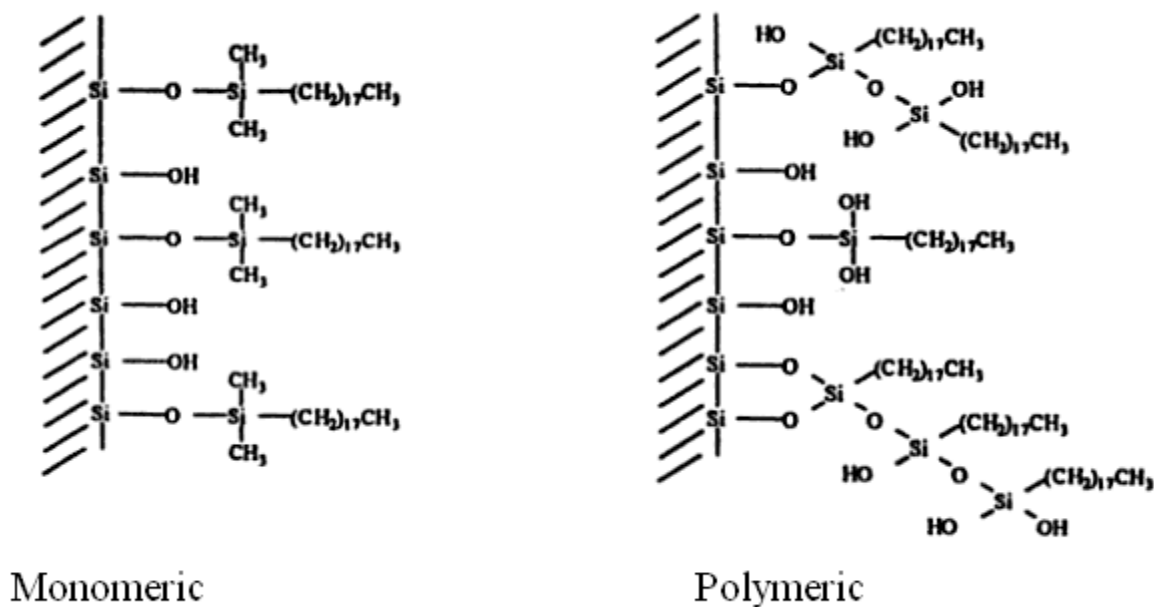


Figure 1-2. Monomeric versus polymeric stationary phase [9].

Since the monomeric stationary phase reaction can be better controlled, they provide a well defined single layer coverage on the silica support. This results in more reproducible stationary phases as well as superior performance due to faster mass transfer kinetics [10, 11]. However, this single layer coverage results in a maximum surface coverage of 4-4.5  $\mu\text{mol}/\text{m}^2$ , leaving approximately half of the silanols unreacted. Alternatively, the polymeric stationary phase has shown bonding densities of up to 6  $\mu\text{mol}/\text{m}^2$  [7]. This higher surface coverage prevents solute interaction with the silica surface which can be problematic. Additionally, it protects the silica from hydrolyzing under extreme pH conditions. Studies have shown them to be more stable at low pH and high pH as compared to monomeric stationary phases. However, because the polymerization process is difficult to control, batch-to-batch reproducibility for polymeric stationary phases proved to be more difficult to produce consistently. In addition, they suffer from peak asymmetry, and irreproducible retention and selectivity [8].

### **1.2.2 Silica based stationary phases**

A majority of the commercially available columns are silica-based. Silica has several advantages which have led to its broad acceptance over other solid support. First, its chemistry is well known and fabrication conditions can be carefully controlled to give a desired product. Silica gels are available with low metal content, narrow pore size distribution, and high porosity and surface area. Silica also has the needed tolerance for the mechanical stress resulting from the pressures seen under HPLC conditions. In addition, these porous particles have very large surface areas, increasing retention and loadability [12].

Of the silica-based stationary phases available, the conventional ligand consists of straight chain alkyl groups. Traditionally, most LC analyses are carried out on  $\text{C}_{18}$  phases, referred to as octadecylsiloxane (ODS), though alkyl chains varying from  $\text{C}_1$  to  $\text{C}_{30}$  are not uncommon. More recently, stationary phases containing a polar group embedded within the alkyl chain have become popular. Common polar-embedded groups include amides, carbamates, or ethers; however, sometimes the functionality is not disclosed by the manufacturer. Typically this polar group is found near the silica surface, attached via a propyl alkyl linker. The remainder of the



chain, which provides for the lipophilic nature of the stationary phase, is the conventional alkyl group, usually C<sub>8</sub> to C<sub>18</sub>. These will be discussed in more detail later.

In addition to the primary bonding reaction of the primary ligand, a secondary reaction involving short chain alkylsilanes such as trimethylchlorosilane is sometimes utilized to react the silanols remaining after the initial reaction. This process, known as end-capping, has shown improved peak shape for certain analytes, as well as improved stability [13, 14, 15]. Similarly, to improve the stability of the silica support, sterically bulky bonded phases may be used. These stationary phases involve monofunctional alkylsilane with bulky side groups that protect the support silica from hydrolyzing.

Bidentate stationary phases also achieve excellent stability, especially at higher pH. These are similar to monomeric stationary phases but have the added feature of a linker group joining adjacent ligands, usually a propylene linker group [14, 16]. With polymer-coated stationary phases, the silica support is first encapsulated with a thin layer of organic silicon layer, ideally to improve the chemical stability of the underlying silica. Subsequent to this, conventional bonded phases are introduced in a separate reaction. Kobayashi *et al.* found that these columns contain a high carbon content, improved peak shape for bases, and improved stability with alkaline mobile phases [17].

Specialized stationary phases have gain popularity recently and are typically used for a specific application. Chiral stationary phases have become particularly useful in pharmaceutical development where enantiomeric separations are important. Typical chiral phases include polysaccharide, proteins, crown ethers, and cyclodextrins [18]. Stationary phases containing phenyl moieties tend to show greater shape selectivity and aromatic selectivity especially towards polycyclic aromatic hydrocarbons (PAHs) [19, 20]. Compared to traditional alkyl ligands, cyano bonded supports are much less hydrophobic, requiring a weaker mobile phase [21], though their stability was problematic [22]. Fluorinated stationary phases have been gaining popularity especially when halogenated analytes are involved, demonstrating longer retention times compared to C<sub>18</sub> columns, and unique selectivity [23]. In addition, these phases have shown promise in other modes of separations such as supercritical fluid chromatography (SFC), micellar electrokinetic liquid chromatography (MEKC), and ion chromatography [24].

### 1.2.3 Other types of stationary phases

In addition to silica based stationary phases, metal oxides such as aluminum oxide, titania and zirconia are also commercially available, though their use is not as extensive. The main advantage of these supports is the improved pH stability. The higher chemical stability of these stationary phases also allows for their uses at higher operating temperatures. Silica-based stationary phases typically have a maximum temperature limit of  $\sim 60^{\circ}\text{C}$ – $80^{\circ}\text{C}$ . However, these metal oxides have shown long-term stability at operating temperatures of  $\sim 200^{\circ}\text{C}$ , which means a lower pressure drop or faster flow rates. This in turn improves on analysis times as well as increases mass transfer kinetics [25].

The different chemistry of these metal oxides, which provides for its improved stability, is also a disadvantage. The metal oxides, having more complex surface chemistry, cannot be modified using the classical silica-based silane chemistry. Though the silica-based supports and the metal oxides all share the common feature of having surface hydroxyl groups, the amount and properties of these hydroxyls vary depending on the type of metal oxide. Further, these metal oxides can act as both ion- and ligand exchangers, thus demonstrating more complex retention behavior [26, 27]. Supports of mixed metal oxides that attempt to combine the stability of metal oxides with the favorable properties of silica (high surface area, good pore size) have also been reported. In their study, J. Ge and coworkers, using an octadecyl bonded on titania coated silica stationary phase, found improved methylene and shape selectivity, as well as improved peak shape [28].

Polymer-based stationary phases also offer better pH stability as compared to silica-based, however, the overall performance is still typically lower. Polystyrene-divinylbenzene (PS-DVB) resins are probably the most common, and are chromatographically most similar to ODS silica-based stationary phase [29]. However, depending on the mobile phase composition, these stationary phases are susceptible to volume changes and thus demonstrate variable efficiencies. Surface derivatized PS-DVBs are also available, uniquely combining the chromatographic behavior of polymer-based stationary phases with alkyl-derivatized stationary phases [9].

Certainly, this is not a complete list but rather a brief overview of the types of stationary phases available. Regardless of the nature of the bonded ligand, the advent of these new stationary phases is driven by the need for improved separations. As analyses become more

complex, newer technologies are developed to achieve the desired separation. An overview of various stationary phases is offered by Buchmeiser [30] and Kirkland [8], while Claessens and van Straten consider their chemical and thermal stability [31].

### 1.3 Peak asymmetry

Peak asymmetry has been a nuisance in the analysis of basic compounds, especially pharmaceuticals which often contain a basic nitrogen moiety. In addition to irreproducible retention times, poor peak shapes lead to difficulties with quantifying sample size and reduced efficiencies [32, 33]. In fact, many of the newer stationary phases were developed in order to combat the poor performance of traditional C<sub>18</sub> phases with basic compounds. Chromatographic efficiencies for a given separation can be characterized by various column parameters.

#### 1.3.1. Descriptors for column efficiency

In LC, the efficiency of a packed chromatographic column is usually measured in the number of theoretical plates,  $N$  :

$$N = \frac{t_R^2}{\sigma^2} \quad \text{Equation 1-1}$$

In equation 1-1,  $t_R$  represents the retention time for a solute and  $\sigma^2$  is the variance, both in time units. The variance is an indication of the peak width; therefore it is a measure of how much an analyte band spreads as it travels through the column. Assuming that the peak is Gaussian, equation 1-1 can be re-written as either of the following equations:

$$N = 5.54 \left( \frac{t_R}{W_{0.5}} \right)^2 \quad \text{Equation 1-2}$$

$$N = 16 \left( \frac{t_R}{w_b} \right)^2 \quad \text{Equation 1-3}$$

In equations 1-2 and 1-3,  $w_{0.5}$  and  $w_b$  represent the peak width at half height and at the base, respectively [34]. However, peaks typically are not symmetric as Gaussian distribution dictates. Therefore, Foley and Dorsey derived an empirical formula for calculating the number of plates based on an exponentially modified Gaussian model [35]. As seen in Figure 1-3, the peak can be asymmetric, and the asymmetry factor is described by the B/A ratio.

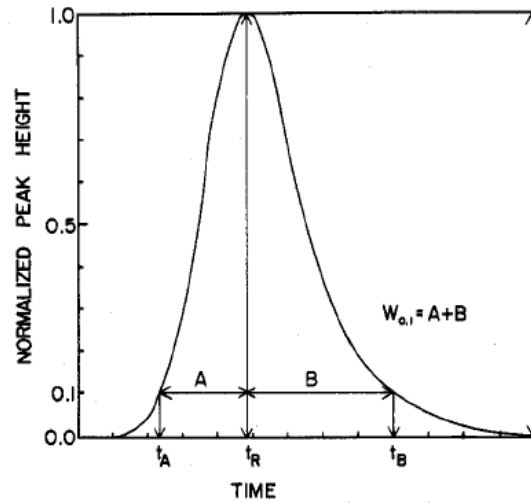


Figure 1-3. Asymmetric peak used for calculating plate count [35].

Using this model, the plate count is given as

$$N = \frac{41.7 \left( \frac{t_R}{w_{0.1}} \right)^2}{1.25 + B/A} \quad \text{Equation 1-4}$$

In this equation,  $w_{0.1}$  represents the peak width at ten percent of its height, and B and A are also measured at ten percent of the peak's height. The ratio  $B/A$  must be greater than unity for the

equation to be accurate, indicating peak tailing. For peaks that are skewed towards the front (fronting), the ratio must be inverted when applying this equation to calculate the number of plates. Berthod has shown that equation 1-4 is superior in accurately calculating the number of plates [36].

As the number of plates for a given column increases, the column efficiency also increases. However, plate count alone cannot adequately signify column performance because columns are available in varying length. To account for this variable, perhaps a better measure of column efficiency is plate height. Plate height,  $H$ , is give as

$$H = \frac{L}{N} \quad \text{Equation 1-5}$$

Here,  $L$  is the column length, and  $N$  is the number of plates for that column. The physical interpretation of this value signifies the thickness of each “plate”. In order to account for columns of varying stationary phase particle diameters, a reduced plate height,  $h$ , can be reported and is a normalized indicator of column efficiency:

$$h = \frac{H}{d_{sp}} \quad \text{Equation 1-6}$$

In equation 1-6,  $d_{sp}$  is the diameter of the stationary phase particle. Both plate height and  $d_{sp}$  are in the same units, therefore  $h$  is unitless, and smaller values are preferable. Typically, efficient RPLC columns will have plate counts of 10,000-20,000, and reduced plate heights in the range of 2-5.

Ultimately, the goal of any chromatographic process is to resolve the analytes in a sample into individual components. Moreover, an efficient column will have the ability to separate a large number of analytes. The maximum number of analytes that can be resolved with a resolution of 1.0 in a given chromatogram is termed peak capacity,  $PC$ , and is given by equation 1-7.

$$PC = 1 + \frac{\sqrt{N}}{4} \ln(1 + k') \quad \text{Equation 1-7}$$

In this equation,  $k'$  is the retention factor and is defined by equation 1-8.

$$k' = \frac{t_R - t_0}{t_0} \quad \text{Equation 1-8}$$

The time required for an unretained solute to travel through the column is designated as  $t_0$ . The implicit constraint in using equation 1-7 is that the solutes be resolved with a resolution of 1.0. The resolution value of two peaks indicates how separated the two analytes are. Assuming Gaussian peaks, a resolution of 1.0 would indicate a contamination of approximately 2.27%. For accurate quantitation, a resolution of 1.5 is required. The resolution of two peaks can be calculated as

$$R = \frac{2(t_{R2} - t_{R1})}{w_{b1} + w_{b2}} \quad \text{Equation 1-9}$$

In equation 1-9,  $t_{R1}$  and  $t_{R2}$  represent the retention times of adjacent peaks, and  $w_{b1}$  and  $w_{b2}$  represent their respective peak width measured at the baseline. Clearly, peak widths are significant in determining the resolution, thus separation efficiency of two components. Wider peaks lead to lower resolution and also lower peak capacities. It is apparent that asymmetric peaks, especially peaks that tail, lead to lower column efficiencies.

For a given analyte pair, selectivity can be used to describe the quality of separation. Selectivity,  $\alpha$ , can be described in two ways. Equation 1-10 gives the conventional definition.

$$\alpha = \frac{k'_2}{k'_1} \quad \text{Equation 1-10}$$

As shown in equation 1-10, selectivity is the ratio of retention factors of an analyte pair. Larger values of  $\alpha$  indicates the ease of separation of the analyte pair, though not as practically descriptive as resolution. Selectivity can also be described in terms of elution order. Any change in elution order possibly indicates important differences in retention mechanism and analyte-stationary phase interaction.

### 1.3.2 Silanols

The ability to derivatize bonded-phases requires chemically reactive sites on the support. For most stationary phases, including zirconia, alumina, titania, and especially silica, the reactive sites are hydroxyl groups. In the case of silica-based stationary phases, these functional groups are termed silanols. Since silica has been well characterized, this discussion will focus on silica-based supports. As mentioned previously, the silica surface also contains siloxane bonds, which typically are hydrophobic in nature. Several studies have shown retention of non-polar analytes using bare silica in a high aqueous mobile phase [33, 37, 38]. The analyte interaction with the siloxane may be the source of retention, however using high aqueous mobile phases is uncommon. For most LC operating conditions, the silanols are of more interest to the chromatographer.

As shown in Figure 1-4, the silanols exist in three distinct forms, as isolated, geminal, or vicinal silanol [39]. There are various chemical and physical methods to assess the total silanols.

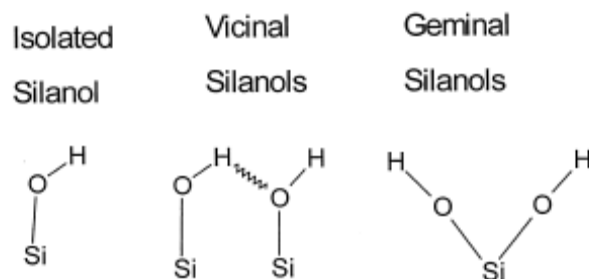


Figure 1-4. Three types of silanols on the silica surface [39].

All the chemical methods exploit the acidic nature of the silanol and include:

1. reactions with methyl lithium and measuring the methane produced
2. reaction with organoboron and measuring the hydrogen produced
3. isotope exchange, using  $D_2O$  or  $^3HHO$
4. titration with  $NaOH$

Physical methods such as infrared spectroscopy (IR) and nuclear magnetic resonance (NMR) are advantageous in their ability to distinguish the various types of silanols. IR can distinguish between isolated and vicinal silanols while NMR can discriminate isolated and geminal silanols [32, 40]. However, these methods are less quantitative than chemical methods.

The accepted belief is that the silanols remaining after derivatization are responsible for asymmetric peaks, especially seen with basic analytes. The acidic nature of these silanols results in their interaction with basic compounds as shown by the equation:



This results in a mixed retention mechanism, absorption/partitioning, hydrogen bonding and ion exchange, resulting in peak tailing. Various studies have investigated the presence and effects of these residual silanols. Fluorescence microscopy showed the presence of strong adsorption sites using fused silica plates derivatized with octadecylsilane. When compared to ODS end-capped phase, a decrease in these sites necessarily meant the silica surface was responsible for these adsorption sites [41]. Neue *et al.* used the change in retention of lithium ions with changes in mobile phase pH as an indication of silanol activity and acidity. Testing several commercial columns resulted in varied results, ranging from the presence of two different types of silanols (Resolve C<sub>18</sub> and Symmetry columns) to no evidence of residual silanols (Symmetry C<sub>18</sub>, XTerra, and XTerra MS C<sub>18</sub>). Anion exchange was even observed on one column under acidic conditions [42]. Breakthrough curves have also been employed to quantitate surface silanols, however, results were much lower than predicted [43]. Recent works by Guiochon and coworkers found that the surface heterogeneity of the silica resulted in multiple active sites with different binding energies. It was hypothesized that the observed peak tailing resulted from the analyte interaction with different energy sites [44].

In addition to silanol activity, it has been argued that the slow kinetics of the solute desorption process can contribute to peak tailing. If this were true, it has been hypothesized that at a high enough temperature, the mass transfer rate coefficient increases enough to minimize this effect on peak shape [45]. An issue with this approach is that care must be taken to ensure the thermal stability of the stationary phase and analytes. Nonetheless, McCalley found that of the four probes studied, only two showed reduced peak asymmetry when the temperature was raised from



20°C to 60°C. Furthermore, this improvement was seen only at pH 7.0, with no significant difference seen in the peak shape at pH 3.0 [46]. In a later study, Buckenmaier and coworkers suggested that improvements in peak shape while running the chromatography at increased temperature were not necessarily due to changes in kinetics but rather the  $pK_a$  of the basic analyte [47]. As the temperature increases, the  $pK_a$  of the analyte decreases. Therefore, at a constant pH, increasing the temperature results in a lower percentage of the basic molecule being protonated, thus interactions between analyte and silanols are reduced.

More recently, Gritti and Guiochon did an extensive investigation into the heterogeneity of the stationary phase and its effect on tailing [44]. Equilibrium isotherm models and affinity energy distribution calculations established the existence of different energy sites that contribute to peak tailing. High energy sites, though low in population, become saturated before low energy sites. The physical origin of these high energy sites are related to regions within the ligand where analytes can become buried, leading to peak tailing. For columns that exhibit two distinct types of energy sites, differences in the adsorption energies and the densities of these sites challenge the idea that these high energy sites are residual silanol groups [48]. However, some columns do exhibit additional high energy sites that seem to better correlate to silanol interactions or ion-exchange interactions.

Further studies by Gritti and Guiochon compared adsorption isotherms of endcapped and endcapped amido-embedded reversed phase columns to conventional non-endcapped  $C_{18}$  columns. It was found that for non-basic compounds, little difference in adsorption behavior can be seen. However, in general, non-endcapped columns showed greater surface heterogeneity, and a greater percentage of high energy sites. Additionally, the choice of organic modifier also affects the surface heterogeneity. By using a stronger organic modifier, e.g., acetonitrile vs methanol, a protective adsorbed organic layer is formed, thus shielding the analyte from the high energy sites [49]. Comparison of an endcapped amido-embedded column to a conventional endcapped  $C_{18}$  column yielded similar adsorption behavior for certain analytes. Yet, other analytes were responsive to the presence of the polar-embedded group and showed an additional high energy site [50]. However, these sites only become important at analyte concentrations that saturated high energy sites.

The available literature suggests that the fundamental reasons for peak tailing are still debatable. As new insight into retention mechanisms is gained and the differences in solute-

stationary phase interactions are investigated through carefully selected probes, we gain a better understanding of the separation process and the role silanols have in chromatographic efficiencies. More importantly, this understanding would aid in the development of improved stationary phases thus increasing the analyst's toolbox for complex separations.

### 1.3.3 Methods to reduce silanol activity

The negative affects of silanols on separation efficiencies have lead to many techniques that attempt to minimize their solute interactions. The development of new stationary phases and manufacturing techniques endeavor to reduce their concentration or apparent concentration. For the chromatographer, mobile phase conditions can be optimized to reduce their deleterious affects.

The acidic nature of silanols is shown by the dissociation reaction:



At 20°C, the  $\text{pK}_a$  of an isolated silanols is about  $6.8 \pm 0.5$  [40]. Thus, by selecting a suitable mobile phase, the ionic interaction can be lessened. One approach is to operate at a low pH, such that  $\text{pH} < \text{pK}_a$  of the silanol, thus the silanol remains protonated. Similarly, operating at a high pH, such that the  $\text{pH} > \text{pK}_a$  of the basic analyte, will suppress the ionization of the analyte.

[14, 15] The dilemma with operating at the pH extreme is the stability of the silica support or bonded-phase. Studies have shown at low pH, the bonded phase can be cleaved from the silica support, and is impacted by the ligand type, bonding density and end-capping [51]. Conversely, at high pH, above 9.0, dissolution of the underlying silica support becomes a problem [52]. Buckenmaier showed that temperature can also be employed to reduce the deleterious effect of silanols. At intermediate pH, basic compounds showed improved peak shape at elevated temperatures [47].

Mobile phase additives, increasing the ionic strength of the mobile phase, and/or changing the sample concentrations have also been studied [53]. The use of a mobile phase modifier to suppress silanol interaction was first suggested by Nahum and Horváth [54]. Ammonium salts

and amines such as triethylamine (TEA) and dimethyloctylamine (DMOA) are most common and have proven to be effective with certain analytes at neutral and acidic pH [55]. The use of buffers not only allow the control of pH, but also the type of buffer used, specifically the cation ( $\text{Na}^+$ ,  $\text{K}^+$ , etc) can act as a silanol suppressor via ion-pairing interactions [56]. The use of divalent cations, which interacts more strongly with silanols, also showed promise. Reta and Carr demonstrated that barium could be used showing peak symmetry and retention comparable with TEA as the modifier, without the deleterious problems of column instability and slow equilibration times often seen with amine additives [57]. Further, increasing the ionic strength of the mobile phase has shown improved peak symmetry. However, using frontal analysis and the adsorption isotherm of propranolol, Gritti and Guiochon concluded that silanols were not solely responsible for adsorption sites leading to asymmetric peaks. In addition, the choice of salts ( $\text{NaCl}$ ,  $\text{KCl}$ ,  $\text{CaCl}_2$ , etc) used to increase ionic strength along with concentration did play an important role in the band profile [58, 59]. Lastly, the sample concentration can be used to minimize the effects of silanols. If the existence of different adsorption sites prove valid [44, 48] then the high energy sites would become saturated first, whether silanols or not. If sorption-desorption from these sites are fast, then too large of a sample would result in distorted peaks.

In addition to these techniques, the stationary phase itself has been designed to help alleviate peak tailing via improved pH stability or decreased silanol accessibility. Kirkland *et al.* found that end-capping reduced stationary phase degradation at intermediate and high pH [15]. Polymeric derivatization has also shown improved peak shape for basic analytes. By cross-linking the stationary phase, the stationary phases have demonstrated increased stability at high and low pH compared to monomeric stationary phases [7, 60]. Surface-modified silica has also shown promise. In one method, the silanols are replaced with methyl groups prior to the reaction with the primary ligand. This leads to the reduction of residual silanols about 50% to approximately 33% [61]. Polymers such as polyethylene and polystyrene used to coat the silica support allow the use of lower pH [17]. Großmann and coworkers reported mixed results when using various post-treatments of the native silica, including an acid wash and calcination step, prior to bonding the  $\text{C}_{18}$  [62]. More recently, Sunseri and coworkers used a thermal pre-treatment to reduce the amount of surface silanol prior to derivatization [6, 63].

## 1.4 Research goals

As seen in Figure 1-5, polar-embedded stationary phases incorporate a polar functional group within the alkyl chain. The presence of the polar group is reported to have several advantages such as unique selectivity and improved peak shape for basic analytes. Since these phases differ from conventional columns, they offer a unique selectivity. This uniqueness presents the possibility of separating complex mixtures conventional columns cannot.

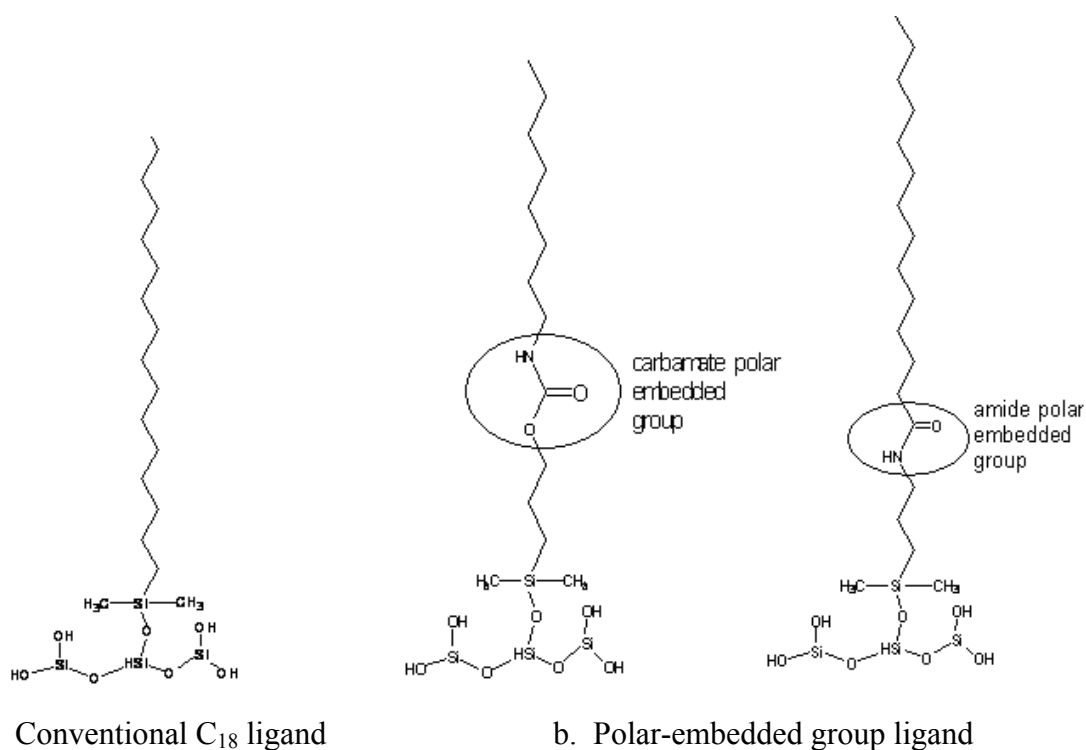


Figure 1-5. Stationary phase of conventional alkyl ligand compared to polar-embedded group.

In addition, it is reported that polar-embedded columns allow for the use of higher aqueous mobile phase. For convention columns with high bonding densities, it was previously argued that chain collapse was an issue in highly aqueous mobile phases. Chain collapse results from the aggregation of the hydrophobic alkyl chain in a highly aqueous mobile phase. This can result

in irreproducible retention times and decreased chromatographic efficiency [64, 65]. Recent works by Walter and coworker have argued that the loss of retention with highly aqueous mobile phase was not due to chain collapse, but rather the extrusion of the mobile phase from the stationary phase pores [66]. The dependence of retention loss on pore size, the correlation between changes in void volume and intraparticle pore volume after flow stoppage, and the pressure dependency of retention loss all corroborate this idea. Furthermore, a C<sub>18</sub>-carbamate embedded group stationary phase showed only a 3% loss in retention compared to a 98% loss for a C<sub>8</sub> and C<sub>18</sub> stationary phase when the mobile phase was changed to 100% aqueous.

Another factor leading to improved peak shape for basic compounds results from the increased wettability of polar-embedded columns [67]. One argument is that the polar group binds a water layer on the silica surface which shields the analyte from the silanols [65]. Others have suggested that the polar group can preferentially interact with the residual silanols [68]. In addition, if the pH of the mobile phase is below the pK<sub>a</sub> of the embedded group, the embedded group will be protonated and positively charged. This can result in electrostatic repulsion of the stationary phase and the analyte, thereby protecting it from the surface silanols.

The uniqueness of these columns also arises from the methods used in the synthesis of the polar-embedded stationary phase. In a two step synthesis, the first step involves bonding the polar group to the silica support via a short chain alkyl linker such as propyldimethylsilane. Next, an alkylsilane is reacted yielding the polar-embedded alkyl ligand. However, like the overall synthesis of conventional columns, the bonding reaction in the second step is incomplete. This results in residual “naked” polar groups remaining on the silica surface. Similar to polar end-capped stationary phases, this incomplete reaction can impart a unique selectivity.

The focus of this research was to evaluate and compare polar-embedded columns to conventional columns. In addition, a comparison of polar-embedded columns from different manufacturers, but same polar group was also investigated. Despite the fact that numerous works on column comparison have been published [2, 8, 67, 69, 70], this research investigated fundamental differences in these columns not yet explored. Ultimately, differences in the separation of basic compounds using these stationary phases were investigated.

The research was divided into two parts: selectivity assessments and thermodynamic studies. Though very general in showing difference between columns, selectivity studies are still beneficial. A mixture of select analytes was injected onto the column and the retention time and

elution order gives insight into differences in columns. More specifically, these columns will be characterized by methylene selectivity using alkyl benzene homologs. Next, retention studies allow for the calculation of thermodynamic values. Retention factors for analytes were measured at various temperatures. From these, van't Hoff plots were constructed and enthalpy and entropic values for methylene selectivity were calculated. In addition, log-log plots will show if analytes experience similar retention mechanism on two columns.

## CHAPTER TWO

### METHODS OF STATIONARY PHASE CHARACTERIZATION

#### 2.1 Introduction

It is well known that the character of the underlying support as well as the type of bonded phase plays a critical role in the efficiency and selectivity of the separation. However, the selection of a column for a particular analysis is not as obvious. Chromatographers often select a stationary phase as well as experimental conditions based on experience without thought to fundamental differences in the packing. To be fair, this is not always the fault of the analyst. Column manufacturers are not always forthcoming with information about these columns and what little information is available can be biased towards a product. With the numerous commercial columns available, the choice of column is not always apparent [71]. Through evaluating and characterizing these columns, a better understanding of column selectivity and important differences can be ascertained. The goals of these assessments are to provide information so that an educated decision on column selection can be made.

Methods of characterizing columns can be placed into four categories: spectroscopic methods, non-linear chromatographic studies, chemometric based modeling, and chromatographic based characterization. Spectroscopic techniques such infrared, fluorescence, and nuclear magnetic resonance (NMR) spectroscopy directly probe the structure of the stationary phase. These are typically used under non-chromatographic conditions, and provide qualitative properties of the support or bonded phase. To probe the specific nuances of the heterogeneous stationary phase, non-linear chromatography is employed. The most frequently used studies of this type involve measuring isotherms which describe the distribution of the solute between the mobile phase and stationary phase. From this, specific adsorption sites can be characterized. Though spectroscopic studies and non-linear chromatographic investigations provide valuable information on the stationary phase, the column performance using typical operating conditions is of more practical utility to the chromatographer. For this, empirical studies and modeling are utilized. Chemometric based modeling attempts to use specific molecular interaction descriptors

to predict selectivity and retention. These descriptors are based on retention data of certain solutes selected to measure specific interactions. Similarly, chromatographic based methods use select solutes to characterize the stationary phase. Generally, these types of studies use elution order or the peak shape of these analytes to evaluate column performance or molecular interactions.

With the ever increasing selection of columns available, the importance of these methods in distinguishing fundamental differences has become imperative. These characterization techniques provide a better understanding of retention and selectivity. For the chromatographer, these investigations aid in column selection or method development. For the manufactures, these methods assist in the development of new stationary phases. Each of these methods provides valuable and complementary information on the stationary phase.

## 2.2 Spectroscopy

NMR is useful for the characterization of structural and dynamic features of the bonded ligand as well as the silica support. In general there are two types of NMR studies: solid-state NMR, which provides structural information of the stationary phase support, and suspended-state NMR, used to provide details on the conformation and motion of the bonded phase. Cross polarization magic angle spinning (CP-MAS)  $^{29}\text{Si}$  NMR can provide information on the type and relative amounts of silanols on the silica. This method can distinguish isolated and vicinal silanols from geminal silanols and surface siloxanes [72]. Sindorf and Maciel first reported the distinct chemical shifts of these moieties [73]. Pfeleiderer and coworkers were able to use  $^{29}\text{Si}$  CP-MAS measurements to quantitate the relative amounts of di- and trifunctionally modified silica derivatized under various reaction conditions [74]. It was found that the presence of water during the synthesis significantly affected the polymerization process and resulting bonded phase.

To study the bonded phase, Sindorf and Maciel used  $^{13}\text{C}$ -CP-MAS NMR to investigate the motional dynamics of  $\text{C}_8$  and  $\text{C}_{18}$  bonded on silica gel. It was found that beyond eight carbons from the silica support surface, molecular motion increased, and overall the motional behavior of the bonded ligand was non-uniform [75]. Jinno *et al.* used  $^{13}\text{C}$  NMR to observe the effects of



bonding density, alkyl chain length, and temperature on alkyl chain conformation [76]. In addition to  $^{29}\text{Si}$  and  $^{13}\text{C}$  NMR, proton NMR can also elucidate conformational information using the  $^1\text{H}$  or  $^2\text{H}$  nuclei. Pursch and coworkers used  $^1\text{H}$ ,  $^{13}\text{C}$ , and  $^{29}\text{Si}$  NMR to examine alkyl ligand spacing, mobility, and order. It was concluded that increasing bonding density resulted in more rigid, ordered stationary phases and enhanced shape selectivity [77]. Sentell and Sanders offer extensive reviews of additional NMR studies [78, 79].

Infrared spectroscopy (IR) can detect the hydroxyl stretch in the  $3700\text{ cm}^{-1}$  to  $2800\text{ cm}^{-1}$  region as well as C–H stretches around  $2900\text{ cm}^{-1}$  to  $2800\text{ cm}^{-1}$  and wagging modes around  $1360\text{ cm}^{-1}$  to  $1350\text{ cm}^{-1}$  [37]. Often, IR spectra are obtained before and after derivatization of the support to gauge the extent of bonding, though elemental analysis is more quantitative and therefore preferred. Diffuse reflectance infrared Fourier transform spectroscopy (DRIFTS) can resolve siloxanes, isolated silanols, and geminal and vicinal silanols. Thus, this is complimentary to NMR, as NMR can distinguish geminal silanols while DRIFTS can resolve free silanols [32]. Sagliano and coworkers used DRIFTS and spectral subtraction to monitor the loss of alkyl bonded phase under acidic conditions. After exposure to the solvent for 18 hours, an observed increase in the intensity of the hydroxyl absorption band along with a decrease in the intensity of the hydrocarbon band corresponded to loss of 17% of the bonded phase [80]. Besides revealing the presence of hydroxyls, IR spectroscopy has been used to study the alkyl ligand. Using Fourier transform infrared spectroscopy (FT-IR), Sander *et al.* examined the conformation of alkyl ligands ranging from  $\text{C}_1$  to  $\text{C}_{22}$ . By comparing bonded-alkyl chains to corresponding liquid alkanes, it was found that the bonded phases were bent; showing some degree of conformational disorder at ambient temperatures. Further, the mobile phase environment resulted in an ordering of the alkyl chains, which was attributed to the binding of the organic modifier to the reversed-phase [81].

Raman spectroscopy also offers information on the conformation of the chromatographic stationary phase, though it is less utilized than FT-IR. Doyle and coworkers were the first to use Raman spectroscopy to examine the stationary phase under chromatographic conditions, i.e., typical mobile phase flow rates and pressures. Previous spectroscopic studies had examined either dry stationary phase, to eliminate the interference from absorbed water, or solvated stationary phase under static flow and atmospheric pressures. By using an LC column that was modified with a quartz window and fitted with a fiber optic probe, it was shown that Raman

spectra could provide a non-invasive, on-column method of characterization [82]. Further, solvent studies using Raman spectroscopy demonstrated that a conformational change of the C<sub>18</sub> ligand did not occur when the solvent was varied from an aqueous to an organic mobile phase; again, contesting the concept of a phase collapse [83]. Liao and coworkers showed the ability of Raman spectroscopy to examine the effects of bonding density, temperature, and polymerization method on the conformation of the alkyl ligand. As expected, it complimented previous NMR studies, showing the dependency of conformation, temperature, and surface coverage on shape-selective retention [84]. A similar study using Raman also considered the effects of pressure on solute retention. It was found that pressure could induce changes in alkyl conformation on par with changes in temperature, but generally smaller than changes caused by certain solvents [85].

Though native silica and alkyl ligands do not naturally exhibit fluorescence, employing fluorescent probes has allowed the use of fluorescence spectroscopy to investigate the silica surface, spatial distribution of bonded ligands, and solute absorption/desorption kinetics. Further, studies have also been carried out with silica modified with pyrene and other fluorescent ligands to evade the issue of the non-fluorescing alkyl bonded silica. One of the earliest studies employing this technique used dansylamide as the fluorescent tag to investigate the heterogeneity and polarity of the silica surface [86]. Changes in the excitation and emission spectra were correlated to changes in the polar environment caused by different solvents. Ståhlberg and Almgren used pyrene modified C<sub>2</sub> and C<sub>8</sub> phase and their emission spectra to investigate changes in polarity due to changes in mobile phase composition. The authors found that increasing the methanol concentration resulted in a decrease in the surface polarity. This trend was also true for acetonitrile, but only up to about 14% acetonitrile (w/w), at which point the polarity of the surface began to increase. The difference in polarity changes was attributed to the hydrogen bonding capability of methanol as compared to that of acetonitrile [87]. Diffusion rates within alkyl chains have also been measured using fluorescent probes. It was found that diffusion rates decreased with decreasing bonding densities, as well as with decreasing alkyl chain length. It was hypothesized that increased surface coverage and chain length resulted in decreased regions of energetically unfavorable regions the probe solute had to traverse, thus resulting in the observed trend in diffusion rates [88]. Ludes and Wirth used single-molecule fluorescence to detail the surface heterogeneity of C<sub>18</sub> modified silica. Based on desorption times of the dye,

three distinct adsorption sites were observed. The use of acetonitrile also increased the observed population of stronger binding sites [89].

The use of various spectroscopic techniques offers details on the surface structure of the chromatographic support and bonded phases. Effects of bonding density, temperature, mobile phase composition, and chain length can be elucidated and from these studies. More importantly, these analyses offer insight into physical properties such as bonded phase conformation, surface heterogeneity, and stationary phase polarity. However, these methods are limited in that these studies often do not simulate chromatographic conditions, e.g. dynamic mobile phase, stationary phase under pressure and flow conditions. However, these techniques are only a portion of the methodologies available that offer direct and versatile means of probing the stationary phase that can complement other methods of characterization.

### **2.3 Non-linear chromatography**

The data have convincingly shown the surface of the stationary phase is heterogeneous [44, 49, 50, 58, 59]. The dilemma arising from the nature of the surface is that linear chromatographic investigations cannot probe this heterogeneity. Typical studies, including spectroscopic studies, measure average properties rather than the microstructure of the support or microenvironment of the solvent-stationary phase interface [90]. Further, most models used in linear chromatography assume that interactions such as hydrophobicity, acid-base pairing, and ion exchange are independent of each other. Thus, if mixed retention mechanisms are involved, the individual contributions of the different sites cannot be resolved. Fortunately, the presence of these different sites on the surface results in a heterogeneous distribution of the adsorption energy of different analytes [44]. At low concentrations, high-energy sites are first populated followed by low-energy sites. Thus by acquiring data using a wide range of concentrations, the various retention mechanisms can be investigated.

To characterize the surface, adsorption isotherms are measured. Essentially, the isotherm describes the distribution of an analyte between two phases. From this, certain parameters such as saturation capacities are determined by fitting the experimental data to a model. The simplest model is the Langmuir model, however more complex models such as bi-Langmuir, quadratic,

Fowler, and Jovanovic models can be utilized [91]. The use of non-linear chromatography has been important in many industrial applications such as extraction and purification of pharmaceutical compounds. Csaba Horváth pioneered the understanding of non-linear chromatography through his works on preparative chromatography and isotherms [92].

Traditionally, isotherms were measured via static methods in which the change in concentration after equilibration of the solute solution with the adsorbent was measured. This so-called shake-flask method was imprecise and labor intensive due to the measurement of discrete points on the isotherm. In addition, non-polar sorbents posed the added difficulty of being poorly wetted by water-rich solvents [93]. Uncertain equilibration times and difficulties in measuring the amounts of solute also detracted from this method. A similar method, adsorption-desorption method, required two steps. Initially, the column is completely equilibrated with a solution of known solute concentration. In the second step, the column is flushed with an eluent, which is subsequently analyzed for the solute amount [94].

Perhaps the most widely used and most accurate method of measuring adsorption isotherms is by frontal analysis (FA), first proposed by James and Phillips [95]. In essence, this method is a titration curve in which the amount of solute needed to saturate the packing is measured. Chromatographic methods were developed to avoid the issues of static isotherms. These methods involve the replacement of the mobile phase with the solute solution at a known concentration. A profile of the mobile phase concentration measure at the column exit versus the elution volume is called the breakthrough curve. Figure 2-1 shows a typical breakthrough curve [44].

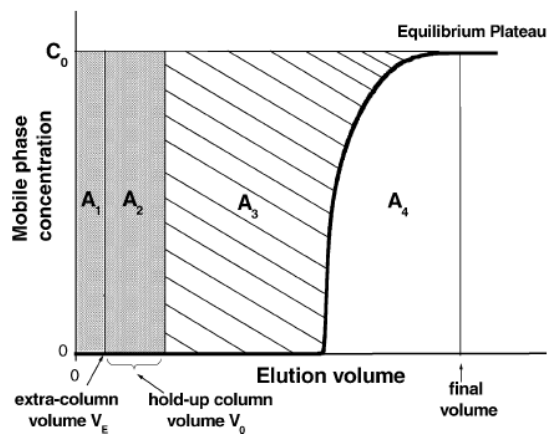


Figure 2-1. Break through curve using frontal analysis [44].

The different regions,  $A_1$ ,  $A_2$ ,  $A_3$ , and  $A_4$ , shown in Figure 2-1 represent the amount of the solute in different parts of the system. The areas shaded  $A_1$  and  $A_2$  represent the mass of solute outside the column between the mixer and detector cell, and the mass of solute in the volume of mobile phase inside the column, respectively. Area  $A_3$  is the amount of solute adsorbed on or in the stationary phase inside the column at equilibrium, while  $A_4$  is the mass of solute exiting the column during the duration of the isotherm measurement. Using  $A_3$ , the concentration of the solute adsorbed on the stationary phase,  $q$ , can be calculated as

$$q = \frac{A_3}{V_{sp}} \quad \text{Equation 2-1}$$

The term  $V_{sp}$  in equation 2-1 represents the volume of sorbent present in the column, which can be calculated as the volume mobile phase subtracted from the volume of the empty column. This saturation amount for various analytes is then used to calculate adsorption energies for various sites and also fitted to a particular isotherm model (e.g., Langmuir) to give information on different adsorption sites.

An important physical property of the support is the surface area of the native silica. This value limits the amount of stationary phase that can be bonded to the surface. The surface area of the bare silica is routinely measured using a gas adsorption isotherm called the BET method, developed by Brunauer, Emmett, and Teller [96]. The amount of nitrogen gas adsorbed on the silica surface is proportional to the surface area of the support. HPLC grade silica has surface area values ranging from 10 to about 500 m<sup>2</sup>/g, depending on the pore diameter and particle size [40]. However, Hägglund and Ståhlberg demonstrated that modified silica may exhibit a different surface area. Based on the adsorption isotherm for a negatively charged solute, the surface area for a C<sub>18</sub> modified stationary phase was significantly lower than the reported value using the BET method on the bare silica [97]. However, the presence of methanol in the mobile phase seemed to increase the area accessible by the solute.

On an analytical scale, operating under condition of non-linear isotherm can result in column overload and can have negative effects on peak shape and efficiencies. In fact, these distorted peaks make it impossible to accurately calculate plates. One method to avoid this error is to reduce the amount of injected analyte so that linear chromatographic conditions apply. The

difficulty in utilizing such methods is that the concentration of analyte may be so small that it becomes lost in the noise. Recently, Dai and coworkers developed a method for determining plate counts under non-linear conditions to avoid the issues surrounding low analyte concentrations [98]. Using a previously developed model, the so-called Wade-Lucy-Carr kinetic non-linear model, it was found that the limiting plate count (i.e., plate count under linear chromatographic conditions) and the sample load that reduced the plate count to half of its limiting value were key to characterizing the overload behavior. By fitting experimental data of higher injected amounts into the model, the limiting plate count was estimated. Further, the authors found that the limiting plate count for columns of similar size, particle size and flow rate was similar, and observed differences were due to loading capacities.

Another method of measuring isotherm is using the frontal analysis by characteristic point (FACP) method. It differs from FA in that the concentration of the solute solution is decreased during the course of the analysis, thus leading to a gradual tailing curve as shown in Figure 2-2.

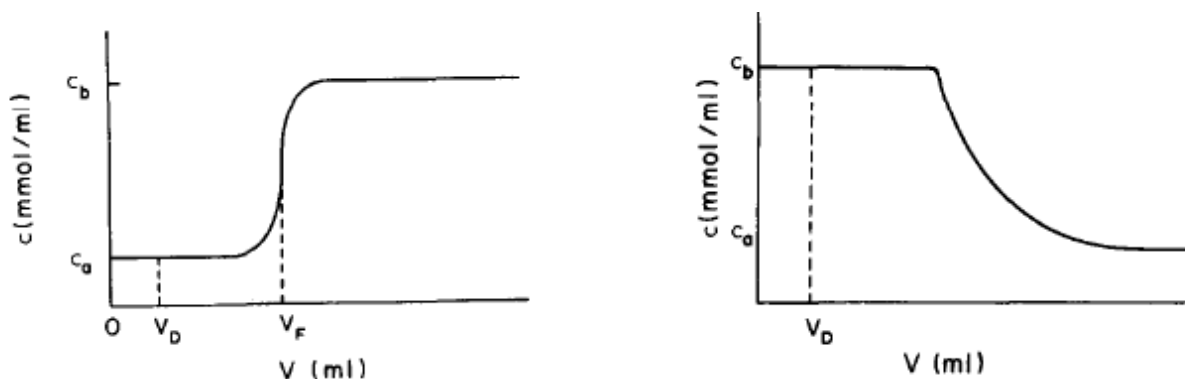


Figure 2-2. Concentration profiles using frontal analysis and frontal analysis by characteristic point.  $C_a$  and  $C_b$  are the initial and final solute concentrations,  $V_D$  is the system dead volume,  $V_F$  is the retention volume of the front [93].

The advantage of FACP is that the entire isotherm is calculated from the one concentration profile experiment. However, the detector signal must be calibrated so that concentration units are evaluated. Elution by characteristic point (ECP) is similar to FACP; however the elution profile of an overloaded peak is used instead of the solute solution profile. Using the peak fitting

method, isotherm parameters are adjusted so that the simulated chromatographic peak best resembles the experimental chromatographic peak [99].

In addition to information on the heterogeneity of the silica surface, adsorption isotherms are also important in understanding and predicting overloaded band profiles. Further, they can be used in the analysis and design of preparative scale chromatographic separations. However, the acquisition of these isotherms is not trivial. These methods are labor intensive, and finicky to experimental conditions such as temperature, flow rate, and mobile phase composition. Gritti and Guiochon demonstrated the effects of varying these conditions using phenol as the solute probe. It was found that increased temperatures resulted in a decrease in the saturation capacity of the high energy sites. Additionally, increasing the organic modifier in the mobile phase also decreased the availability of these sites. Quantitatively, a 1 K deviation in temperature or a change in mobile phase concentration of 0.3% was found to have resulted in a change in saturation capacity of 1.5% [100]. Despite the long and tedious nature of these methods, adsorption isotherms provide an additional, complementary method for the characterization of the stationary phase; giving added insight into the nature of the retention process and ultimately, the separation process.

## **2.4 Modeling**

Characterization using spectroscopy and non-linear chromatography provides valuable information of the stationary phase; however, most chromatographers are interested in the practical performance of the stationary phase (i.e., column) under chromatographic operating conditions. With the vast amount of columns available, and an equally daunting variety of analytes to be separated, chemometric based modeling attempts to characterize columns based on specific solute parameters and system parameters, which include stationary phase and mobile phase properties. These parameters are based on evaluation of column performance using select test analytes to measure specific properties including hydrophobicity, methylene selectivity, steric selectivity, and stationary phase acidity and basicity. The belief is that properties of the chemical compounds, including chemical structure along with solvent and stationary phase properties can be used as predictors of chemical behavior. Empirical measurements provide the

parameters needed to develop these models that attempt to correlate retention and selectivity to physicochemical properties of the stationary phase and analyte.

Since the inception of LC, the importance of the mobile phase was acknowledged. Early attempts to characterize and model retention focused on solvent properties. Rohrschneider attempted to correlate gas-liquid partition coefficients with solvent polarity and solubility using six solutes and 82 different liquids [101]. From this, Snyder modeled a P' scale describing solvent polarity and categorized solvents based on proton donor ability, proton acceptor ability, and polarity [102]. Kamlet, Taft, and Abboud developed the solvatochromic model to characterize solute-solvent interactions [103, 104, 105]. The authors used spectroscopic measurements to evaluate various solvents based on dipolarity/polarizability. Using the effect of the solvent on the maximum UV/Vis absorbance on some 40 different polar aromatic compounds, a  $\pi^*$  scale of solvent polarities was developed. Subsequently, solvatochromic scales for solvents' hydrogen bond donor acidity and hydrogen bond acceptor basicity were also developed.

Though solvent characterizations were an important step in modeling and predicting chromatographic performance, solute properties needed to be taken into account. Some of the earliest attempts to analyze solute factors leading to solute retention arose out of solvophobic theory, initially developed by Sinanoğlu. Horváth and coworkers adapted the solvophobic theory to LC, correlating retention factors to the hydrocarbonaceous surface area of the solute [106]. The retention process was viewed from a solute-solvent hydrophobic interaction. However, solvophobic theory failed to account for the role of the stationary phase in the retention process; ignoring effects of stationary phase ligand type and bonding density [107]. Though this theory is still applied to retention in LC, studies by Carr *et al.*, Tan and Carr, and Dorsey and Dill have shown the importance of the stationary phase's role in retention, accordingly the limitation of this model [108, 109, 110].

Hafkenschied and Tomlinson established a linear correlation between water solubilities, octanol/water partition coefficients and retention factors using 32 solutes in three different mobile phases [111, 112]. It was modeled on the following relationship

$$\kappa = \kappa_w + B\phi \quad \text{Equation 2-2}$$



In equation 2-2,  $\kappa$  represent the logarithm of the retention factor,  $\kappa_w$  is the logarithm of the retention factor of the solute in pure water, and  $\varphi$  is the volume fraction of organic modifier. In essence, equation 2-2 is the linear solvent strength (LSS) model more often represented by

$$\log k = \log k_w - S\varphi \quad \text{Equation 2-3}$$

LSS relates the retention factor to the volume fraction of organic modifier in the mobile phase. The coefficient  $S$  is a constant related to the chromatographic system [113]. One problem of equation 2-3 lies in the difficulty of measuring retention in a pure aqueous mobile phase, denoted by  $\log k_w$ . As Hafkenscheid and Tomlinson demonstrated,  $\log k_w$  can be correlated to octanol/water partition coefficients which have been used extensively to model lipophilicity, an important factor in metabolism, absorption, bioavailability, and pharmacological activity [114]. Extrapolation of a plot of  $\log k$  vs  $\varphi$  allows  $\log k_w$  to be calculated; however studies have shown such extrapolations are prone to errors, possibly due to the disregard of the stationary phase's role in the LSS model [115].

From the solvatochromic model, the solvent properties as a bulk liquid were converted to solute parameters. Though it is not necessarily accurate to characterize an individual solute in a solvent based on the solute's bulk liquid properties, it provided an initial foundation [116]. The recognition of the importance of solute parameters has led to the development of quantitative structure-retention relationships (QSRR). QSRR are statistically derived models that aim to predict retention based on molecular structure. These models also provide a means of evaluating the stationary phase and offer insight into the mechanism of retention. Of the QSRR models, the most widely used is linear solvation energy relationship (LSER), also referred to as linear free energy relationship (LFER) [117, 118].

In general, QSRR parameters are evaluated based on several physicochemical properties that are strongly correlated to retention data. Hydrophobicity is derived from stationary phase factors including ligand length, bonding density, pore diameter, and surface area. These all influence the retention times of solutes that can establish dispersion interaction with the bonded phase. A similar and often confused parameter is hydrophobic selectivity, or methylene selectivity. Methylene selectivity is the variation in retention due to the addition of a methylene group on a

solute. Steric selectivity and shape selectivity are also often erroneously used interchangeably. Steric selectivity, also called steric resistance, is a measure of a solute's ability to penetrate the stationary phase based on its size. It is manifested as a reduction in retention as molecular volume increases, and increases with high bonding density. Shape selectivity, though related to steric selectivity, is a descriptor related to the ability of a stationary phase to discriminate between isomers that have different three-dimensional shape. For example, isomers in which one is narrow and elongated and the other is wide, but short; or differences in planarity of isomers. Lastly, silanol activity describes the hydrogen bonding between solutes and residual silanols on the support surface. Hydrogen bonding can occur between acidic or basic solutes and the neutral silanol, or ionized acidic or basic solutes and ionized silanols. This also provides a measure of the stationary phase's ability for ion-exchange [118, 119].

Abraham and coworkers first adapted the solvatochromic model into a LSER model for HPLC [120]. The authors correlated dipolarity/polarizability, hydrogen bonding properties and molar volume to solubility properties using equation 2-4.

$$SP = SP_0 + m\bar{V}_2/100 + s\pi_2^* + b\beta_2 \quad \text{Equation 2-4}$$

In equation 2-4,  $SP$  denotes the solubility properties; the coefficients  $m$ ,  $s$ , and  $b$  are related to the chemical nature of the stationary phase and mobile phase, and  $\bar{V}_2$ ,  $\pi_2^*$ ,  $\beta_2$  denote the molar volume, polarizability and hydrogen bonding properties of the solute, respectively.  $SP_0$  is a correction factor, possibly related to the amount of bonded phase. A more general formalism of the relation to retention is given as

$$\log k = c + rR_2 + s\pi_2^* + a\sum\alpha_2^H + b\sum\beta_2^H + \nu V_x \quad \text{Equation 2-5}$$

In equation 2-5, the solvation parameter  $R_2$  is the excess molar refraction,  $\pi_2^*$  is solute dipolarity/polarizability,  $\sum\alpha_2^H$  is the overall hydrogen bond donor acidity,  $\sum\beta_2^H$  is the overall hydrogen bond basicity, and  $V_x$  is the molar volume, known as the McGowan volume [121]. The coefficients  $r, s, a, b$ , and  $\nu$  are determined by multivariate regression analysis and

characterize the system complementary properties. For example, if  $\sum \alpha_2^H$  represents hydrogen bond acidity, the coefficient  $a$  represents the hydrogen bond basicity of the phase. The determination of these solvation parameters has been reviewed and numerous solute parameters have been reported in the literature [122]. The solvation parameter model and LFER are essentially LSER models [123, 124, 125]

Another powerful tool in characterizing HPLC columns is principle component analysis (PCA). Like LSER, it is based on a linear relationship given by

$$\log k_{i,j} = \log k_{ref,j} + \sum_{k=1}^n SP_{i,k} \cdot CP_{j,k} \quad \text{Equation 2-6}$$

In equation 2-6,  $\log k_{i,j}$  represents the retention factor of a compound, under  $j$  conditions (e.g., temperature, mobile phase composition, etc). It is related to the retention of a reference compound,  $\log k_{ref,j}$  and a combination of solute properties and stationary phase properties,

$\sum_{k=1}^n SP_{i,k} \cdot CP_{j,k}$  [126]. Whereas LSER models are based on empirical data, PCA is a mathematical approach which defines a new, reduced set of variables, called principal components, from original variables (e.g.,  $SP_{i,k}$  and  $CP_{j,k}$ ). These principle components represent a simplification of the original data set with minimal loss of information. PCA has been used for comparison and classification of stationary phases [69, 126]. Such assessment would be valuable in method development, selection of an equivalent replacement column, or entirely different column for a desired separation. In addition, PCA can be used to reduce the number of test compounds for a characterization method, such as LSER. Vervoort and coworkers used PCA to reduce a set of 32 test solutes used in a previous study to five [127].

More recently, Snyder *et al.* published a very comprehensive review that examined the hydrophobic-subtraction model [70]. In this assessment of column selectivity, five column properties and five complementary solute properties were measured for over 300 columns. The five solute-column interactions include hydrophobicity ( $H$ ), steric selectivity ( $S^*$ ), hydrogen bond acidity ( $A$ ), hydrogen bond basicity ( $B$ ), and cation-exchange activity ( $C$ ). In this approach, using ethylbenzene as a reference analyte, the values of  $\log k$  were measured for 90

solutes on similar type columns, e.g., type-B C<sub>18</sub> columns, and then averaged. Next, log k values for each column were correlated to the average log k values, and deviations were measured,  $\delta \log k$ . Finally, values of  $\delta \log k$  for deviant analytes were plotted against values of  $\delta \log k$  for all other deviant analytes for all the columns in the group. Correlations in this plot were attributed to a single solute-analyte interaction other than hydrophobicity. Multiple linear regressions were then performed to assign values to the five solute-column descriptors. These interactions were correlated to retention by the following:

$$\log \left( \frac{k}{k_{EB}} \right) = \eta' H - \sigma' S^* + \beta' A + \alpha' B + \kappa' C \quad \text{Equation 2-7}$$

The variables  $\eta'$ ,  $\sigma'$ ,  $\beta'$ ,  $\alpha'$ , and  $\kappa'$  represent the complementary solute property related to the corresponding stationary phase property. Later studies using cyano and phenyl bonded phases concluded that  $\pi$ - $\pi$  interactions and dipole-dipole interaction also contribute to retention [128]. From these a modified hydrophobic subtraction model was proposed, presented as

$$\log \left( \frac{k}{k_{EB}} \right) = \eta' H - \sigma' S^* + \beta' A + \alpha' B + \kappa' C + \pi' P + \mu' D \quad \text{Equation 2-8}$$

However the authors did stipulate that the  $\pi$ - $\pi$  interactions, denoted by  $P$  and its complementary solute contribution  $\pi'$ , were only present for cyano and phenyl columns; and dipole-dipole interactions, denoted by  $D$  and its complementary solute contribution  $\mu'$ , were only present for cyano columns. For all other columns,  $P$  and  $D = 0$ , and equation 2-8 reverts back to equation 2-7. Further, these two interactions were found to be mobile phase dependent. Mobile phases containing acetonitrile demonstrated decreased  $\pi$ - $\pi$  selectivity compared to methanol using phenyl columns [129].

Though various models have been developed, each with different considerations, all have the common goal of better understanding the retention process. Fundamentally, these models are based on the premise that structural aspects of an analyte contain physicochemical properties needed to predict retention. These models not only allow for the characterization of these

columns but also give insight into individual solute-stationary phase interactions. These interactions play a role in the retention process, and understanding these interactions aids the chromatographer in selecting an appropriate column for a given separation.

## 2.5 Chromatographic

Similar to chemometric based models, chromatographic based studies attempt to characterize stationary phases based on test solutes. The use of specific solutes allows the elucidation of various column properties such as silanol activity, hydrophobicity, or shape selectivity. The advantage of these tests over chemometric based models is that a single column can be characterized with a few experiments. With modeling, a large empirical data set is required to generate the molecular descriptor values. In addition, unlike non-linear chromatographic studies and spectroscopic studies, these investigations use typical chromatographic conditions. Many of these tests provide qualitative assessments based on elution order of specific solutes or the peak shape of a particular solute.

Sander and Wise developed a test to examine a column's ability to differentiate solutes based on shape. This so-called shape selectivity is based on differences in molecular structure, rather than chemical differences in the solutes, and is important for classes of solutes including polycyclic aromatic hydrocarbons, polycyclic aromatic sulfur heterocycles, polychlorinated biphenyl congeners, and steroids [130, 131]. The shape selectivity arises from conformational constraints of these molecules due to fused rings, double bonds, and/or sterics. The National Institute of Standards and Technology uses this test through standard reference material 869a as a measure of column selectivity. It is based on the selectivity and elution order of 1,2:3,4:5,6:7,8-tetrabenzonaphthalene (TBN), benzo[*a*]pyrene (BaP), and phenanthro[3,4-*c*]phenanthrene (PhPh) using a 85/15 acetonitrile/water mobile phase at 25°C [132]. The selectivity is measured as a ratio of  $k'$  of TBN and  $k'$  of BaP, with values of less than one implying enhanced shape selectivity, and greater than 1.7 implying reduced selectivity. In addition, the elution order of the three components is an indicator of bonding type, monomeric versus polymeric. However, this test was developed on C<sub>18</sub> columns, and may be restricted to these types of bonded phase.

Engelhardt and coworkers developed a series of tests to characterize hydrophobicity, silanol activity, and polar interactions [133]. Solutes for the Engelhardt test include ethylbenzene, toluene, phenol, *p*-ethylaniline, aniline, ethylbenzoate, N, N-dimethylaniline, and *o*-, *m*-, and *p*-toluidine isomers. The mobile phase is a 49/51 (w/w) methanol/water or 55/45 (v/v) methanol/water and the operating temperature is 40°C. The retention of ethylbenzene and toluene is used as a measure of hydrophobicity, and subsequently, is indicative of the percent carbon load. As the two solutes differ by a methylene group, the selectivity value can also be used as a measure of methylene selectivity. However, Claessens *et al.* suggested that the methylene selectivity is an inadequate measure of hydrophobicity, and absolute retention factor values should be used instead [134]. To measure silanophilic interactions, the elution order of phenol and aniline, separation of the toluidine isomers, as well as the peak shape of *p*-ethylaniline is used. The authors stated that if aniline eluted before phenol then the silanophilic interactions can be considered negligible. This is also true if the toluidine isomers were not separated since they only differ in basicity. In addition, the peak asymmetry of *p*-ethylaniline, measured at 10% height, was suggested as an indication of silanol activity. Interestingly, phenol and ethylbenzoate were mentioned as indicators of polar interaction, however no interpretation was provided.

Tanaka and coworkers developed another commonly used test to evaluate column character [135]. Various alkylbenzenes were used to test hydrophobic character, using 80/20 (v/v) methanol/water mobile phase. In contrast to Engelhardt, Tanaka reported a linear dependence of methylene selectivity versus percent carbon content. This allowed the authors to infer information on surface area and amount of alkyl chains from the methylene selectivity. Shape selectivity was gauged using the separation factor of triphenylene and *o*-terphenyl, also using 80/20 (v/v) methanol/water. In addition, the functionality of the stationary phase could be predicted based on the selectivity of these two analytes. Caffeine and theophylline were used to test the hydrogen bonding ability of the stationary phase using 30/70 (v/v) methanol/water. The selectivity between benzylamine and phenol using a methanol/phosphate buffer, buffered at pH 7.6 and pH 2.7 was used to evaluate ion exchange capacity, taken as a measure of silanol activity. However, it was stated that any alkyl amines with  $pK_a > 9$  such as procainamide or N-acetylprocainamide could be used as long as it was normalized with phenol or benzyl alcohol to cancel out the hydrophobic character of the stationary phase.

Neue and coworkers used a modified Engelhardt test, employing a mixture of neutral, acidic, and basic compounds to measure hydrophobic, silanophilic and ion-exchange properties [136, 137]. Using a 65/35 (v/v) methanol/phosphate buffer, pH 7, toluene, naphthalene, and acenaphthalene were used to measure hydrophobicity. Propyl- and butyl-parabens and dipropyl- or di-butylphthalates were used to test for polar interactions. In addition, propranolol and amitriptyline, which are basic analytes, were used to investigate ionic interactions, thus silanol activity. Similar to the data treatment Tanaka used, qualitative determination of the properties being measured were based on plots of selectivity of different analytes or known physical properties of the column being tested.

Euerby and coworkers also used a modified Tanaka test to characterize columns [138]. Amount of alkyl chain was based on the peak shape of amylbenzene, hydrophobicity was based on the selectivity of amylbenzene compared to butylbenzene, shape selectivity was determined using triphenylene and *o*-terphenyl, all analyzed using 80/20 (v/v) methanol/water. In addition, hydrogen bonding capacity was measured using caffeine and phenol, employing a 30/70 (v/v) methanol/water mobile phase. Finally, ion exchange capacity was evaluated at pH 7.6 and pH 2.7 using a 30/70 (v/v) methanol/water. The retention factor of benzylamine compared to phenol was used as an indicator of this interaction. The authors also introduced a dihydroxynaphthalene efficiency ratio test (DERT) to investigate surface metals. However, the surface metal contribution of the stationary phase to this parameter was determined to be small and dependent on column history. Subsequently, the DERT value was reported for only one column and subsequently abandoned. A modified test was reported in 2007 that included aromatic selectivity for phenyl phases [139].

Other empirical tests have also been developed based on the retention, selectivity, and peak shape of select solutes. The Goldberg test uses dimethylphthalate and diethylphthalate to measure hydrophobicity, while caffeine, theophylline and benzoic acids measure acid/base character. Galushko uses toluene and benzene in 60/40 methanol/water to evaluate hydrophobicity, and aniline and phenol to gauge silanol acidity. Daldrup and Kardel use diphenhydramine and diazepam to measure ion exchange activity at low pH [134, 140]. Verzele and Dewaele use naphthalene, 1-nitronaphthalene, and acetylacetone to measure silanol activity. McCalley also focuses on silanol activity through the use of basic test solutes [141].

Being able to characterize the stationary phase can have a tremendous impact on LC applications and development. Identifying the various interactions and column properties would allow the analyst to make an educated selection of a column for an analysis. Chromatographic based methods offer these characterizations by means evaluating retention times, peak shape, selectivity values of select solutes. However, the availability of these tests is not of concern, it is the variable conclusions that these tests result in that is troublesome. Vervoort *et al.* compared the results of several tests on seven commercially available stationary phases [142]. It was found that qualitative comparisons of the stationary phases based on several tests including the Tanaka, Engelhardt, Galushko, and McCalley test, produced different assessments. For example, the Luna C<sub>18</sub> column was found to be suitable for the analysis of basic analytes based on the results of a McCalley and Engelhardt test. However, characterization of the same column using the Tanaka test produced disagreeing assessments. These varying conclusions partly arise from the different methodologies each test necessitates. Neue *et al.*, Engelhardt *et al.*, and Tanaka *et al.* all evaluate the hydrophobic character of a column, however, different analytes under different mobile phase conditions are suggested. Wilson and coworkers found that changing the temperature and mobile phase composition unquestionably changed retention and column performance [143, 144]. Therefore, it is not surprising that these tests produce different conclusions. However, the authors did find that for a given solute, changing experimental conditions produced the same relative changes in retention on different columns.

Regardless of the method used to evaluate particular properties of the column, the need for them is undeniable. Each method, whether using spectroscopic methods, non-linear chromatography, chemometric based modeling, or empirical chromatographic experiments, provides useful physical or chemical information that helps the chromatographer better understand retention mechanisms, molecular interactions, or physicochemical properties. None of these methods alone provide a complete characterization, but together offer the analyst complementary information that assists in method development, application, or product development.



## CHAPTER THREE

### VAN'T HOFF ANALYSIS

#### 3.1 Introduction

In the investigation of chromatographic retention, the elucidation of thermodynamic information often takes the form of van't Hoff analysis. In one of the earliest van't Hoff studies, Knox and Vasvari calculated heats of transfer of select solutes to characterize Permaphase, a stationary phase developed by DuPont [145]. The retention factor,  $k'$ , was related to thermodynamic parameters as

$$\log k' = \log f + \frac{\Delta H_{s \rightarrow m}}{RT} - \frac{\Delta S_{s \rightarrow m}^\circ}{R} \quad \text{Equation 3-1}$$

In equation 3-1,  $\Delta H_{s \rightarrow m}$  is the heat of transfer from the stationary phase to the mobile phase,  $\Delta S_{s \rightarrow m}^\circ$  is the standard entropy of transfer from the stationary phase to the mobile phase,  $R$  is the gas constant, and  $T$  is the absolute temperature. The phase ratio, the volume of the stationary phase to volume of the mobile phase,  $f$ , was estimated to be 1/25 using physical properties of the stationary phase such as weight percent polymeric phase, density of the support, and porosity. For the ODS column, the authors found that retention increased with increasing heats of transfer and increasing entropy change, partly attributed to the strong orientation of the solute on the surface.

Though equation 3-1 is valid, classical van't Hoff analysis considers the retention process as the transfer of the solute from the mobile phase to the stationary phase. In chromatography, the retention factor is defined by equation 1-8, and can be related to the equilibrium constant,  $K$ , as

$$k' = \frac{t_R - t_0}{t_0} = K \frac{V_s}{V_m} \quad \text{Equation 3-2}$$

in which  $V_s$  and  $V_m$  are the volume of the stationary phase and mobile phase, respectively. This ratio is usually represented as  $\phi$ , the phase ratio. The distribution of the solute between the stationary phase and mobile phase is related to the standard free energy change,  $\Delta G^\circ$ , associated with the transfer of the solute into the stationary phase by equation 3-3.

$$\Delta G^\circ = -RT \ln K \quad \text{Equation 3-3}$$

The free energy change is also related to the standard enthalpy and entropy as

$$\Delta G^\circ = \Delta H^\circ - T\Delta S^\circ \quad \text{Equation 3-4}$$

Substituting equation 3-2 and 3-3 into equation 3-4 yields

$$\ln k' = \frac{-\Delta H^\circ}{RT} + \frac{\Delta S^\circ}{R} + \ln \phi \quad \text{Equation 3-5}$$

Equation 3-5 is the classical representation of the van't Hoff equation [146]. Opposite to equation 3-1, here,  $\Delta H^\circ$  and  $\Delta S^\circ$  represents the enthalpy and entropy of transfer of the solute from the mobile phase to the stationary phase. A plot of  $\ln k'$  versus  $1/T$  produces a linear plot (van't Hoff plots) with slope equal to  $-\Delta H^\circ$ ; and if the phase ratio is known,  $\Delta S^\circ$  can be calculated from the intercept provided both are invariant over the temperature range studied. Through the variations in retention as a function of temperature, the stationary phase can be investigated.

Cole and Dorsey examined whether partitioning or adsorption was the mode of retention by calculating the  $\Delta H^\circ$  and  $\Delta S^\circ$  of transfer for benzene on columns of differing bonding densities ranging from 1.60 to 4.07  $\mu\text{mol}/\text{m}^2$ . It was found that as the bonding density increased the entropic contribution to retention became more important. This trend was concluded to support the partitioning model of retention. Further, the authors noted that at bonding densities at and

above  $2.84 \mu\text{mol}/\text{m}^2$  non-linear van't Hoff plots were obtained, corresponding to a phase transition [147].

Grushka and coworkers used van't Hoff plots to investigate the behavior of alkylbenzene homologs using three different mobile phases. As expected, for two of mobile phases studied,  $\Delta H^\circ$  became more negative with increasing alkyl chain length, corresponding to a more favorable retention process. In addition, by comparing the data for 9:1 methanol/water and 4:1 methanol/water mobile phase, the higher aqueous content mobile phase demonstrated more favorable retention, contributed to solvophobic interaction. Methylene selectivity was also found to decrease with increasing temperature. For the third mobile phase of pure methanol, no trend in  $\Delta H^\circ$  was reported, faulted to the difficulty in measuring  $t_0$ . This demonstrated the importance of measuring  $t_0$  accurately, as small changes dramatically altered the retention data. [148]

McCalley used van't Hoff plots to evaluate the effects of temperature on retention of basic compounds. For most compounds, van't Hoff plots show a positive slope and therefore  $\Delta H^\circ$  is negative over the temperature range studied. However, McCalley found that two compounds demonstrated a negative slope. Nortriptyline showed a negative slope at pH 7.0, but a slightly positive slope at pH 3.0 while pyridine showed a negative slope at pH 3.0 and a positive slope at pH 7.0. This anomalous result was attributed to the change in the  $\text{pK}_a$  of the base with temperature, and an increase in hydrophobic interaction relative to ion-exchange [46].

Vervoort and coworkers also investigated the retention of basic compounds by collecting thermodynamic data [149]. Over the temperature range studied, the authors did not report any deviation in linearity for the compounds studied. In addition, a positive slope was seen for nortriptyline, which contrasts the study by McCalley [46]. It was also found that the addition of the silanol blocking agent N, N-dimethyloctylamine (DMOA) produced a less negative  $\Delta H^\circ$  and  $\Delta S^\circ$  value for protonated basic compounds. This was interpreted to mean that retention of the compounds were less favorable due to blocking of the silanol sites and ion exclusion.

Additional van't Hoff studies include the studies of Philipsen *et al.* on the retention of polystyrene and polyester oligomers [150], the effect of mobile phase on the separation of enantiomers by Kazusaki *et al.* [151], and the investigation of Purcell *et al.* on secondary structure of peptides and interactions with hydrophobic surfaces [152]. Clearly, van't Hoff

analysis offers chromatographers an additional method of characterizing the stationary phase, as well as understanding the retention process.

### 3.2 Phase ratio

When using van't Hoff plots, the determination of the standard entropy of transfer of a retained solute from the mobile phase to the stationary phase is contingent on knowing the phase ratio. However, manufacturers do not determine the phase ratio as part of quality control; therefore its determination is not trivial. As mentioned previously, the volume phase ratio is defined as

$$\phi = \frac{V_s}{V_m} \quad \text{Equation 3-6}$$

There have been various methods utilized to determine the volume of the mobile phase which will be discussed in the next section. The definition of stationary phase volume is not as clear and is still subject to debate. Much of the debate arises from the fact that there is no distinct boundary between the stationary phase and mobile phase. Further, studies have shown that the bonded phase is preferentially solvated by the organic component of the mobile phase [153]. The assignment of this solvated layer to the stationary phase or mobile phase would change the calculated volume phase ratio. In addition, Alhedai and coworkers have argued that the mobile phase may consist of as many as four distinct regions, including stagnant and moving mobile phase regions [154]. The assignment of these stagnant regions confuses the issue more. This ambiguity has led to the several methods used to determine the volumes. The various method of determining the stationary phase volume is discussed in section 3.2.2.

### 3.2.1 Mobile phase volume

The lack of convention in defining  $V_m$  has resulted in the use of different methods in its determination. In addition to the ambiguity caused by the solvated organic layer, the vagueness arises from the porous nature of the support. Small solutes can access the pores while larger solutes cannot due to sterics. Knox and Kaliszan differentiated these regions as the kinetic dead volume and the thermodynamic dead volume [155]. The kinetic dead volume only included interparticle void while the thermodynamic dead volume includes the additional volume of mobile phase within the pores. Similarly, Alhedai and coworkers noted that the kinetic void volume only comprised of the moving portion of the mobile phase and was common to all solutes. However, the thermodynamic dead volume included the stagnant mobile phase within the pores and was unique to each solute [154]. Thus, depending on the method used, slightly different  $V_m$  are calculated. However, all measurements involve the determination of the void volume,  $V_0$ , which is taken to be  $V_m$ .

Pycnometry is the most often used static method, also known as the weight difference method. In this method, a column is equilibrated with a solvent and the mass is measured. Subsequently, the column is filled and equilibrated with a second solvent of differing density and the mass is again measured. The void volume is calculated as

$$V_0 = \frac{M_x - M_y}{\rho_x - \rho_y} \quad \text{Equation 3-7}$$

In equation 3-7,  $M$  represents the mass of the column filled with either solvent  $x$  or  $y$  and  $\rho$  represents the density of those solvents [156]. In general, this method gives the maximum possible value because it does not differentiate between the mobile phase within the pore and interparticle mobile phase. Typically, solvents with large differences in densities give the best results. Commonly used solvents include methanol, carbon tetrachloride, acetonitrile, and chloroform. However, Guiochon and coworkers did show that this method underestimated the true value, taken to be the difference between the volume of the empty column and the volume of

the packing. Further, the error was dependent on the carbon content of the bonded phase, with higher carbon content showing greater error [157].

Perhaps the most widely used method due to its ease of measurement is the use of an unretained, neutral solute. The difficulty lies in finding a solute that explores the mobile phase yet does not interact with the stationary phase. Various solutes have been used including thiourea, acetone, and uracil. Acetone has the advantage of being highly sensitive over a wide range of wavelengths [158]. However, a study by Nowotnik and Narra found that it showed slight retention and was deemed unsuitable [159]. The use of uracil is also very common and Bidlingmeyer found it less retained than acetone, thus more suitable [160].

Similar to the use of an unretained solute, the method of minor disturbance allows the determination of  $V_0$  in a fast and easy manner. This method involves injecting a mobile phase component or isotopically labeled mobile phase component that results in a disturbance in the baseline. In one technique, the retention volume of the minor disturbance is plotted against the mobile phase composition. The integral average of the minor disturbance peak is used to calculate  $V_0$  [161]. Another technique involves simply injecting a mobile phase component which should produce a disturbance peak. However, the choice of injection solvent should be judicious such that it is not bonded or solvated by the stationary phase. Most mobile phase contains some percentage of water, thus it is the most obvious choice. However it has been shown to produce multiple peaks [156, 162]. An initial peak corresponds to the elution of the water. A vacancy peak is observed next, resulting from the disturbance of the equilibrium between the bulk mobile phase and stationary phase. And lastly, a third peak is seen due to a slight excess of organic solvent immediately following the injected water. To avoid the issue of multiple peaks, the injection solvent composition should match the bulk mobile phase, but be isotopically labeled. The use of deuterated solvents is the most common type of solvent using this method [154, 156, 162]. The different refractive index of the deuterated solvent produces a minor disturbance in the baseline.

The determination of  $V_0$  can also be made by the use of an unretained salts such as  $\text{NaNO}_3$ ,  $\text{NaNO}_2$ ,  $\text{KBr}$ ,  $\text{KI}$ ,  $\text{NH}_4\text{NO}_3$  [163, 164]. The disadvantage of this method arises from the residual silanols on the silica support. Depending on mobile phase conditions, these silanols can possibly exclude charged ions from probing the pore volume. This electrostatic effect is known as Donnan exclusion. The use of buffers or large salt concentrations has been suggested as a

method of masking the silanols. Engelhardt and coworkers found that as the salt concentration increased, the elution time increased [162]. The authors also found that the sample size, mobile phase pH, and organic composition of the mobile phase affected the retention of the salt.

In the method of homologous series, a plot of retention versus homolog number produces a linear relationship. An extrapolation of the plot to the zeroth homolog is taken to be  $V_0$ . As with the use of any test solute, the selection of the homologs must be chosen carefully. First, the homologs must be soluble in the mobile phase. Also, a minimum of three homologs must be available in order to construct the plot. Obviously, the homologs must be detectable in the chromatographic system. Various homologs have been used including alcohols [164], alkylbenzene [160, 165], nitrosamine [165], and alkanes [166]. However, discontinuities in the plots have been observed when the length of the homolog exceeds the length of the bonded alkyl chain [166].

### 3.2.2 Stationary phase volume

The ambiguity in defining the volume of the mobile phase also necessitates an uncertainty in the determination of the volume of the stationary phase. If the solvated organic layer is assigned to  $V_s$ , the effective stationary phase volume that participates in the partition or adsorption process will certainly change along with  $\phi$ . Further, the type of bonded ligand, the bonding density, pore size, and surface area of the stationary phase all effect  $V_s$ . For proprietary reasons, column manufacturers do not always report this information. Thus, between the lack of information and the ambiguity in defining  $V_s$ , there is no consensus on how it is calculated. As a result, various approaches have been reported in the literature.

Guiochon defines that the stationary phase “as the fraction of the column that is not occupied by the mobile phase [167].” Based on this, the phase ratio is defined as

$$\phi = \frac{V_G - V_m}{V_m} \quad \text{Equation 3-8}$$

where  $V_G$  is the geometric volume of the empty column. The inaccuracy in using this definition is that the volume of the underlying silica support is included in  $V_s$ . Retention is an equilibrium process and therefore the phase ratio should only include the volume of stationary phase that participates in the equilibrium.

Sentell and Dorsey realized the fallacy in using the volume definition as stated by Guiochon [168]. As an alternative, the authors proposed a calculation based on the carbon load of the stationary phase and the mass of the packing contained within the column. From these values, the stationary phase volume can be calculated as

$$V_s = \frac{(\%C)(M)(W_p)}{(100)(12.011)(n_c)(\rho)} \quad \text{Equation 3-9}$$

In equation 3-9,  $\%C$  is the percent carbon,  $M$  is the molecular weight of the bonded phase in g/mole,  $W_p$  is the mass of packing material contained within the column in grams,  $n_c$  is the number of carbon atoms per mole silane, and  $\rho$  is the density of the ligand in  $\text{g/cm}^3$ . The percent carbon is the grams of carbon per 100 grams of bonded silica and can be determined from elemental analysis or gravimetric analysis. Essentially, this calculates the spatial volume occupied by the ligand in units of  $\text{cm}^3$ .

Chan and coworkers defined the stationary phase as the total pore volume while differentiating the mobile phase as the interparticle volume [170]. Using excess adsorption isotherms, the authors investigated the extent of organic solvent accumulated on the stationary phase surface. It was found that acetonitrile occupied up to 60% of the pore volume while methanol occupied up to 12%. Based on the interaction of solute with this adsorbed layer, along with the fact that solutes within the pores were effected by this layer; the authors proposed defining the stationary phase as the pore volume. This definition also implies that the stationary phase volume is dependent on the mobile phase composition.



### 3.3 Research goals

Despite the lack of consensus in defining the mobile and stationary phase volumes, thus the inability to determine  $\Delta S^\circ$ , van't Hoff analysis still proves to be useful. Occasionally,  $\frac{\Delta S^\circ}{R} + \ln \phi$  is reported to avoid the issue of  $\phi$  and as long as  $\phi$  remains constant over the temperature range studied, general trends in  $\Delta S^\circ$  can be analyzed [149]. However, there have been reports in the literature where van't Hoff plots are not linear [171, 172, 173]. Typically these non-linear plots are attributed to changes in retention mechanism, i.e., changes in  $\Delta H^\circ$  and/or  $\Delta S^\circ$ , with changes in temperature.

Chester and Coym have argued the possibility that changes in the phase ratio result in non-linear van't Hoff plot [174]. Using data from Cole *et al.* [171], the authors manipulated the results such that the phase ratio was allowed to change as a function of temperature while keeping  $\Delta H^\circ$  and  $\Delta S^\circ$  fixed. The calculated hypothetical phase ratio as a function of temperature is shown in Figure 3-1.

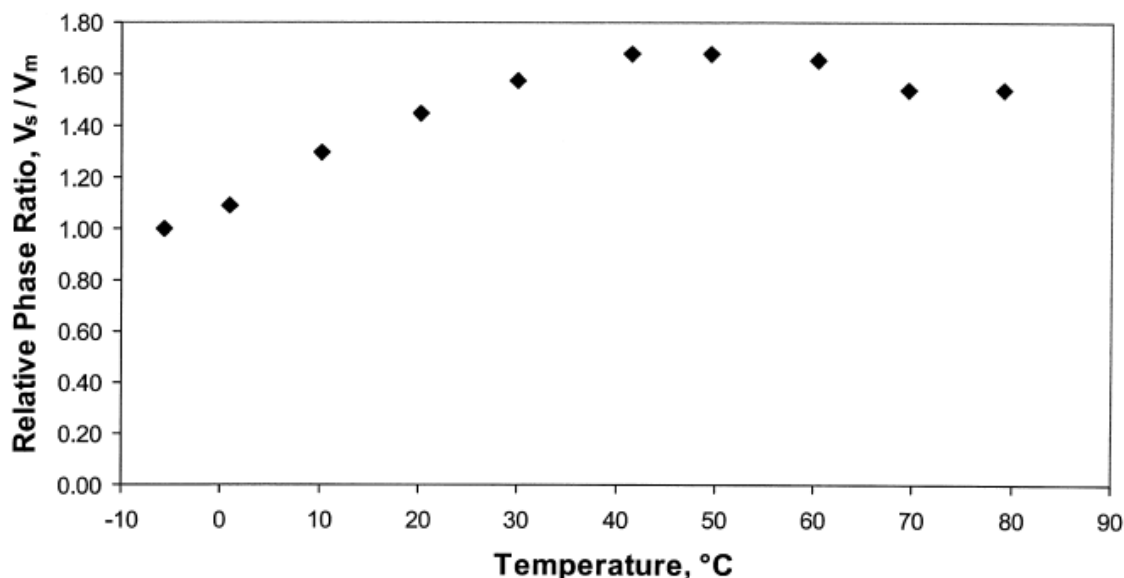


Figure 3-1. The hypothetical change in the phase ratio as a function of temperature when  $\Delta H^\circ$  and  $\Delta S^\circ$  are constant [174].

As seen, the relative phase ratio varied from approximately 1.00 at the low temperature to a maximum value of about 1.70 at intermediate temperatures. This represents a variation in  $\phi$  of approximately 70%. It was suggested that to avoid the assumption of a constant phase ratio, thermodynamic data for solutes that differ by a molecular moiety be reported. For example, the enthalpy of transfer for a methylene group,  $\Delta\Delta H^\circ$ , can be determined by plotting van't Hoff plots for two solutes that differ by a methylene group. The difference in these plots represents a methylene selectivity plot. Mathematically, this is represented by

$$\begin{aligned} \ln \alpha_{CH_2} &= \ln k_{i+1} - \ln k_i \\ &= \frac{(-\Delta H_{i+1}^\circ + \Delta H_i^\circ)}{RT} + \frac{(\Delta S_{i+1}^\circ - \Delta S_i^\circ)}{R} \end{aligned} \quad \text{Equation 3-10}$$

where  $i + 1$  and  $i$  represent the solutes that differ by a moiety to be investigated. The absence of  $\phi$  in equation 3-10 results from the assumption that changes in the phase ratio due to temperature should be observed by both solutes, thus cancel out. The slope of the difference plot would equal  $\frac{-\Delta\Delta H^\circ}{RT}$  and the intercept strictly represents  $\frac{\Delta\Delta S^\circ}{R}$ .

Obviously, the implication of a changing phase ratio would alter the interpretation of van't Hoff plots. So this begs the question of whether non-linear van't Hoff plots are a result of changes in  $\phi$  or changes in retention mechanism [175]. The observed parabolic van't Hoff plot for benzene reported by Cole and coworkers has been attribute to a well characterized phenomenon known as the hydrophobic effect rather than a change in the phase ratio. This explanation for the van't Hoff plot is corroborate by the observed maximum retention of benzene corresponding to a minimum in the solubility of benzene in water at nearly the same temperature [176]. The hydrophobic effect arises from the strong attractive forces between water molecules. The presence of a non-polar solute within the mobile phase disrupts this network resulting in a decrease in entropy. This aversion towards non-polar solute results in a favorable entropic change when the solute is transferred into the stationary phase [177, 178].

Sentell and Henderson also noted non-linear van't Hoff plots while investigating the effects of temperature on the selectivity of polycyclic aromatic hydrocarbons. Using a high density monomeric column, the authors noted a curvature in the van't Hoff plots at around 25°C, which

was not seen in the low density column. This anomaly was attributed to a phase transition in the stationary phase in which the ligand changed from a crystalline-like state to a liquid like state. At lower temperatures, the ligand is more rod-like and extended. The shape selectivity of the high bonding density column supported this theory [179].

Using a hybrid C<sub>18</sub> column, Liu and coworkers obtained an unusual van't Hoff plot studied over a wider temperature range, 30°C to 200°C. For toluene, the authors observed two linear regions disjointed at around 97°C. Like Sentell and Henderson, this was attributed to a change in the stationary phase conformation. Differential scanning calorimetry (DSC) experiments showed an abrupt transition around 97°C. This correlated to the temperature at which a change in slope of the van't Hoff plot was observed [180]. The study also demonstrated that the observed van't Hoff plots may be linear if the temperature range is not large enough.

The concept of a changing phase ratio was also discussed by Bidlingmeyer and Henderson. In the investigation of retention of basic compounds using bare silica stationary phase, the authors observed non-linear van't Hoff plots for all four analytes studied using a 70/30 methanol/water mobile phase. Since bare silica was used, the observed van't Hoff plot could not be explained by a phase transition or a change in the phase ratio. Two possible explanations were proposed for the curvature seen in the plots. The first hypothesis was that a relative change in adsorptive force to electrostatic resulted in a change in the retention mechanism. Secondly, the increase in temperature changed the amount of adsorbed mobile phase on the silica surface. Of course, it is also possible that a combination of these two affected the observed plots [181].

Obviously, the occurrence on non-linear van't Hoff plot is not an anomaly. The issue lies in the rationale of such observation. If Chester and Coym are correct in suggesting that such curvature is a result of changes in the phase ratio, then the utility of these analyses have been diminished. Non-linear plots could be attributed to changes in  $\Delta H^\circ$ ,  $\Delta S^\circ$ ,  $\phi$ , or a combination of the three. As a result, the deconvolution of contributing changes would be impossible. In addition, if  $\phi$  is found to vary with temperature, previous interpretation of van't Hoff plots would have to be revisited. However, if the phase ratio were constant, then non-linear van't Hoff plots would be due to changes in the thermodynamics of retention. In this case,  $\Delta H^\circ$  could still be derived from the differential of the plot of  $\ln k'$  versus  $1/T$ . The determination of  $\phi$  is not

practical until a clear definition of the two phases is agreed upon. But rather the goal of this portion is to determine whether the phase ratio changes with temperature.

## CHAPTER FOUR

### POLAR-EMBEDDED COLUMNS

#### 4.1 Introduction

The analysis of basic compounds has been a concern for chromatographers because of poor peak shape and low efficiencies often seen with such compounds. Conventional thought has attributed the poor chromatography on silanols, though more recent research has shown that the fundamental reasons are more complex. Regardless of the reasons, the development of new stationary phases has attempted to improve the chromatography when basic analytes are present.

One such stationary phase utilizes a polar-embedded group. These stationary phases differ physically from conventional bonded phases in that they incorporate a polar group within the alkyl chain. The limited reports available have shown that these columns do offer unique selectivity and improved column performance for certain compounds. However, because these phases are relatively new, the characterizations of these columns are still ongoing. The evaluation of these columns can offer insight into the retention process. In addition, column comparisons allow for the selection of columns to incorporate into method development or as a replacement when conventional columns fail to provide a given separation.

The following studies evaluate the character of seven polar-embedded columns and one conventional alkyl column. Selectivity studies, using a mixture of acids, bases and neutral compounds, provide information on the uniqueness of these columns and highlight distinct differences between the columns. Next, van't Hoff studies offer insight into the thermodynamics of retention and retention mechanisms. In addition, the use of homologous analyte pairs allow for the determination of methylene selectivity. Lastly, log-log selectivity plots provide direct column comparisons.

## 4.2 Instrumentation

Experiments for the evaluation of polar-embedded columns were performed on a Hewlett-Packard 1100 liquid chromatography system (Agilent Technologies, Palo Alto, CA) equipped with a vacuum degasser, binary pump, autosampler, and variable wavelength detector. Data collection was performed using Chemstation (Agilent Technologies, Palo Alto, CA). Column temperature was maintained using a water jacket connected to a circulator bath.

## 4.3 Columns

Columns used for the selectivity studies and retention studies are shown in Table 4-1.

Table 4-1. Columns and their physical properties.

Column	Manufacturer	Dimension (mm)	s.p. diameter	Pore (Å)	Surface Area (m <sup>2</sup> /g)	Carbon Load	End capped?	Polar Embedded Group
Synergi Fusion RP, C18	Phenomenex	4.6 x 75	4 µm	80	475	Unknown	Yes	Unknown
Synergi Max C12	Phenomenex	4.6 x 75	4 µm	80	475	17%	Yes	N/A
Polaris C8-Ether	Varian	4.6 x 75	3 µm	180	Unknown	Unknown	Unknown	Ether
Polaris C8-A	Varian	4.6 x 75	3 µm	Unknown	Unknown	Unknown	Unknown	Unknown
Symmetry Shield C8	Waters	4.6 x 75	3.5 µm	100	Unknown	15%	Yes	Carbamate
Zorbax Bonus RP C14	Agilent	4.6 x 75	5 µm	100	160	9.5%	Yes	Amide
Discovery Amide C16	Supelco	4.6 x 150	5 µm	180	200	11%	Yes	Amide
Dionex Acclaim PA, C16	Dionex	4.6 x 50	5 µm	120-140	290-320	16.6%	Unknown	Sulfonamide

Column manufacturers included Phenomenex (Torrance, CA), Varian (Palo Alto, CA), Waters (Milford, MA), Agilent (Wilmington, DE), Supelco (Bellefonte, PA), and Dionex (Sunnyvale, CA). Information labeled “unknown” in Table 4-1 was not available from the manufacturer. The Synergi Max is not a polar-embedded column, thus is labeled as N/A in the last column listing the polar-embedded group

#### 4.4 Experimental

HPLC grade acetonitrile was obtained from EMD Chemical Inc (Gibbstown, NJ). Water for the preparation of buffers was deionized and filtered through a Millipore Milli-Q water purification system (Bedford, MA). All analytes were prepared in the same composition as the mobile phase and injected in triplicate. Test analytes were obtained from Sigma-Aldrich Corp. (St. Louis, MO) or Mallinckrodt Baker (Phillipsburg, NJ).

*Selectivity studies* – Test mixture 1 consisted of thiourea, amitriptyline, 4-*n*-butylbenzoic acid, benzonitrile, and *trans*-chalcone. Test mixture 2 consisted of thiourea, N, N-diethylacetamide, ethylbenzene, acetophenone, and anisole. All analytes were prepared at a concentration of 0.05 mg/mL and injected individually as well as in a mixture with an injection volume of 5  $\mu$ L. For the low pH studies, the mobile phase was 50/50 ACN/30 mM phosphate buffer, pH 3.0. For the intermediate pH studies, the mobile phase was 50/50 ACN/60 mM phosphate buffer, pH 7.0. Columns were maintained at 35°C and equilibrated for at least an hour prior to injection. A flow rate of 1.0 mL/min was used except with the Discovery Amide column, in which a flow rate of 2.0 mL/min was used. The detection wavelength was 205 nm.

*van't Hoff studies* – Analytes used in this portion of the study were 4-*n*-propylbenzoic acid, 4-*n*-butylbenzoic acid, toluene, ethylbenzene, benzonitrile, phenylacetone, 4-pentylaniline, and 4-hexylaniline with thiourea used as the void volume marker. These were prepared at a concentration of 0.05 mg/mL and the injection volume was 5  $\mu$ L. The mobile consisted of a 50/50 ACN/10 mM phosphate buffer, pH 3.0. Retention times were measured for 5°C to 55°C at 10°C increments. The column was allowed to equilibrate at temperature for a minimum of 1 hour before injections. A flow rate of 1.0 mL/min was used except for the Discovery Amide column, in which a flow rate of 2.0 mL/min was used. Data were collected at a wavelength of

205 nm. For the higher temperature van't Hoff studies on the Zorbax Bonus RP column, the same conditions were used except the temperature range. Retention times were measured for 5°C to 85°C at 5°C increments. Only 4-pentylaniline and 4-hexylaniline were injected, both in triplicate with thiourea as the void volume marker.

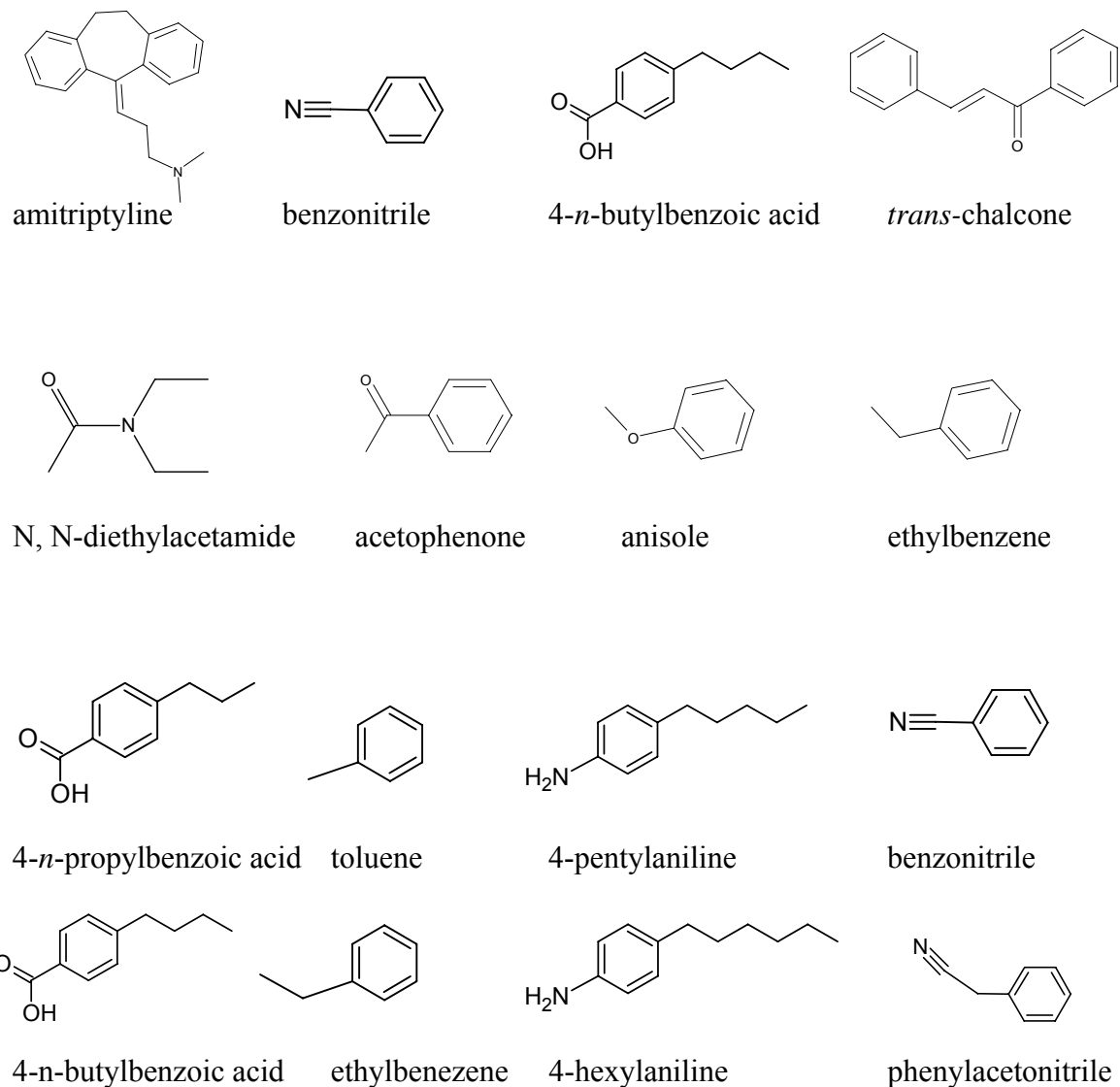


Figure 4-1. Analytes used for selectivity and retention studies.



## 4.5 Results and discussion

### 4.5.1 Selectivity studies

Analytes in mixture 1 and mixture 2 were chosen from ref [182] so that different solute-stationary phase interactions were probed. Chromatograms for mixture 1 at pH 3.0 are shown in Figure 4-2. *Trans*-chalcone demonstrated dual peaks possibly due to impurities. For six of the eight columns, the elution order was amytriptyline, benzonitrile, 4-*n*-butylbenzoic acid, and *trans*-chalcone. Only the Discover Amide and the Zorbax Bonus RP columns demonstrated differences in elution order. On the Discovery Amide column, 4-*n*-butylbenzoic acid eluted between the two *trans*-chalcone peaks, while on the Zorbax Bonus RP column it eluted last. Though both of these columns are known to contain an amide polar group, the selectivity and peak shape of 4-*n*-butylbenzoic acid on these columns are quite different. The amide group, with a  $pK_a$  of around 10, is protonated at the mobile phase pH of 3.0. Therefore, hydrogen bonding between the carboxylate group of 4-*n*-butylbenzoic acid with the protonated amide results in a difference in selectivity. In addition, 4-*n*-butylbenzoic acid showed significant tailing on the Zorbax Bonus RP column with a B/A asymmetry factor of 7.1 measured at 10% of peak height. In comparison, the tailing factor on the Discovery Amide column was 1.1. This difference in tailing can partly attributed to the manufacturing process. In the bonding reaction of the chromatographic phase to the support, a one or two-step bonding reaction can be utilized. If a two-step synthesis is employed, an aminopropylsilane group is first bonded to the silica support followed by acylation of a lipophilic ligand. Incomplete reaction in the second step would result in a stationary phase consisting of unreacted amino groups in addition to the polar-embedded amide groups [183]. At low pH, these sites are protonated and serve as ion exchange sites, which lead to the observed tailing. The marked tailing for acids resulting from a positively charged column was also observed by Wilson and coworkers [182]. Not only does this reduce efficiency, but O’Gara *et al.* also demonstrated that a single step synthesis was preferable in terms of reproducibility and more homogeneous silica surface [184].

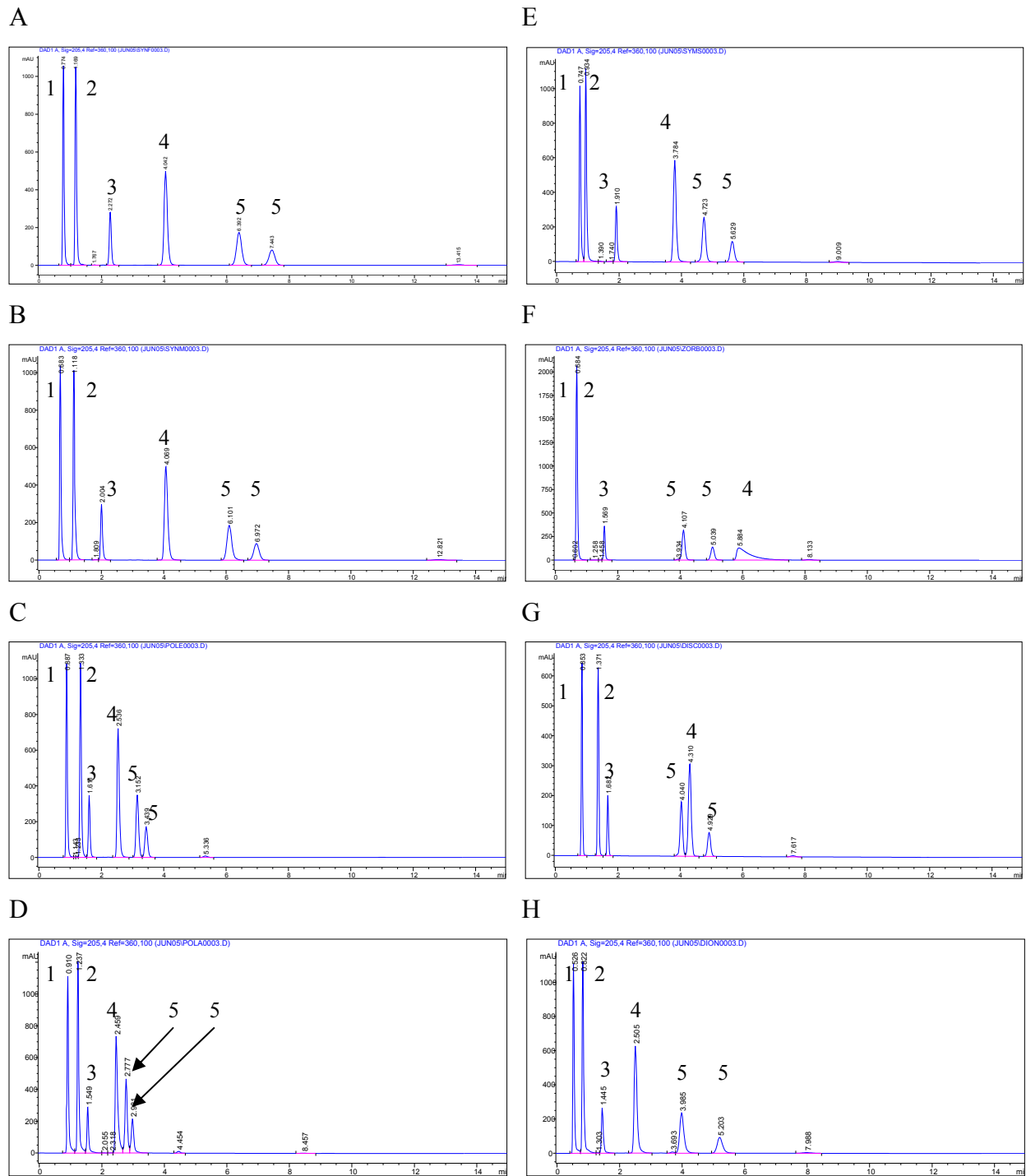


Figure 4-2. Chromatograms for test mixture 1, pH 3.0. Columns are A. Synergi Fusion RP; B. Synergi Max; C. Polaris C8-Ether; D. Polaris C8-A; E. Symmetry Shield; F. Zorbax Bonus RP; G. Discovery Amide; H. Dionex Acclaim. Test mixture 1: 1. thiourea, 2. amitriptyline, 3. benzonitrile, 4. 4-*n*-butylbenzoic acid, 5. *trans*-chalcone.

Amitriptyline, with a  $pK_a$  of 9.4, was chosen to gauge silanophilic interactions and column performance with basic compounds. For this particular base, the polar-embedded columns did show improved peak shape when compared to a conventional column at low pH. The asymmetry factor for this analyte on the Synergi Max column, which lacks a polar-embedded group, was 1.7, the largest for the eight columns. On the Zorbax Bonus RP column, amitriptyline, with a retention factor of 0.136, co-eluted with the void marker (Figure 4-2F). Again, this can be explained by the residual amines resulting from the two-step manufacturing process. At low pH, the amines and amides of the stationary phase, as well as amitriptyline, are positively charged. This electrostatic repulsion results in decreased retention.

Figure 4-3 shows the chromatograms for mixture 1 at pH 7.0. At this pH, many of the residual silanols are in ionized form ( $Si-O^-$ ), thus ion-exchange mechanisms become important for charged analytes. This can result in changes in elution order for these analytes as well as asymmetric peaks. As seen in the chromatograms, 4-*n*-butylbenzoic acid is less retained at this pH, eluting second on all the columns, often with a retention factor  $< 1.0$ . With a  $pK_a$  of 4.2, it is mostly ionized at pH 7.0 and anionic exclusion by the ionized silanols resulted in decreased retention. For amitriptyline, cation exchange and hydrogen bonding become important mechanisms in retention. The protonated amitriptyline interacts with the ionized silanols resulting in longer retention times as well as increased peak tailing. When compared to the pH 3.0 studies, the B/A tailing factor for amitriptyline increased for all of the columns. Improved peak shape for basic analytes at lower pH has been reported by others and is generally attributed to the suppression of silanol ionization [185-187]. However, the improvement in peak shape at lower pH cannot be generalized for all analytes. Four of the columns showed slightly lower asymmetry factors for 4-*n*-butylbenzoic acid at pH 7.0 compared to pH 3.0.

At pH 7.0, amitriptyline demonstrated significant tailing on the Synergi Fusion RP column. Unfortunately, the polar-embedded group for this column was not disclosed by the manufacturer, but the presence of a mixed-mode mechanism of retention is possibly responsible. In contrast, the two neutral analytes, benzonitrile and *trans*-chalcone, did not demonstrate any significant change in selectivity or efficiency at this higher pH on all of the columns. This is not surprising since the dominant retention mechanism for these analytes is hydrophobic interaction and changing the pH would not affect neutral analytes as much.

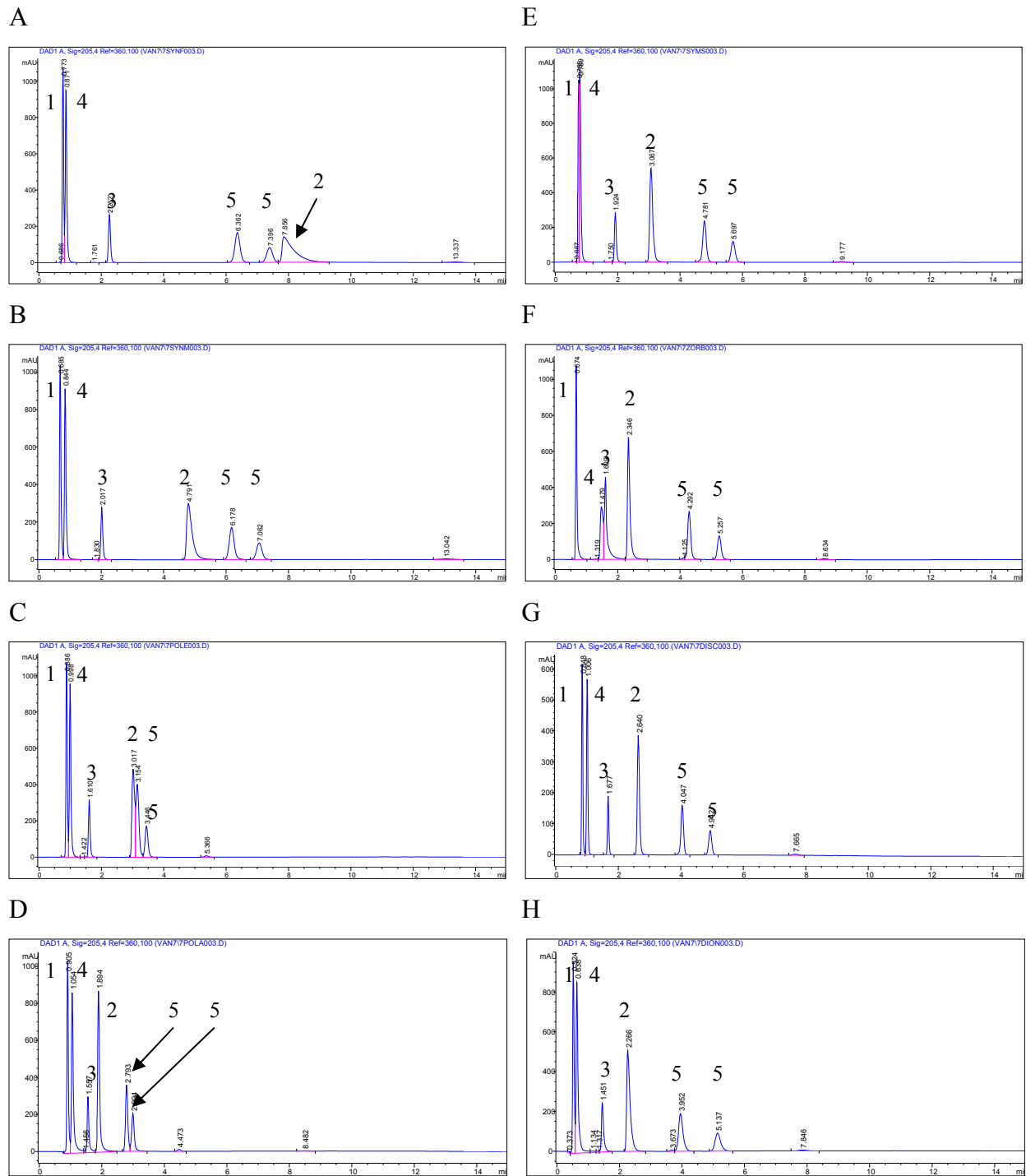


Figure 4-3. Chromatograms for test mixture 1, pH 7.0. Columns are A. Synergi Fusion RP; B. Synergi Max; C. Polaris C8-Ether; D. Polaris C8-A; E. Symmetry Shield; F. Zorbax Bonus RP; G. Discovery Amide; H. Dionex Acclaim. Test mixture 1: 1. thiourea, 2. amitriptyline, 3. benzonitrile, 4. 4-*n*-butylbenzoic acid, 5. *trans*-chalcone.

For mixture 2, all eight columns showed very similar selectivity and good peak shape. The elution order for the mixture was the same in both the pH 3.0 and pH 7.0 mobile phase. N, N-diethylacetamide eluted first, followed by acetophenone, anisole, and then ethylbenzene. Table 4-2 shows the selectivity values for adjacent peaks. That is, the value labeled peak 3/2 is the ratio of retention factor for acetophenone to N, N-diethylacetamide; the third and second eluting analytes, respectively. As shown in the table, for most of the analyte pairs, the selectivity values at pH 3.0 did not vary drastically. For example, for peak 4/3, the selectivity values ranged from 1.62 to 1.88. Moreover, the selectivity values at pH 3.0 only varied slightly when compared to the selectivity value for the same analyte pair at pH 7.0.

Table 4-2. Selectivity data for adjacent peaks in mixture 2.

pH 3.0	Synergi Fusion RP	Synergi Max	Polaris C8-Ether	Polaris C8-A	Symmetry Shield	Zorbax Bonus RP	Discovery Amide	Dionex Acclaim PA
	peak 3/2	4.24	4.46	3.54	3.86	5.00	4.82	4.74
peak 4/3	1.73	1.88	1.64	1.62	1.70	1.68	1.75	1.81
peak 5/4	2.46	2.81	2.25	1.75	2.28	2.46	2.53	2.40
pH 7.0	Synergi Fusion RP	Synergi Max	Polaris C8-Ether	Polaris C8-A	Symmetry Shield	Zorbax Bonus RP	Discovery Amide	Dionex Acclaim PA
	peak 3/2	4.18	4.47	3.51	3.74	4.86	4.76	4.68
peak 4/3	1.73	1.88	1.64	1.61	1.69	1.68	1.75	1.80
peak 5/4	2.46	2.82	2.25	2.10	2.28	2.45	2.53	2.38

The identification of similar columns can be useful in method development or routine analysis. During the course of analyses, column degradation may require an equivalent column be substituted if the original is not available or discontinued by the manufacturer. Conversely, in method development, recognizing similar columns would aid in choosing columns of differing character. One method of comparing two columns is through log-log plots. The selectivity values for a series of analytes on one column are plotted against their selectivity values for a second column. Selectivity values are plotted as opposed to retention times because, for an isocratic separation, selectivity is independent of flow rate. Thus adjusting the flow rate for a column can match the retention time for a second column without effecting selectivity. Figure 4-

4 shows four columns comparisons at pH 3.0. All the analyte selectivity values were measured against ethylbenzene. The more linear the log–log plot, the more similar the retention mechanism is between the two columns. A correlation coefficient,  $R^2$ , for perfectly matching columns would be 1.0. Of course this is never exactly the case except for the possibility of identical columns from the same production batch. As seen in Figure 4-4, the Synergi Max and Synergi Fusion RP show very similar selectivity for these analytes. This is unusual since the Synergi Max column is a traditional  $C_{12}$  bonded phase, while the Synergi Fusion RP column is polar-embedded bonded phase. However, both these columns are manufactured by Phenomenex and most likely use similar silica support (see Table 4-1). It is known that the character of silica support can affect the overall stationary phase property, thus similar supports would show more similar retention behavior.

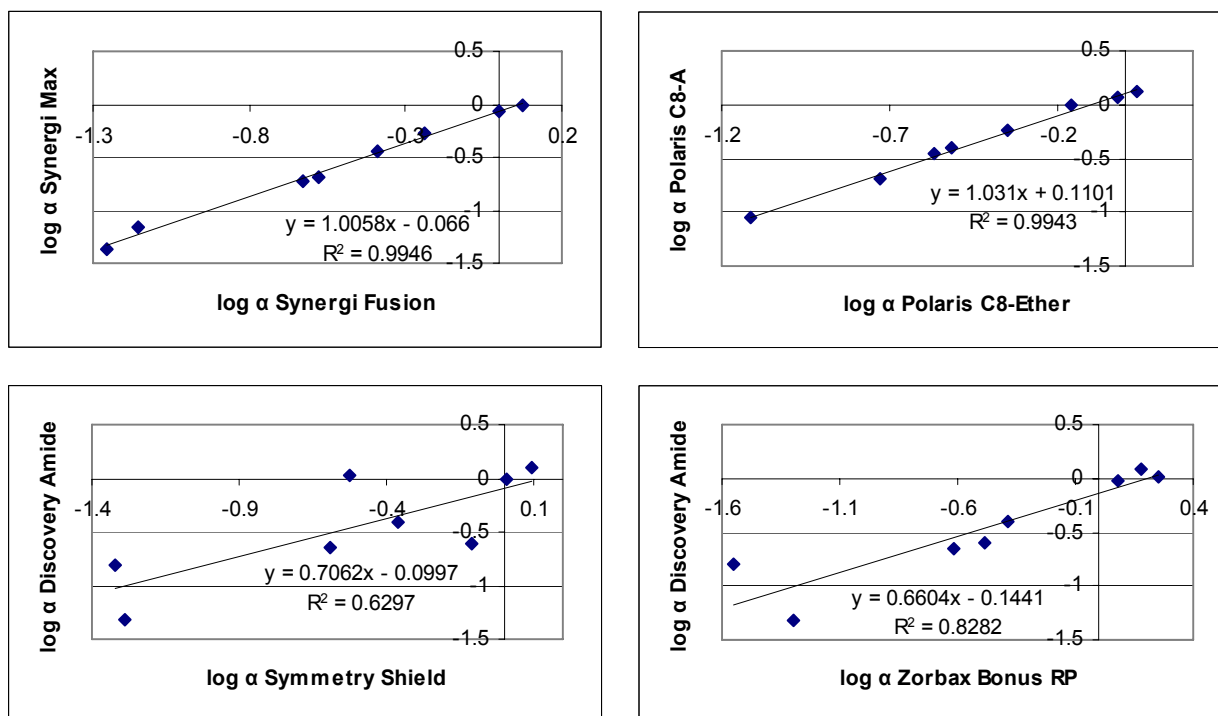


Figure 4-4. Log–log plots for selectivity values at pH 3.0. Reference analyte was ethylbenzene.

The Polaris C8-A and Polaris C8-Ether columns also show similar selectivity. Though the polar group of the Polaris C8-A column is unknown, both columns are manufactured by Varian. Again, the use of similar silica supports may result in similar chromatographic properties. In contrast, the log–log plot for the Discovery Amide and Zorbax Bonus RP column corroborate differences seen in the chromatograms, especially for 4-*n*-butylbenzoic acid. The low  $R^2$  value of 0.828 indicated poor correlation even though both incorporate an amide group. Comparison of the Discovery Amide and Symmetry Shield columns demonstrated the lowest correlation.

Figure 4-5 shows the log–log plot for the same four sets of columns but for selectivity values at pH 7.0. Similar to the pH 3.0 selectivity plots, the Synergi Max and Synergi Fusion RP as well as the Polaris C8-A and Polaris C8-Ether columns showed good correlation; however, the correlation factor did decrease slightly. This was also the case for the Discovery Amide and Zorbax Bonus RP columns, but to a larger extent. However, the Discovery Amide and Symmetry Shield showed improved correlation at pH 7.0 compared to pH 3.0.

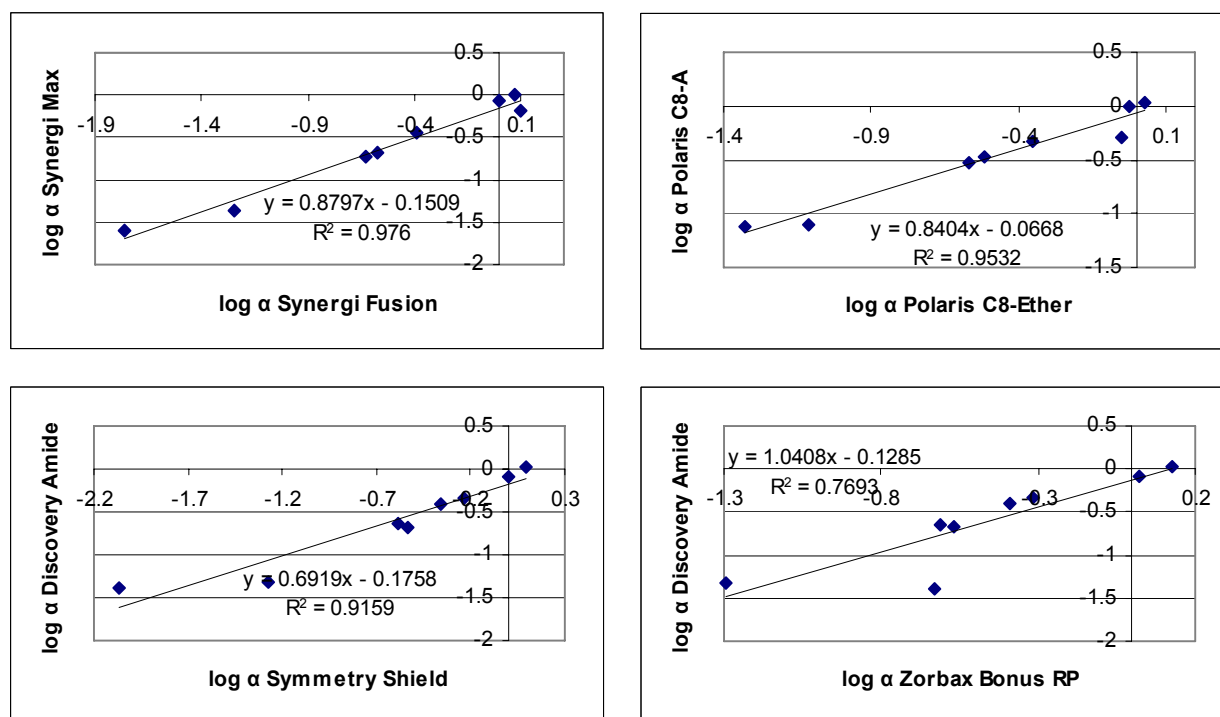


Figure 4-5. Log–log plots for selectivity values at pH 7.0. Reference analyte was ethylbenzene.

#### 4.5.2 van't Hoff studies

Though selectivity studies can illuminate fundamental differences between columns, van't Hoff studies provide thermodynamic information related to the retention process. A plot of  $\ln k'$  vs  $1/T$  typically produces a linear relationship. The slope of that plot is related to the enthalpy of transfer of the solute from the mobile phase to the stationary phase. The intercept is related to the entropy of transfer and the phase ratio. Unfortunately, the phase ratio is often not known, partly due to the ambiguity in its definition, and therefore the entropy of transfer cannot be determined. However, assuming the phase ratio remains constant over the temperature range being studied, reporting  $\Delta S^\circ/R + \ln \phi$  for homologous analytes can provide trends related to the entropy of transfer.

Of the eight columns used in the selectivity studies, four were chosen based on their unique behavior to further investigate using van't Hoff analysis. The four columns were the Zorbax Bonus RP, Discover Amide, Synergi Fusion RP, and the Symmetry Shield. All retention times were reproducible with relative standard deviations of 0.004 or less. Again, the Zorbax Bonus RP and Discovery Amide columns both contain an amide polar-embedded group. This allows the direct comparison of similar functionalities, but from different manufacturers (and apparently different manufacturing processes). The Symmetry Shield contains a carbamate functionality, while the polar-embedded group of the Synergi Fusion RP is unknown.

The pairs of analyte chosen for use in this study were a homologous series that differ by a methylene group ( $\text{CH}_2$ ). The four sets of analytes also represented different functional classes of compounds, acids, anilines, nitriles, and neutral, non-polar aromatics. van't Hoff analysis was performed to elucidate standard molar enthalpy of transfer. Since the phase ratios are not known for these columns, only trends in the molar entropy of transfer will be discussed. However, by choosing homologous analytes that differ by a methylene group, the methylene selectivity of the columns can be evaluated. Methylene selectivity is the ease in which a stationary phase can differentiate two solutes that differ by a methylene group. Reporting the enthalpy and entropy of transfer of a methylene group,  $\Delta\Delta H_{\text{CH}_2}^\circ$  and  $\Delta\Delta S_{\text{CH}_2}^\circ$ , avoids the issue of the phase ratio because both analyte should experience similar phase ratios at a given temperature, and thus the selectivity values are independent of the phase ratio.



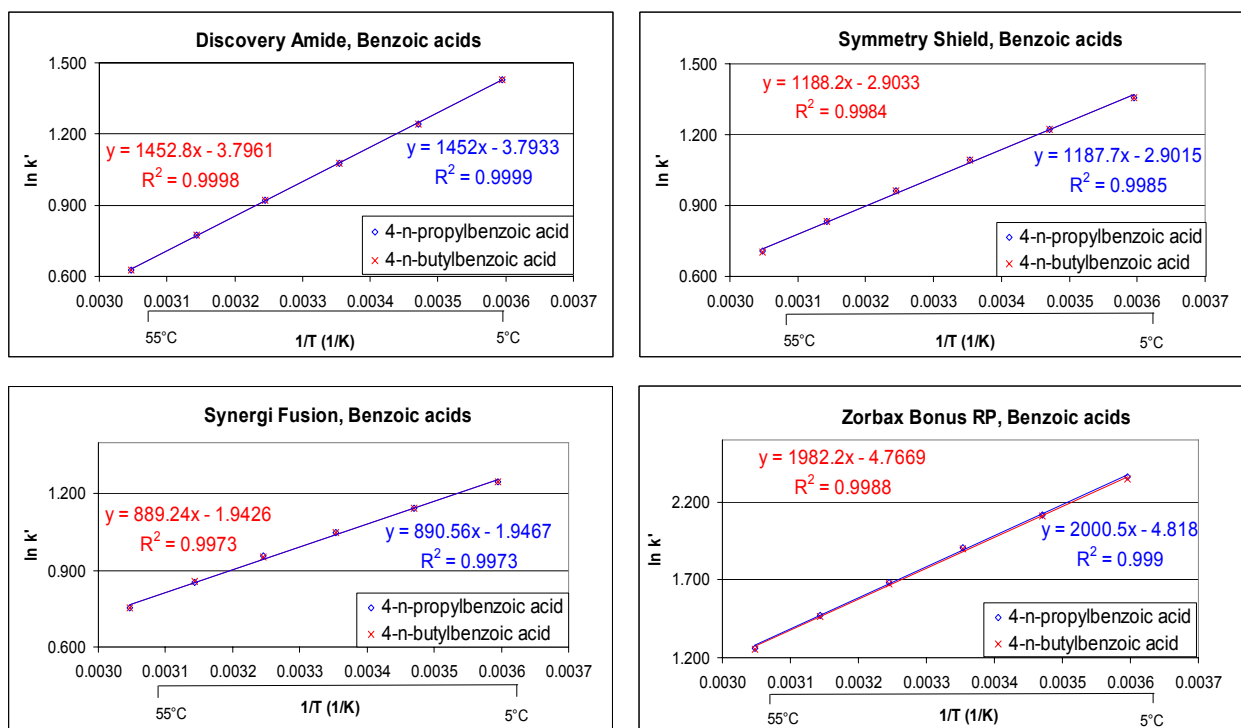


Figure 4-6. van't Hoff plots for 4-*n*-propylbenzoic acid and 4-*n*-butylbenzoic acid. Mobile phase: 50/50 ACN/10 mM phosphate buffer, pH 3.0.

Figure 4-6 shows the van't Hoff plots of 4-*n*-propylbenzoic acid and 4-*n*-butylbenzoic acids on the four columns over the temperature range 5°C to 55°C. Though it is difficult to see due to the overlap of the lines, each plot contains two linear regressions plots; one for each analyte. All eight regressions showed great linearity with  $R^2 > 0.997$ . For all the van't Hoff plots in this section, the homolog with the lower carbon number will be noted in the plots in blue, and the higher carbon containing homolog in red. The linearity of these plots is taken to indicate that no change in retention mechanism occurred over the temperature range studied. The extensive overlap in the plots of 4-*n*-propylbenzoic acid and 4-*n*-butylbenzoic acids revealed that all four columns showed poor methylene selectivity. That is, separation of this analyte pair would be difficult on these four columns using the 50/50 ACN/10 mM phosphate buffer, pH 3.0 mobile phase. The more separated the van't Hoff plots, the greater the ability of the column to differentiate a methylene group. One possible interpretation of this overlap is that the methylene group is not partitioned into or adsorbed onto the stationary phase. At pH 3.0, the polar-

embedded carbamate group and amide group are protonated and the benzoic acids are partially ionized. If the carboxylic acid portion of the analytes are preferentially interacting through ion-pairing or hydrogen bonding, then the orientation of the solute may limit the propyl and butyl structural moiety, which are directly opposite of the carboxylic acid functional site, from partitioning fully into the stationary phase. Insight into this hypothesis may be provided by using *ortho*- and *meta*- isomers, in which the alkyl moiety is structurally closer to the carboxylic acid functionality, thus can interact more with the bonded phase.

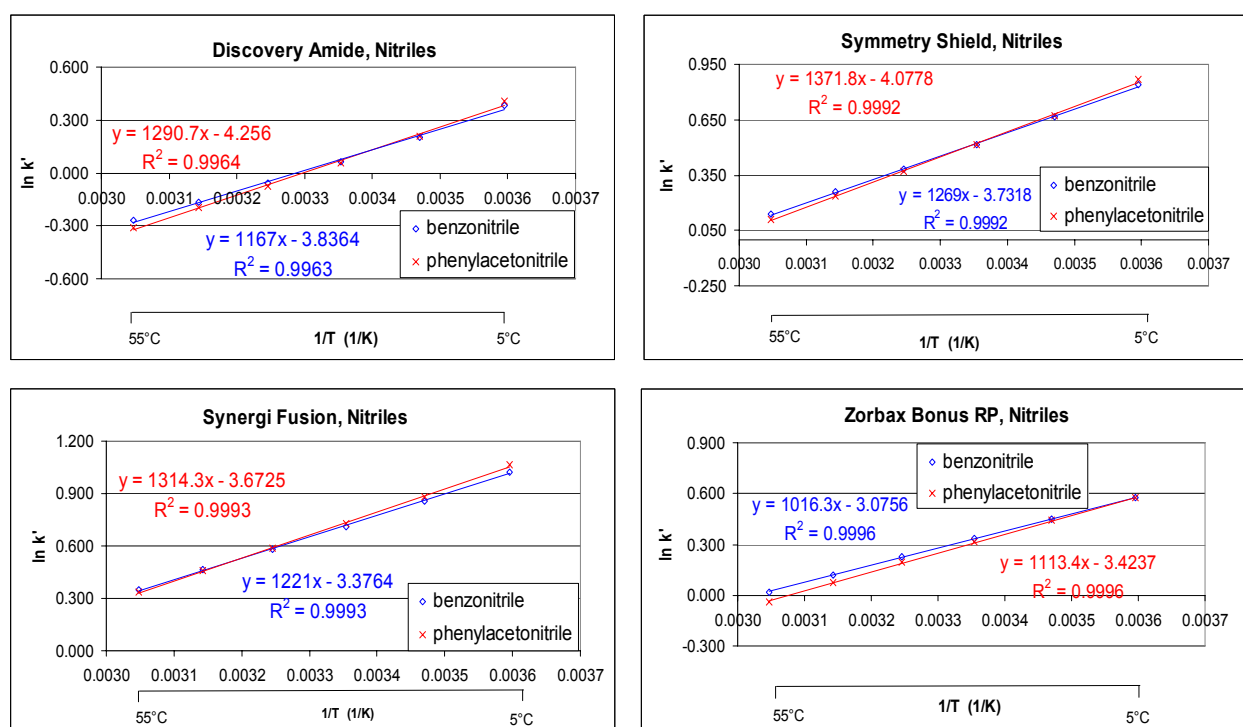


Figure 4-7. van't Hoff plots for benzonitrile and phenylacetonitrile. Mobile phase: 50/50 ACN/10 mM phosphate buffer, pH 3.0.

van't Hoff plots for benzonitrile and phenylacetonitrile are shown in Figure 4-7. All four plots for the nitrile homologs showed good linearity with  $R^2 > 0.996$ . With respect to these analytes, the columns showed nominal methylene selectivity at most temperatures. Interestingly, there is a reversal of elution order illustrated by the crossing of the van't Hoff plots. Others have

reported such temperature dependent selectivity, mainly with ionizable solutes [188, 189]. Such changes are attributed to variations in the extent of ionization or dissociation of the analytes with temperature [190].

Comparison of the columns using neutral, non-polar probes are shown in Figure 4-8. The van't Hoff plots of toluene and ethylbenzene all had linear correlation with  $R^2 > 0.986$ . In comparison to the methylene selectivity for benzoic acid homologs, all four columns show great methylene selectivity with respect to non-polar benzene homologs. It should be noted that a close inspection of the toluene plots for the Discovery Amide and Zorbax Bonus RP columns shows slight curvature, thus resulting in a lower linear correlation value. It is possible that the temperature range is not large enough to reveal non-linearity. Depending on the temperatures being studied, van't Hoff plots may appear linear over a small range, yet overall demonstrate non-linear behavior over a broader temperature range [180].

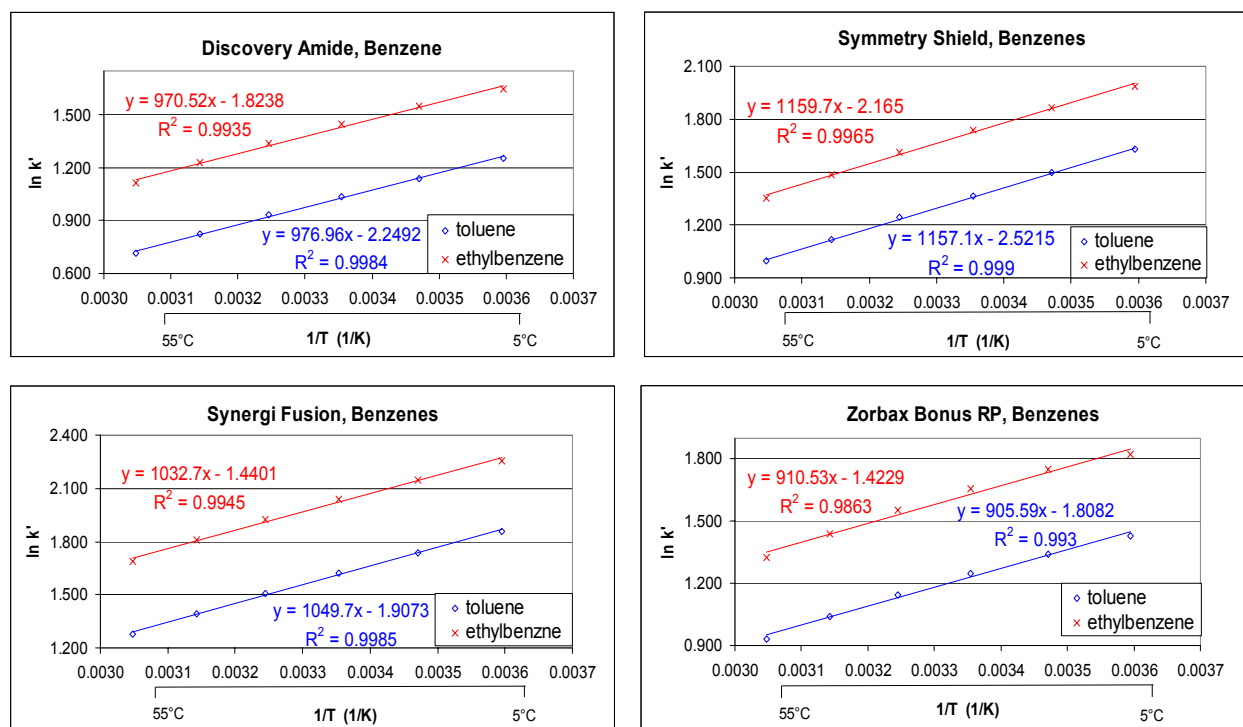


Figure 4-8. van't Hoff plots for toluene and ethylbenzene. Mobile phase: 50/50 ACN/10 mM phosphate buffer, pH 3.0.

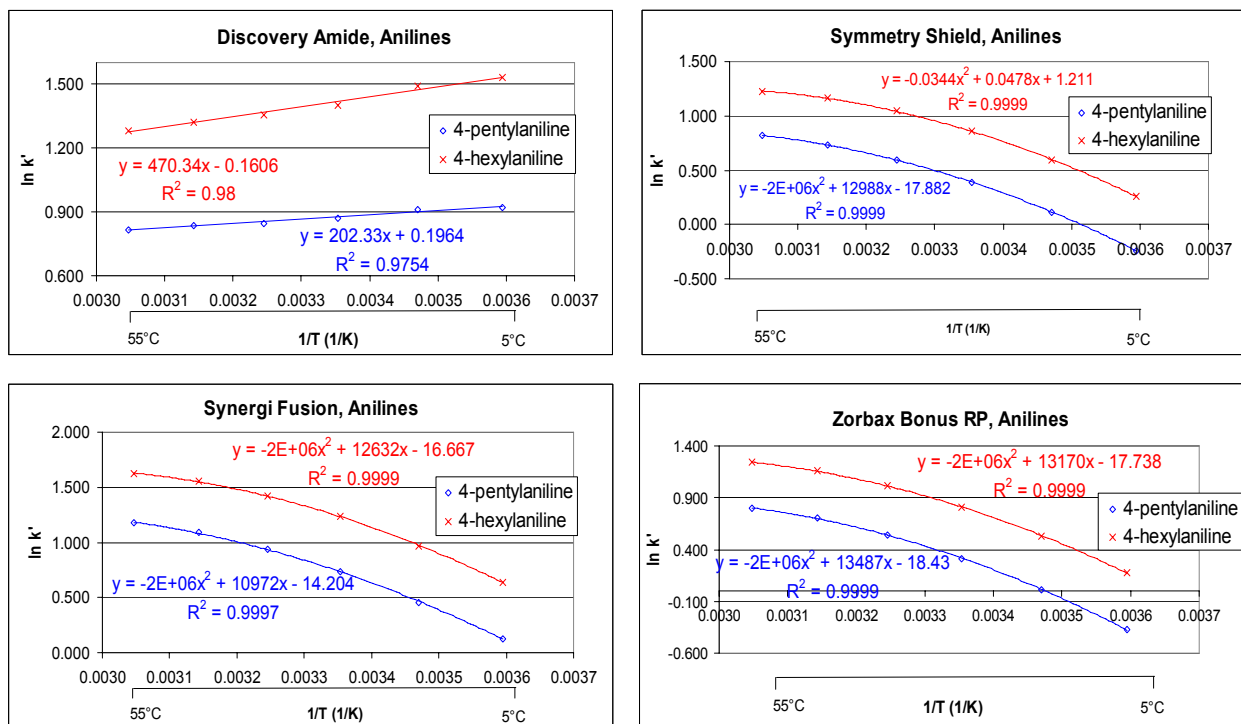


Figure 4-9. van't Hoff plots for 4-pentylaniline and 4-hexylaniline. Mobile phase: 50/50 ACN/10 mM phosphate buffer, pH 3.0.

The last pair of analytes investigated via van't Hoff plots are shown in Figure 4-9. Only the van't Hoff plot for the Discovery Amide column produced a linear relationship with  $R^2 > 0.975$ . For the other three columns, 4-pentylaniline and 4-hexylaniline had curved van't Hoff plots fitted to second order polynomial with  $R^2 > 0.999$ . Undoubtedly, fitting a plot to a higher order polynomial will produce a better correlation value. However, one must be judicious in that the relationship is not intrinsically linear before fitting the plot to a higher order polynomial. Though the van't Hoff plots for the Discovery Amide and Zorbax Bonus RP columns with toluene and ethylbenzene demonstrated slight curvature, the limited data range prohibited the conclusion that a non-linear fit was required and therefore a linear regression was imposed. For the columns that showed curved van't Hoff plots with the anilines, fitting the plots to a linear regression only resulted in the lowest  $R^2$  value of 0.958, which was for 4-hexylaniline on the Symmetry Shield column. Thus, to verify the appropriateness of a non-linear fit, retention data were collected for a wider temperature range, specifically from 5°C to 85°C in 5°C increments,

on the Zorbax Bonus RP column. Figure 4-10 shows the van't Hoff plot for 4-pentylaniline and 4-hexylaniline using the same chromatographic conditions. The samples were injected in triplicate and retention factors had an RSD of 0.004 or less. Clearly, the van't Hoff plots are non-linear. The nature of the curve also indicates that retention increased with increasing temperature until a maximum retention was reached near 70°C. McCalley also observed increased retention with temperature, but was using a conventional ODS column. In addition, the atypical retention behavior was pH dependent [46]. At low pH, pyridine demonstrated increased retention with increasing temperature, but at pH 7.0 exhibited a decrease in retention with temperature. Strangely, nortriptyline followed the opposite pattern with respect to pH. Nonetheless, both analytes had atypical retention behavior, but still had linear van't Hoff plots. Non-linear, atypical retention was observed by Cole and coworkers [171]. Using a high aqueous mobile phase, the authors noticed a parabolic van't Hoff plot for benzene that paralleled the solubility of benzene. Such retention behavior is normally attributed to the hydrophobic effect in which the analyte is excluded from the mobile phase into the stationary phase resulting in increased retention.

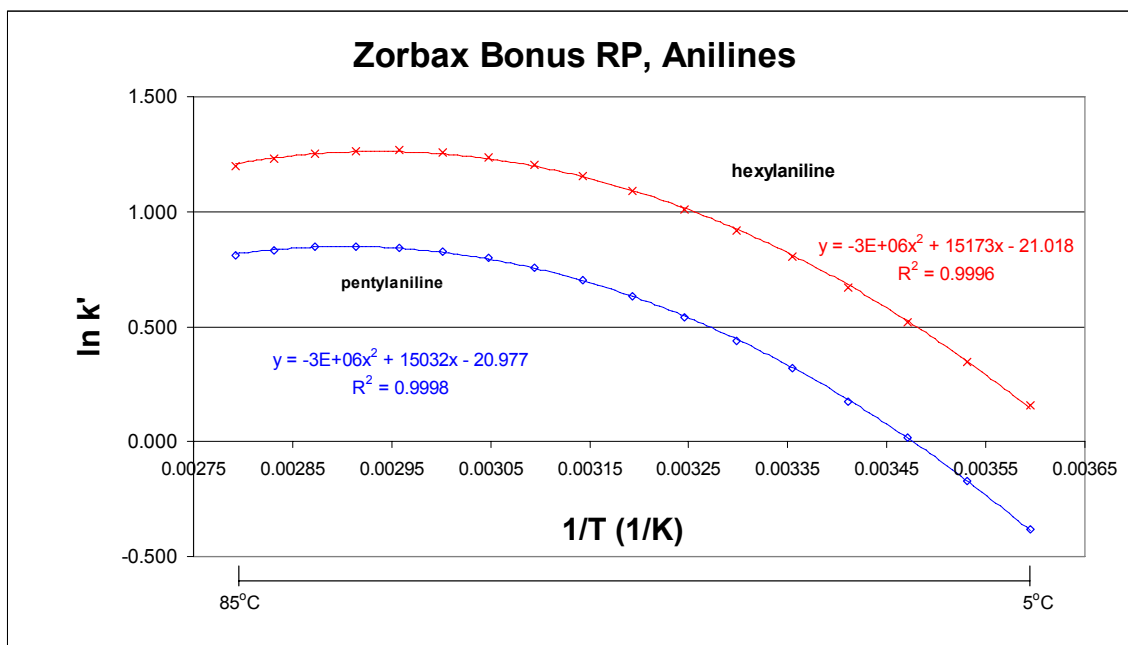


Figure 4-10. van't Hoff plot of the anilines for temperatures of 5°C-85°C. Mobile phase: 50/50 ACN/10 mM phosphate buffer, pH 3.0.

Table 4-3. Molar enthalpies of transfer and  $\Delta S^\circ / R + \ln \phi$  values from van't Hoff plots. Mobile phase: 50/50 ACN/10 mM phosphate buffer, pH 3.0.

<b>Enthalphy (kJ/mol)</b>	propylbenzoic acid	butylbenzoic acid	toluene	ethylbenzene	benzo-nitrile	phenyl-acetonitrile	pentylaniline	hexylaniline
Zorbax Bonus RP	-16.69	-16.53	-7.55	-7.60	-8.48	-9.29	na	na
Discovery Amide	-12.07	-12.08	-8.12	-8.07	-9.70	-10.73	-1.68	-3.91
Symmetry Shield	-9.88	-9.88	-9.62	-9.64	-10.55	-11.41	na	na
Synergi Fusion	-7.40	-7.39	-8.73	-8.59	-10.15	-10.93	na	na
<b><math>\Delta S^\circ / R + \ln \phi</math></b>	propylbenzoic acid	butylbenzoic acid	toluene	ethylbenzene	benzo-nitrile	phenyl-acetonitrile	pentylaniline	hexylaniline
Zorbax Bonus RP	-4.82	-4.77	-1.81	-1.42	-3.08	-3.42	na	na
Discovery Amide	-3.79	-3.80	-2.25	-1.82	-3.84	-4.25	0.20	-0.16
Symmetry Shield	-2.90	-2.90	-2.52	-2.17	-3.73	-4.08	na	na
Synergi Fusion	-1.95	-1.94	-1.91	-1.44	-3.38	-3.67	na	na

Further insight into the retention process can be elucidated from the thermodynamic data. The molar enthalpies of transfer for the analytes are listed in Table 4-3. These were calculated from the slopes of the van't Hoff plots. The “na” (not available) listed for the anilines are a consequence of non-linear van't Hoff plots. Negative values of enthalpy of transfer indicate an energetically favorable retention process. That is, with only consideration to enthalpic contributions, the more negative enthalpy value results in longer retention times. Note the large  $\Delta H^\circ$  values for the benzoic acid homologs on the Zorbax Bonus RP column. The relatively large enthalpy energy is possibly due to the ion pairing or hydrogen bond interaction which is manifested as the severe tailing seen, e.g. 4-*n*-butylbenzoic acid in the selectivity studies (Fig. 4-2). Excluding the aniline homologs because of the lack of data,  $\Delta H^\circ$  for toluene and ethylbenzene were the lowest in magnitude. For toluene, the values ranged from  $-7.55$  kJ/mol to  $-9.62$  kJ/mol, while ethylbenzene had enthalpy values ranging from  $-7.60$  kJ/mol to  $-9.64$  kJ/mol. As a comparison, Cole and Dorsey, using a monomeric ODS column, reported values of  $-12.01$  kJ/mol and  $-11.21$  kJ/mol for toluene and ethylbenzene, respectively, measured in a 60/40 ACN/H<sub>2</sub>O mobile phase [147]. In comparison, Chen and Horváth calculated retention enthalpies of  $-8.58$  kJ/mol for toluene and  $-9.20$  kJ/mol for ethylbenzene using a Zorbax ODS column; also in a 60/40 ACN/H<sub>2</sub>O mobile phase [191]. Oddly, the retention of toluene was

avored over ethylbenzene in the Cole and Dorsey studies, while the retention of ethylbenzene was favored in the Chen and Horváth studies. In general, for RPLC, where hydrophobic interactions are the dominant retention mechanism, retention times should increase as the alkyl side chain increases. However, for this study, no trend in the retention enthalpies for the homologous analyte pairs was discernable. For some homologous pairs, the analyte with more carbons had a larger  $\Delta H^\circ$ , while on another column it had the smaller  $\Delta H^\circ$ . One possible reason is that the presence of the polar-embedded group introduced a mixed-mode retention mechanism that is solvent and solute dependent.

Since the phase ratio is not known for any of the columns, the intercept value,  $\Delta S^\circ / R + \ln \phi$ , is reported. For a given column, the phase ratio should be constant; therefore the  $\Delta S^\circ / R + \ln \phi$  values are indicative of the relative standard molar entropy of transfer. The most notable trend is that all the values are negative and considerably smaller than the enthalpy values. The difference in the intercept values between the homologs can also be considered. The benzoic acid analogs had relative  $\Delta S^\circ$  values that were very similar in magnitude. For the benzene homolog, toluene had less negative values than ethylbenzene. Justifiably, for non-polar solutes, the entropy of transfer should increase (become less negative) with increasing carbon number for a homologous series. These solutes disrupt the hydrogen bonding network of the aqueous solvent, thus it is entropically more favorable to exclude the larger solute from the mobile phase into the stationary phase – the hydrophobic effect. However, this was not the case for benzonitrile and phenylacetonitrile; the more hydrophobic analyte had the less favorable  $\Delta S^\circ$  value. It is noteworthy to mention that, as seen in the van't Hoff plots (Fig 4-7), phenylacetonitrile is more retained at low temperatures while benzonitrile is more retained at higher temperatures. This makes sense if the  $\Delta H^\circ$  values are also considered. The retention enthalpies for phenylacetonitrile were more negative on all the columns. Thus at low temperatures, enthalpy is the dominant force for retention. However, as the temperature is increased, entropy becomes more important and benzonitrile has the more favorable entropy of transfer values. As a result, at higher temperature, benzonitrile is more retained and the reversal of elution order was observed.

### 4.5.3 Methylene selectivity

When non-linear van't Hoff plots are observed, the conventional interpretation is that a change in retention mechanism occurred over the temperature range studied. However, Chester and Coym proposed the possibility that the phase ratio could be temperature dependent [174]. As a result, entropic contributions to retention cannot be calculated when non-linear van't Hoff plots are present, even when the phase ratio is known. Instead, the authors recommended selectivity plots be employed instead. Such plots evaluate the enthalpy of transfer for a structural moiety through the use of homologous compounds. The principle is that if the phase ratio is temperature dependent, resulting in a non-linear van't Hoff plot, the selectivity plot would still remain linear because the homologous solutes should experience the same change in phase volumes.

The methylene selectivity plots using 4-*n*-propylbenzoic acid and 4-*n*-butylbenzoic acids are shown in Figure 4-11. Plots for the Discovery Amide, Symmetry Shield and Synergi Fusion columns all resulted in scattered  $\ln \alpha$  values centered on zero. Only the plot for the Discovery Amide column is shown as an example. These plots are not surprising since the van't Hoff plots were nearly superimposable. The similar retention times of the two solutes results in a selectivity value of one and  $\ln \alpha$  of zero. The Zorbax Bonus RP column plot was less scattered, but produced a poor correlation ( $R^2 = 0.75$ ). Since these plots showed poor or non-existing correlation, the enthalpy and entropy of methylene transfer using these acids were not calculated.

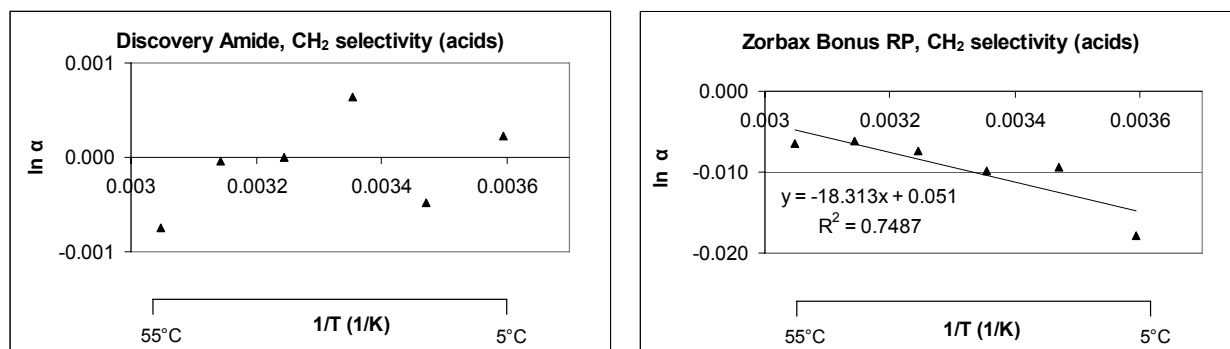


Figure 4-11. Methylene selectivity plots for 4-*n*-propyl benzoic acid and 4-*n*-butylbenzoic acid.



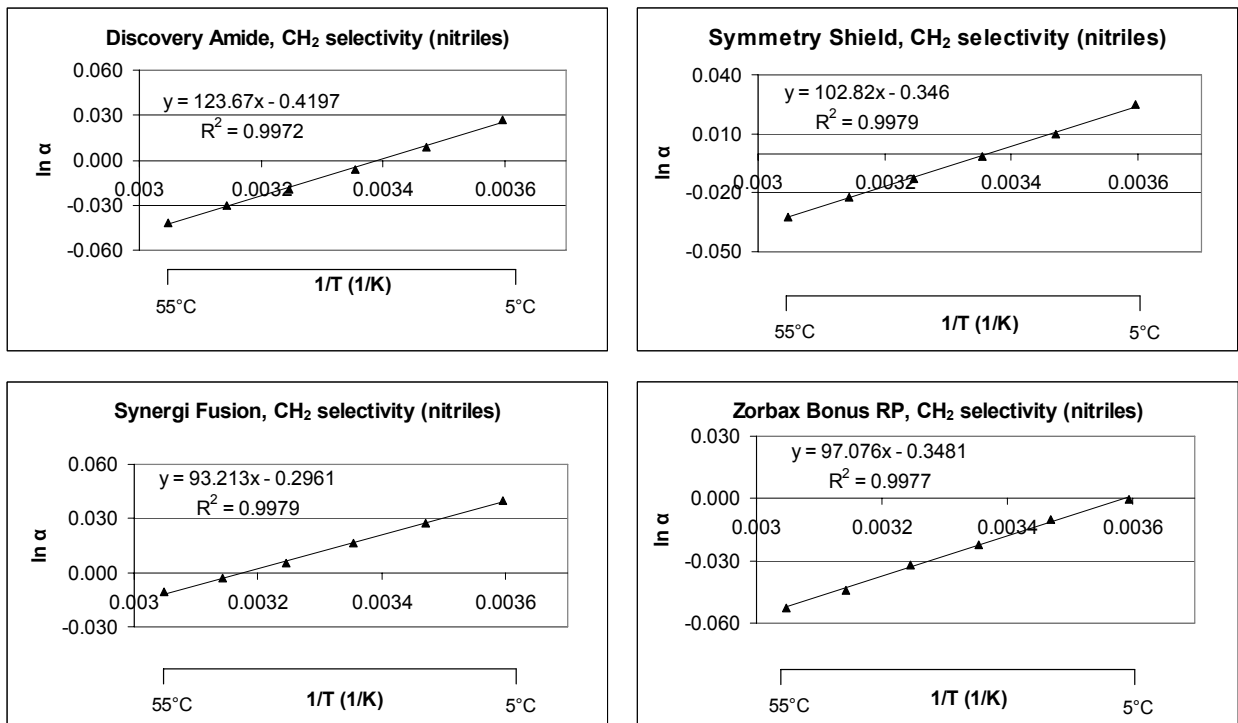


Figure 4-12. Methylene selectivity plots for benzonitrile and phenylacetonitrile.

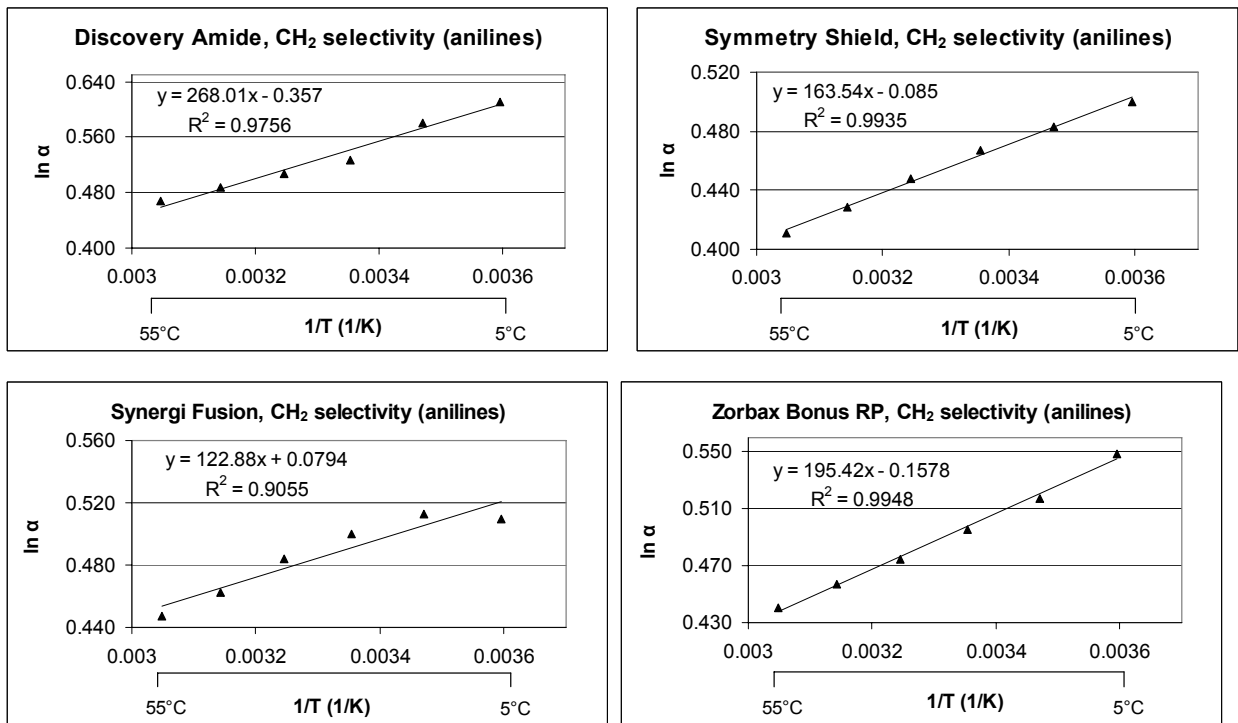


Figure 4-13. Methylene selectivity plots for 4-pentylaniline and 4-hexylaniline.

The methylene selectivity plots using the nitrile and aniline homologs are shown in Figure 4-12 and Figure 4-13. The nitrile plots all demonstrated good linearity with  $R^2 > 0.997$ . Similarly, even though the van't Hoff plots for the anilines on the Symmetry Shield and Zorbax Bonus RP were parabolic, the selectivity plots were linear over the temperature range studied. However, this was not the case for the methylene selectivity plot for the Synergi Fusion, which also had a non-linear van't Hoff plot. At low temperatures, a downward curvature was apparent. The slope of a  $\ln \alpha$  vs  $1/T$  plot is related to the transfer enthalpies of a methylene group from the mobile phase to the stationary phase. Curvature in this plot would imply that the retention enthalpies and/or entropies are temperature dependent. For purpose of calculating these thermodynamic values, the Synergi Fusion plot was fitted to a linear regression, yielding  $R^2 = 0.906$ . Table 4-4 contains the enthalpies and entropies for the selectivity of a methylene group based on the nitrile and aniline homologs. Negative enthalpy values favor the retention of the methylene group. For all the columns, the  $\Delta\Delta H^\circ$  values for the anilines were larger in magnitude when compared to the values for the nitrile homologs. In comparison, Chester and Coym calculated methylene transfer energies of  $-2.33$  kJ/mol and  $-2.48$  kJ/mol using an ODS stationary phase in 60/40 MeOH/H<sub>2</sub>O [174]. Ranatunga and Carr, using *n*-hexadecane as a model for the stationary phase, estimated a methylene transfer energy of  $-2.78$  kJ/mol [178]. Using a polar-embedded column, Coym calculated a molar transfer energy of  $-2.48$  kJ/mol using a 20/80 MeOH/H<sub>2</sub>O mobile phase [192]. Though different mobile phases were used, the values in Table 4-4 are in reasonable agreement.

Table 4-4. Thermodynamic values for methylene selectivity.

	nitriles		anilines	
	$\Delta\Delta H^\circ$ (kJ/mol)	$\Delta\Delta S^\circ$ (J/mol)	$\Delta\Delta H^\circ$ (kJ/mol)	$\Delta\Delta S^\circ$ (J/mol)
<b>Discovery Amide</b>	-1.03	-3.49	-2.23	-2.97
<b>Synergi Fusion RP</b>	-0.78	2.46	-1.02	0.66
<b>Symmetry Shield</b>	-0.85	-2.88	-1.36	-0.71
<b>Zorbax Bonus RP</b>	-0.81	-2.89	-1.62	-1.31

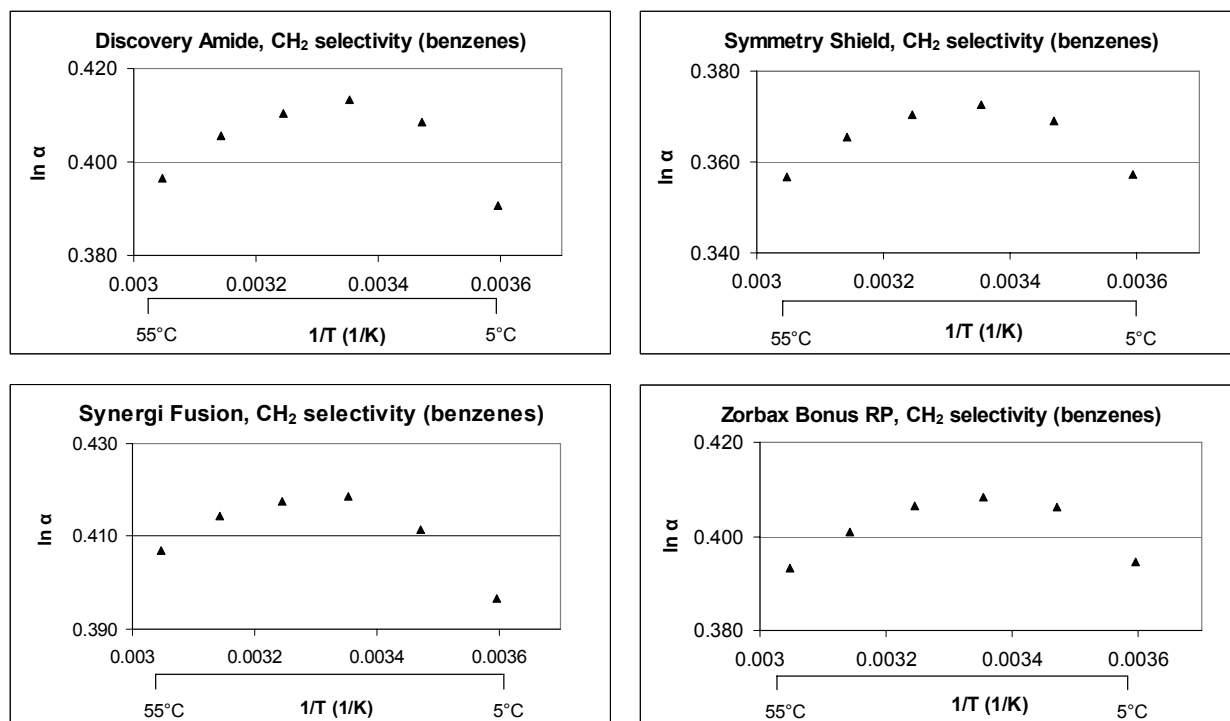


Figure 4-14. Methylene selectivity plots for toluene and ethylbenzene.

The methylene selectivity plots for the benzene homologs are shown in Figure 4-14. Clearly none of the plots are linear. The argument made by Chester and Coym is that even if curvature is observed in the van't Hoff plot, the selectivity plots should still be linear [174]. However, non-linear selectivity plots were observed for the benzene homologs. Discontinuous methylene selectivity plots were reported by Sentell and coworkers [193]. The authors noticed that some selectivity plots exhibited two linear regions. The temperature dependent selectivity was attributed the temperature-induced ordering of the stationary phase. As a result, two different transfer enthalpy and entropy values were reported for the appropriate temperature range. Regardless of the reason, linearity in the selectivity plot is required to evaluate the enthalpy and entropy values. Chester and Coym did address the issue that was seen in this study with the selectivity plots using 4-*n*-propylbenzoic acid and 4-*n*-butylbenzoic acid, namely, three of the selectivity plots were essentially linear plots with a slope of zero. In those cases, the  $\Delta H^\circ$  and

$\Delta S^\circ$  for both probes were not different enough to measure  $\Delta\Delta H^\circ$  of the methylene group. This is seen as overlapping van't Hoff plots. In a second possibility, if  $\Delta H^\circ$  for two solutes were different, but changed in a similar fashion with changes in temperature, a selectivity plot with a slope equal to zero would also arise. The van't Hoff plots of such solutes would be parallel but not overlapping. However, the authors did not consider the possibility of non-linear selectivity plots as seen in Figure 4-14. In comparison, the authors reported a linear methylene selectivity plot with a  $\Delta\Delta H^\circ$  of  $-2.48$  kJ/mol using benzene and toluene.

If the methodology behind selectivity plots is considered, then the proposition that non-linear van't Hoff plots arise from changes in  $\Delta H^\circ$  and/or  $\Delta S^\circ$  rather than a change in the phase ratio seems to be valid. First, consider that selectivity is related to the inverse temperature through equation 3-10, given here again.

$$\begin{aligned} \ln \alpha_{CH_2} &= \ln k_{i+1} - \ln k_i \\ &= \frac{(-\Delta H_{i+1}^\circ + \Delta H_i^\circ)}{RT} + \frac{(\Delta S_{i+1}^\circ - \Delta S_i^\circ)}{R} \end{aligned} \quad \text{Equation 3-10}$$

The benefit of this equation over the van't Hoff equation is that it is phase ratio independent. That is, even if non-linear van't Hoff plots are a result a changing phase ratio, the selectivity plots would still be linear. This would imply that curvature in the selectivity plot cannot be accounted for by a changing phase ratio, regardless of the nature of the van't Hoff plot. In cases where the van't Hoff plot is curved, the hydrophobic effect is often cited as the cause. This results in an entropically favorable transfer of the solute into the stationary phase. Chester and Coym further suggested that since the transfer entropy is temperature dependent, then the enthalpy transfer must also change since both are related through the constant-pressure heat capacity. This necessarily dictates that the selectivity plots should be non-linear. In contradiction, the authors found that the methylene selectivity plots were linear even though the van't Hoff plots were not. However, it should be noted that the test solutes were benzene and toluene. Arguably, those analytes differ by a methyl group and thus are not representative of methylene selectivity. The observed non-linear selectivity plots for toluene and ethylbenzene in this study suggest that changes in  $\Delta H^\circ$  and/or  $\Delta S^\circ$ , rather than a changing phase ratio, is a more reasonable explanation.

## CHAPTER FIVE

### THE PHASE RATIO

#### 5.1 Introduction

The temperature dependency of retention is given by the van't Hoff equation. In plotting  $\ln k'$  vs  $1/T$ , a linear plot with a slope of  $-\Delta H^\circ / R$  and intercept of  $\Delta S^\circ / R + \ln \phi$  is often obtained. However, reports of non-linear plots have raised the question of whether the observed non-linearity arises from a change in the thermodynamics of retention, i.e.,  $\Delta H^\circ$  and/or  $\Delta S^\circ$ , or as a result of a temperature dependent change in the phase ratio. Cole *et al.* reported a parabolic van't Hoff plot for benzene using a 5/95 1-PrOH/H<sub>2</sub>O (v/v) mobile phase [171]. The non-linearity was attributed to the hydrophobic effect under these conditions, and accordingly, temperature dependent thermodynamic values were reported. This effect was also observed with a 65/35 MeOH/H<sub>2</sub>O (v/v) mobile phase, but not with a 60/40 ACN/H<sub>2</sub>O (v/v) mobile phase. Thus, hydrophobic theory of retention seemed to be inadequate in explaining the retention mechanism under all conditions.

Chester and Coym raised the possibility that non-linear van't Hoff plots may be due to changes in the phase ratio [174]. This would redefine how non-linear van't Hoff plots were interpreted. Non-linearity would not necessarily be due to changes in the retention mechanism as a function of temperature, but rather may be due to changes in the volumes of the stationary phase and mobile phase. To further investigate this possibility, the retention behavior of benzene, toluene and 4-hexylaniline, were measured using a traditional C<sub>18</sub> phase and a C<sub>1</sub> phase. Typically, when non-linear van't Hoff plots were reported in the literature, a traditional C<sub>18</sub> phase was used. However, this may be due to their higher frequency of use. In addition, these stationary phases also allow for the supposition that conformational changes and/or sorbed mobile phase could result in changes in the phase ratio. If true, changes in the phase ratio are thought to arise from the different conformations of the C<sub>18</sub> ligand as a result of changes in temperature. Thus, an extended C<sub>18</sub> rod-like ligand would exhibit a different volume than a partially collapsed ligand. However, using similar logic, it must follow that a C<sub>1</sub> phase cannot

exhibit such changes in the phase ratio since conformational changes are structurally impossible. Therefore, if non-linear van't Hoff plots are observed using a C<sub>1</sub> phase, the argument that non-linearity is a result of a change in the phase ratio must be precluded. It should be noted that the purpose of this study is not to determine the actual phase ratio, but more importantly, to understand the thermodynamics of retention and whether those values are temperature dependent.

## **5.2 Instrumentation**

Experiments were performed on a Shimadzu LC-10ADVP HPLC system consisting of a dual pump, DGU-14A degasser, SIL-10A automatic sample injector and SPD-10A UV-Vis detector. Data were collected using Shimadzu Class-VP v.503 automated software system. Column temperatures were maintained using a Fisher Scientific Isotemp Refrigerated Circulator Model 9100 and a glass water jacket. Columns were equilibrated to temperature for a minimum of 1 hour prior to injections.

## **5.3 Columns**

The columns used in these experiments were the Synergi Hydro-RP (Phenomenex, Torrance, CA), a C<sub>18</sub> bonded phase; the Zorbax TMS (Agilent, Wilmington, DE), a C<sub>1</sub> bonded phase; and the Spherisorb (Waters, Milford MA), also a C<sub>1</sub> bonded phase.

## **5.4 Experimental**

HPLC grade acetonitrile was obtained from Mallinckrodt Baker (Phillipsburg, NJ). Purified water from a Barnstead Nanopure II water purification system (Debuque, IA) was used for the preparation of the mobile phase. The mobile phase was degassed via vacuum filtration through a 0.45 μm nylon filter prior to use. The analytes used were benzene (Fisher Scientific, Hampton,

NJ), toluene, (Fisher Scientific, Hampton, NJ), and 4-hexylaniline (Aldrich Chemical, Milwaukee, WI) with thiourea (Fisher Scientific, Hampton, NJ) as a void marker. The mobile phase additive, 1-propanol (1-PrOH), was obtained from Fisher Scientific (Hampton, NJ). Mobile phases used were 30/70 ACN/H<sub>2</sub>O (v/v), 30/70 ACN/H<sub>2</sub>O (v/v) with 3% 1-PrOH, and 5/95 1-PrOH/H<sub>2</sub>O (v/v). The analytes were all prepared at a concentration of 0.05 mg/mL in the same composition as the mobile phase except for benzene. Benzene was prepared in a 30/70 ACN/H<sub>2</sub>O (v/v) injection solution for all the experiments. Each sample was injected in triplicate with a volume of 5  $\mu$ L. Columns and mobile phases were equilibrated for at least an hour. A flow rate of 1.0 mL/min and detection wavelength of 254 nm were used.

## 5.5 Results and Discussion

Figure 5-1 shows the van't Hoff plots for benzene on the Synergi Hydro-RP (C<sub>18</sub>) and Zorbax TMS (C<sub>1</sub>) columns using a 30:70 ACN/H<sub>2</sub>O mobile phase. As expected, both show good linearity with R<sup>2</sup> values of 0.9914 and 0.9897, respectively. From the slopes, the enthalpy of transfer of benzene from the mobile phase to the stationary phase were calculated to be -9.32 kJ/mol for the Synergi Hydro-RP column and -15.88 kJ/mol for the Zorbax TMS column.

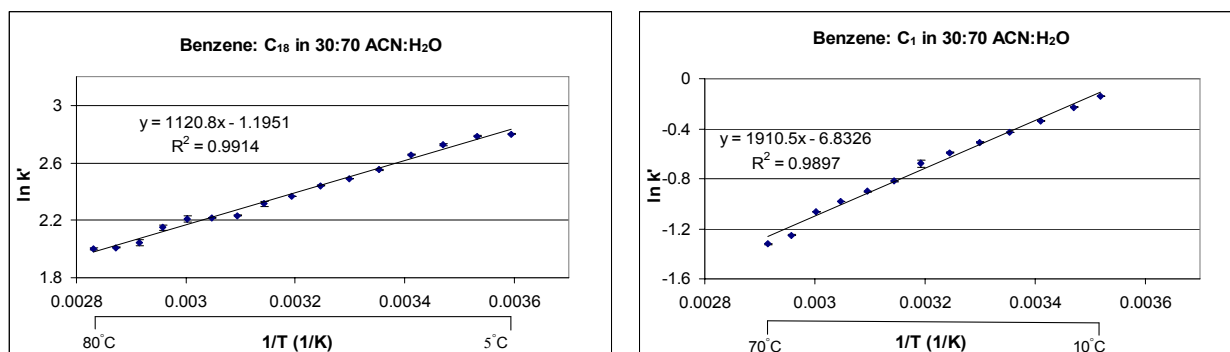


Figure 5-1. van't Hoff plots for benzene using the Synergi Hydro-RP (C<sub>18</sub>) and Zorbax TMS (C<sub>1</sub>) columns, mobile phase 30/70 ACN/H<sub>2</sub>O (v/v).

These values are comparable to enthalpy values reported by others. McCalley reported a value of approximately -10.5 kJ/mol using an Inertsil ODS-3V column in a 35/65 ACN/phosphate buffer, pH, 3.0 [46]. Vervoort and coworkers, using six different RPLC ODS columns, reported values between -9.79 kJ/mol and -11.72 kJ/mol [149]. Using a 60/40 ACN/H<sub>2</sub>O mobile phase, Cole and Dorsey reported a transfer enthalpy of -12.84 kJ/mol using in-house manufactured C<sub>18</sub> columns [147]. Unfortunately, comparable values using C<sub>1</sub> phases were not available in the literature due to the limited use of these types of columns. Since negative  $\Delta H^\circ$  values favor retention, a more hydrophobic phase should have a more negative  $\Delta H^\circ$  value. However, the less favorable value of  $\Delta H^\circ$  for the C<sub>18</sub> phase seems to contradict the trend in retention of non-polar solutes. Using benzene, Cole and Dorsey considered the effects of bonding densities on retention and calculated  $\Delta H^\circ$  values of -12.84 kJ/mol for a C<sub>18</sub> column with a bonding density of 1.60  $\mu\text{mol}/\text{m}^2$ , compared to a value of -9.16 kJ/mol for a column with a bonding density of 2.84  $\mu\text{mol}/\text{m}^2$  [147]. From a retention point of view, the phase with the higher bonding density would be more hydrophobic, thus show larger retention values for non-polar analytes. Though this appears not to be the case, the incongruity can be explained when the entropy of transfer is considered. Cole and Dorsey found that as the bonding density increased, the entropic contribution to retention becomes more significant (more positive) relative to the enthalpic contribution. Thus, retention on the phase with the higher bonding density was greater due to entropic contributions. It should be noted though, that above a critical bonding density, partitioning of the solute into the stationary phase may become entropically disfavored. For this study, the C<sub>18</sub> phase is obviously more hydrophobic in character, compared to the C<sub>1</sub> phase, though the  $\Delta H^\circ$  of retention for benzene was less favorable. This would suggest that the entropic contribution is significantly larger on the C<sub>18</sub> column. Considering that a C<sub>18</sub> ligand is expected to have less conformational constraints than the C<sub>1</sub> ligand, this assumption would seem reasonable. In addition, high energy sites are more accessible by the solute on the C<sub>1</sub> phase. This would result in stronger enthalpic interactions. Therefore, the discrepancy in the  $\Delta H^\circ$  value can be attributed to the entropic contributions of benzene partitioning into a C<sub>18</sub> phase as well as enthalpic contributions of the C<sub>1</sub> stationary phase.

Studies have shown the preferential sorption of the organic component of a hydroorganic mobile phase by the stationary phase [153, 194, 195]. In addition, the temperature dependency



of the sorbed organic layer has been investigated and demonstrated to have an inverse relationship [196]. As the temperature is increased, the thickness of the sorbed layer on the stationary phase surface decreases. Of the common organic solvents used, the volume fraction of organic solvent sorbed into the bonded phases increases with dispersive interaction: methanol, then acetonitrile, followed by tetrahydrofuran. Some researchers have included this solvated layer as part of the stationary phase volume [154, 195, 196, 197]. Since the physical molecular volume of the bonded alkyl ligand cannot change, any hypothetical change in the phase ratio would have to result in the inclusion of the organic layer as part of the volume of the stationary phase. Cole and Dorsey utilized this sorption phenomenon to reduce the equilibration time for gradient elution methods, a technique in which the percentage of organic modifier is increased during the course of the separation [198]. The authors used 3% 1-propanol (vol %) as a mobile phase additive and attributed the reduction in equilibration time to the constant wetting of the stationary phase. Using this principle, the next set of van't Hoff experiments show the temperature dependence of retention in a 30/70 ACN/H<sub>2</sub>O (v/v) mobile phase with 3% 1-PrOH added. The 1-PrOH should be solvated onto or into the stationary phase, albeit to a greater extent on the C<sub>18</sub> phase. If the inclusion of the temperature dependent solvation layer is correct, then a change in the phase ratio should be observed with respect to changes in temperature. Such a dependency would be exhibited as a non-linear van't Hoff plot.

Figure 5-2 shows the van't Hoff plots for benzene, toluene and 4-hexylaniline using a 3% propanol modified mobile phase. The C<sub>1</sub> column was replaced by the Spherisorb column because the Zorbax TMS column demonstrated a loss of stationary phase evident by the gradual loss of retention. This loss was due to exceeding the normal life of the column rather than mobile phase or temperature exacerbated degradation. Nevertheless, all four plots had great linearity with  $R^2 > 0.995$ . For the Synergi Hydro-RP, the transfer enthalpy of benzene was calculated to be -12.88 kJ/mol. The presence of 1-PrOH results in an enthalpically favorable increase (more negative  $\Delta H^\circ$ ) in retention as compared to the mobile phase without the 3% 1-PrOH (Figure 5-1). However, retention factors for the 30/70 ACN/H<sub>2</sub>O (v/v) mobile phase were greater; thus entropically, the addition of 1-PrOH appears to have resulted in an ordering of the stationary phase. On the Spherisorb column, the  $\Delta H^\circ$  of retention for benzene, toluene and 4-hexylaniline were calculated to be -14.60 kJ/mol, -15.65 kJ/mol, and -21.69 kJ/mol, respectively. Though these values seem unusually large for retention enthalpies of non-polar solutes, the

presence and accessibility of the ionized surface silanols may account for these anomalous values. Nevertheless, the absence of non-linear van't Hoff plots weakens the rationale that non-linear van't Hoff plots arise from a change in the phase ratio. This is validated by the fact that the solvated layer is temperature dependent, and its inclusion into the stationary phase would result in a change in the phase volumes.

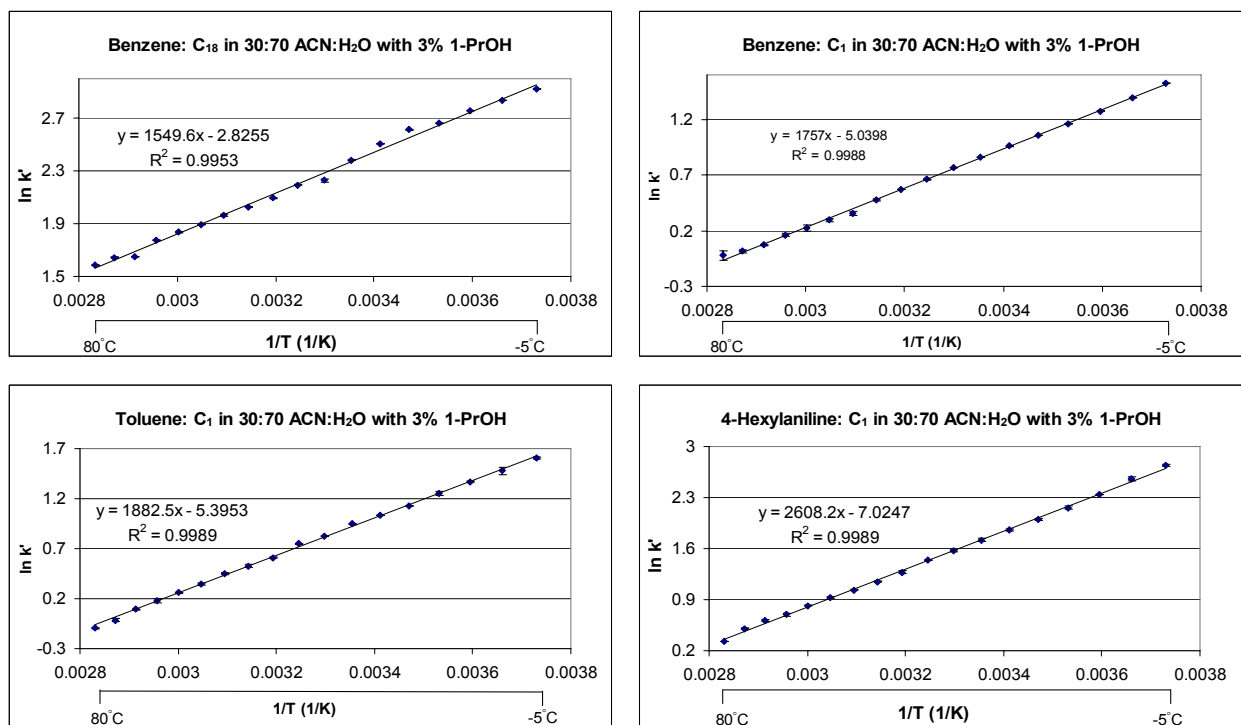


Figure 5-2. van't Hoff plots using the Synergi Hydro-RP ( $C_{18}$ ) and Spherisorb ( $C_1$ ) columns, mobile phase 30/70 ACN/H<sub>2</sub>O (v/v) with 3% 1-PrOH.

The hydrophobic effect, in which an entropically favorable exclusion of the solute from the mobile phase into the stationary phase, has been proposed as one reason for non-linear van't Hoff plots. Evidence for this line of reasoning is shown by considering the van't Hoff plot of benzene as obtained by Cole and coworkers [171]. Using an ODS column with a bonding density of  $2.39 \mu\text{mol}/\text{m}^2$  and a mobile phase of 5/95 1-PrOH/H<sub>2</sub>O, the authors observed a parabolic van't Hoff plot with a maximum retention around 22°C. Interestingly, this retention behavior mirrors the solubility of benzene in water. That is, benzene exhibits a minimum

solubility at around 22°C [176]. Thus, in a chromatographic system, benzene is forced into the non-polar stationary phase, and therefore retained longer by its solubility behavior in aqueous media. To exploit this phenomenon, a highly aqueous mobile phase was selected to evaluate the retention behavior of the three analytes. Non-linear van't Hoff plots using the C<sub>1</sub> column would further reject the concept that a change in the phase ratio could be responsible for non-linearity.

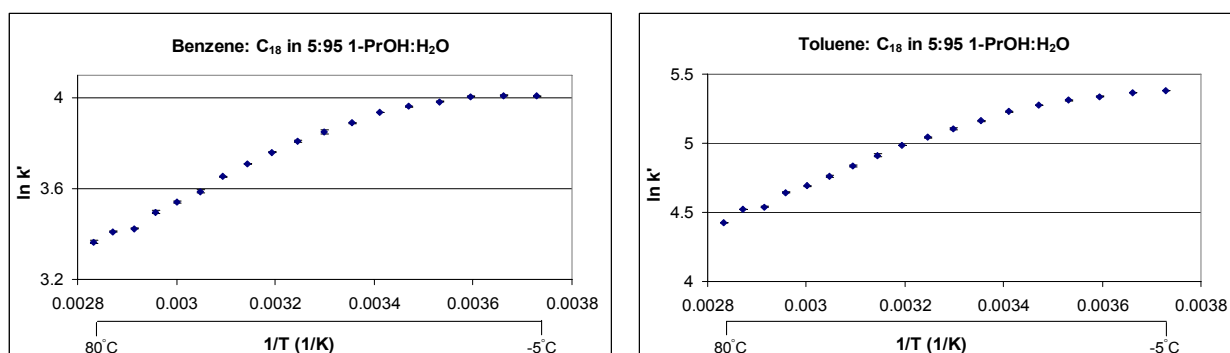


Figure 5-3. van't Hoff plots for benzene and toluene using the Synergi Hydro-RP (C<sub>18</sub>) column, mobile phase 5/95 1-PrOH/H<sub>2</sub>O (v/v).

van't Hoff plots for benzene and toluene on the Synergi Hydro-RP column are shown in Figure 5-3. As expected for a high aqueous mobile phase, non-linear plots were obtained for both analytes, which displayed slight curvatures at lower temperatures. However, unlike the plot reported by Cole *et al.*, the maximum retention for benzene and toluene in this study was around 0°C. Since both plots demonstrated curvature and the lack of information on the phase ratio, enthalpies and entropies of transfer could not be calculated. Although, debatably, the structural difference between benzene and toluene is not representative of a methylene group, the enthalpy and entropy of methylene selectivity was calculated from the  $\ln \alpha$  vs  $1/T$  plot (not shown,  $R^2 = 0.98$ ). The  $\Delta\Delta H^\circ$  of a methylene group was calculated to be -2.70 kJ/mol and the  $\Delta\Delta S^\circ$  was 1.45 J/mol. In comparison, the values obtained for the polar-embedded columns, reported in Chapter 4, varied from -0.78 kJ/mol to -2.23 kJ/mol for the enthalpies of transfer, and -3.49

J/mol to 0.66 J/mol for the entropies of transfer. The more favorable values on the more hydrophobic C<sub>18</sub> column are in agreement with hydrophobic theory.

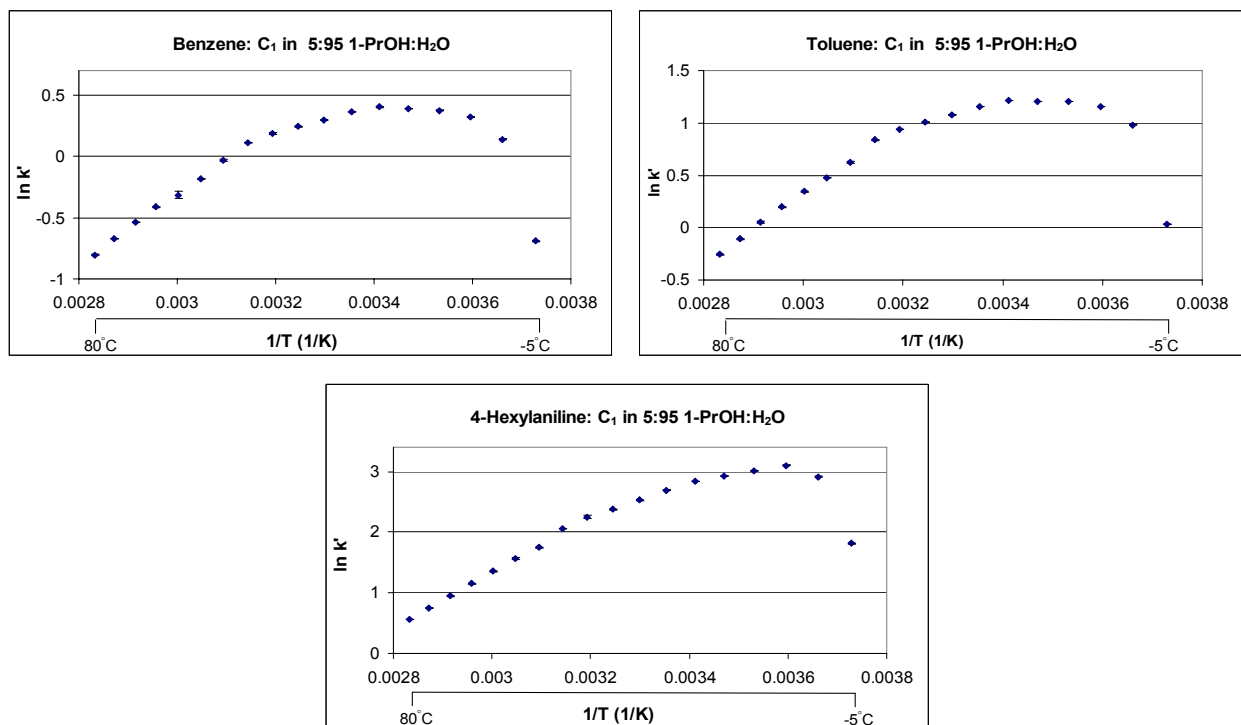


Figure 5-4. van't Hoff plots for benzene, toluene, and 4-hexylaniline using the Spherisorb (C<sub>1</sub>) column, mobile phase 5/95 1-PrOH/H<sub>2</sub>O (v/v).

The curvatures seen in Figure 5-4 using the Spherisorb C<sub>1</sub> phase reaffirms the credence that a change in the phase ratio is not responsible for non-linear van't Hoff plots. Clearly, all three analytes demonstrate parabolic retention profiles, with benzene and toluene showing a maximum retention around 15°C, while 4-hexylaniline has a maximum retention around 5°C. Since a C<sub>1</sub> phases cannot demonstrate any conformational changes, the non-linearity in the van't Hoff plot must be attributed to changes in the enthalpy and/or entropy of retention. Again, using the selectivity of toluene and benzene as an indicator of methylene selectivity,  $\Delta\Delta H^{\circ}$  and  $\Delta\Delta S^{\circ}$  were found to be -2.56 kJ/mol and -0.23 J/mol, respectively ( $R^2 = 0.76$ ). The poor correlation coefficient may be due to a slight curvature in the selectivity plot. This curvature would

reinforce the conventional belief that changes in the thermodynamic values can occur as a function of temperature. It is also noteworthy to point out the similar value of  $\Delta\Delta H^\circ$  for both the  $C_{18}$  and  $C_1$  columns. Since the  $C_{18}$  phase is expected to have a more favorable enthalpy of retention, the comparable values points to the importance of the role of the mobile phase in the retention process, specifically the hydrophobic effect. The  $\Delta\Delta S^\circ$  values also reaffirm this idea. The small  $\Delta\Delta S^\circ$  value for the  $C_1$  phase is due to the fact that the short ligands offers no entropic advantage for the solute to transfer into since a partitioning mechanism is not available. That is, the ordering of the  $C_1$  phase is unchanged by the solute.

## CHAPTER SIX

### SUMMARY AND CONCLUSIONS

Reversed-phase liquid chromatography is the most widely used liquid chromatographic technique used today. Its versatility, sample compatibility, and ability for automation have made it an indispensable tool for the routine separation and analysis of complex mixtures. However, one major concern with RPLC is the performance associated with the analysis of basic compounds. This is particularly problematic for pharmaceutical industries in that many drug compounds contain a basic moiety. These bases tend to demonstrate peak tailing, irreproducible retention times, and loss of efficiency which lead to difficulties in quantitation. The conventional belief is that the unreacted silanols remaining on the silica surface are responsible. More recent works have shown that the heterogeneous surface of the stationary phase is a contributing factor. The existence of multiple active sites with different binding energies results in incongruent analyte interactions that manifest as asymmetric peaks.

Various techniques have been employed to alleviate the deleterious effects of the silanols including the use of mobile phase additives such as triethylamine and dimethyloctylamine or the use of buffered mobile phase to control the pH. In addition, novel stationary phases have been developed to address the issues associated with the separation of basic compounds. One particular type of stationary phase that has been gaining popularity is the polar-embedded phases. Unlike conventional RPLC columns which utilize an alkyl bonded phase, polar-embedded phases incorporate a polar functional group within the alkyl chain. Studies have shown that these stationary phases offer improved peak shape and column efficiencies for bases. However, because of the relative novelty of these phases, the characterization of these columns is limited. This research evaluated seven polar-embedded columns and one traditional column in terms of selectivity and performance with different classes of compounds.

Various techniques have been utilized to characterize and evaluate HPLC columns. These methods can be categorized as spectroscopic methods, non-linear chromatographic studies, chemometric based modeling and empirical chromatographic based methods. These methods offer different and complementary information about the stationary phase, as well as the

retention process itself. However, empirical based methods have the advantages of simulating real chromatographic conditions of high pressures and flow conditions.

The seven columns used in the first portion of the studies contained various polar-embedded groups, some of which were not disclosed by the manufacturer. The first set of experiments used to assess the eight columns focused on column selectivities. Selectivity is defined as the ratio of the retention factors of two analytes and is indicative of the ease of separation of those two analytes. Using two different mixtures of acids, bases, and neutral test analytes, under two different pH conditions, column performances were evaluated. Overall, the columns did show improved peak shape for basic compounds as exemplified by the peak shape of amitriptyline, a common basic test solute. Moreover, the mobile phase pH seemed to have considerable effects on selectivities and efficiencies. On the Synergi Fusion RP column, amitriptyline demonstrated dramatic tailing at pH 7.0, as compared to pH 3.0. The change in pH also resulted in changes in elution order of the compounds for several of the columns. In agreement with reports in the literature, column performance was better at pH 3.0 when compared to pH 7.0. This difference was attributed to the ionization of the silanols at the higher pH.

It was also concluded that the manufacturing process can greatly influence stationary phase character. Though the Discovery Amide column and Zorbax Bonus RP column both contain an amide functional group, the columns' performances differ drastically. Using 4-*n*-butylbenzoic acid as an acid test solute, the Zorbax Bonus RP column demonstrated poor efficiencies towards this class of compound based on the significant tailing observed. In contrast to a B/A tailing factor of 7.1 on the Zorbax Bonus RP column, the tailing factor on the Discover Amide column was 1.1. This disparity was attributed to a two-step synthesis utilized in the manufacturing of the Zorbax Bonus RP column. As opposed to a one-step process, the two-step process results in a stationary phase with unreacted aminopropyl groups in addition to the desired amide-embedded alkyl ligand. At low pH, these groups are protonated which lead to ionic and hydrogen bonding interactions between the analyte and stationary phase. This mixed retention mechanism on the Zorbax Bonus RP results in the observed asymmetric peak of 4-butylbenzoic acid.

The underlying silica also plays an important role in separation efficiencies. Research has shown that physical properties such as particle size, pore size, surface area, and metal content all affect the overall stationary phase character. This factor was observed with the Synergi Max and Synergi Fusion RP columns as well as with the Polaris C8-A and Polaris C8-Ether columns.

Using log-log selectivity plots, the Synergi Max and Synergi Fusion RP columns showed very similar character. With log-log selectivity plots, the selectivity values for a series of analytes on one column are plotted against the selectivity values for a second column. Increased linearity in the plots suggests similar retention mechanisms between the columns. Though the Synergi Max is a traditional C<sub>12</sub> column and Synergi Fusion RP is a polar-embedded column, their log-log selectivity plot had a correlation coefficient of 0.995. This similarity was attributed to the probability that both columns have similar underlying silica since both columns are manufactured by Phenomenex. Likewise, the Polaris C8-A and Polaris C8-Ether columns demonstrated similar selectivity, but most likely contain different polar groups (the polar group of the Polaris C8-A is unknown). Again, the fact that both are manufactured by Varian contributes to the similarity.

The log-log plot using the Discovery Amide and Zorbax Bonus RP columns corroborate the differences observed in the chromatograms. The poor linear correlation in selectivity values confirm that similar stationary phases do not necessarily show similar chromatographic behavior. This poses a challenge if one is interested in the identity of the phase since manufacturers do not always report the structural property of the bonded phase for proprietary reason. This information can be of value in modeling separations since it is believed that structural properties can be used as predictors of chemical behavior.

In addition to the mobile phase composition, pH, and flow rate, the effects of temperature can also be utilized to adjust retention, selectivity and efficiency. Improved peak shape at elevated temperatures has been reported and generally attributed to increased diffusion coefficient, increased sorption-desorption kinetics, and reduced mobile phase viscosity. The relationship between retention and temperature is given by the van't Hoff equation. Besides modeling retention with respect to temperature, van't Hoff analysis allows for the possible determination of the enthalpy and entropy of retention. Plotting  $\ln k'$  vs  $1/T$  typically results in a linear relationship with a slope of  $\frac{-\Delta H^\circ}{R}$  and intercept of  $\frac{\Delta S^\circ}{R} + \ln \phi$ . The thermodynamic values  $\Delta H^\circ$  and  $\Delta S^\circ$  represent the energies associated with the transfer of the solute from the mobile phase into the stationary phase. Since the phase ratio is normally not available, the entropy of transfer is generally not reported. In addition, if homologous analytes are selected, a plot of



$\ln \alpha$  vs  $1/T$  also produces a linear relationship that is phase ratio independent, assuming both analyte experiences the same phase ratio at the given temperature. This permits for the determination of the enthalpy and entropy of transfer for the structural difference of the homologs. For example, if the analytes differ by a methylene group, then the selectivity plots gives the  $\Delta\Delta H^\circ$  and  $\Delta\Delta S^\circ$  values of a methylene group.

Of the eight columns, four were selected to further investigate using van't Hoff analysis. Four pairs of analytes were chosen that differ by a methylene group, and represent different classes of compounds – acids, anilines, nitriles, and neutral, non-polar aromatics. van't Hoff plots highlighted the differences in these classes of compounds. In using 4-*n*-propylbenzoic acid and 4-*n*-butylbenzoic acids, none of the four columns demonstrated significant methylene selectivity. That is, the van't Hoff plots of the two analytes were overlapping. This suggests that the alkyl constituent of the acid is not partitioned or adsorbed into the stationary phase. In contrast, the columns showed improved selectivity using toluene and ethylbenzene. This is not surprising since the dominant retention mechanism for these columns is still hydrophobic interactions even though a polar embedded group is present. The most unusual behavior was seen in the van't Hoff plots of 4-pentylaniline and 4-hexylaniline. Three of the four columns exhibited non-linear van't Hoff plots. Since most non-linear van't Hoff plots demonstrate linearity over a small temperature range, the curvature was verified using a larger temperature range on the Zorbax Bonus RP column. Transfer enthalpies of toluene and ethylbenzene as well as  $\Delta\Delta H^\circ$  and  $\Delta\Delta S^\circ$  values for methylene selectivity were in good agreement with reported values in the literature. In addition, the thermodynamic values explained the temperature dependent reversal of elution order seen with benzonitrile and phenylacetonitrile. At low temperatures,  $\Delta H^\circ$  governs retention and benzonitrile is eluted first. However, at higher temperatures the entropic value increases relative to  $\Delta H^\circ$ , and phenylacetonitrile, with a more favorable entropy of transfer value, elutes first.

Non-linear van't Hoff plots have previously been reported by other researchers and have been attributed to the hydrophobic effect. This phenomenon is a result of an entropically favorable exclusion of a hydrophobic analyte from a high aqueous mobile phase into the hydrophobic stationary phase. Traditionally, the non-linear van't Hoff plots are interpreted as a temperature induced change in the retention mechanism. However, recent debate has raised the possibility

that a temperature dependent phase ratio may be responsible for the non-linearity. This not only changes the conventional interpretation, but questions the overall value of van't Hoff plots, even when linearity is observed. If the phase ratio is temperature dependent, then its value should vary for all van't Hoff plots, regardless of whether a linear trend is observed or not.

Part of the controversy surrounding the phase ratio arises from the ambiguity in defining the two phases. Simplistically, it is defined as the ratio of the volume of the stationary phase over the volume of the mobile phase. The uncertainty in its value is not a result of a lack of methods in measuring the individual volumes, but rather how each particular volume is defined. Some researchers have included the silica support as part of the stationary phase volume, while others clearly exclude this. The existence of a stagnant sorbed mobile phase within the bonded phase, as well as stagnant mobile phase within the pores adds to the debate in assigning phases.

Regardless of the how the phase ratio is calculated, the research present here has demonstrated that the phase ratio is temperature independent. Consideration of experimental van't Hoff plots obtained using a C<sub>18</sub> and C<sub>1</sub> phase has shown that a change in the phase ratio cannot be responsible for the observed curvature. A temperature dependent change in the phase ratio must arise from conformational changes in the ligand or a change in the solvation layer. However, the use of a C<sub>1</sub> phase, which clearly cannot experience conformational changes, resulted in non-linear van't Hoff plots for benzene, toluene and 4-hexylaniline. In addition, linear van't Hoff plots using the mobile phase additive 1-PrOH preclude the effects of the sorbed mobile phase on the phase ratio. Studies have shown that the amount of sorbed mobile phase is temperature dependent, thus its inclusion in the stationary phase should result in non-linear van't Hoff plots. However, van't Hoff plots for a C<sub>18</sub> phase using 30/70 ACN/H<sub>2</sub>O (v/v) with 3% 1-PrOH demonstrated good linearity. Recognizing that the layer of sorbed mobile phase changed without curvature in the van't Hoff plot implies that the phase ratio did not change. This also suggests that this sorbed layer should not be included in calculating the volume of the stationary phase. The confirmation that non-linear van't Hoff plots are not due to a change in the phase ratio is supported by the works of Bidlingmeyer and Henderson [181]. Non-linear van't Hoff plots were observed by the authors using bare silica. Obviously, since there is no bonded phase, a change in the volume of the phases is an impractical conclusion. Lastly, since two analytes would experience the same phase volumes, selectivity plots necessarily eliminate the possible effects of the phase ratio. Thus, even if non-linear van't Hoff plots are observed, the selectivity

plots should be linear. The non-linear methylene selectivity plots observed using toluene and ethylbenzene (Figure 4-14) further substantiate the fact that the phase ratio is not temperature dependent. The plots clearly show a change in the enthalpy and entropy of transfer as a function of temperature.

The importance of this conclusion lies in the usefulness of van't Hoff analysis. These plots are an added tool in evaluating column behavior. These evaluation techniques not only give insight into the retention mechanism, but also allow for the identification of similar or dissimilar columns. In addition to aiding method development, such information can also be used in designing the next generation of columns. The development of polar-embedded columns was facilitated by the need for different selectivity as well as improving efficiencies with basic compounds. This research did expose some differences in these columns, but there is still more that can be investigated. Non-linear van't Hoff plots have been attributed to changes in the thermodynamics of retention rather than a change in the phase ratio. Typically, the hydrophobic effect has been cited as the reason. However, non-linear van't Hoff plots observed for a 50/50 ACN/H<sub>2</sub>O (v/v) mobile phase using the polar-embedded columns, as well as various maximums in retention seen in the van't Hoff plots using a C<sub>18</sub> and C<sub>1</sub> that don't mirror the solubility of the analyte, suggest that a more complex process may be the reason. The nature of the stationary phase, the composition of the mobile phase, the physiochemical characteristic of the analyte all add to the complexity of the separation process. However, the variability of these factors also contributes to the versatility of liquid chromatography, making it one of the most useful analytical techniques.

## REFERENCES

- [1] A.J.P. Martin, R.L.M Syngé, *Biochem. J.* 35 (1941) 1358-1368.
- [2] R.J.M. Vervoort, A. J.J. Debets, H.A. Claessens, C. A. Crammers, G.J. de Jong, *J. Chromatogr. A* 897 (2000) 1-22.
- [3] J.G. Dorsey, W.T. Cooper, *Anal. Chem.* 66 (1994) 857A-866A.
- [4] J. Nawrocki, C. Dunlap, A. McCormick, P.W. Carr, *J. Chromatogr. A* 1028 (2004) 1-30.
- [5] L.C. Sander, S.A. Wise, *Crit. Rev. Anal. Chem.* 18 (1987) p.300.
- [6] J.E. Sandoval, *J. Chromatogr. A*, (1999) 375-381.
- [7] C.A. Rimmer, L.C. Sanders, S.A. Wise, J.G. Dorsey, *J. Chromatogr. A* 1007 (2003) 11-20.
- [8] J.J. Kirkland, *J. Chromatogr. A* 1060 (2004) 9-21.
- [9] C.A. Doyle, J.G. Dorsey; *Reversed-Phase HPLC: Preparation and Characterization of Reversed-Phase Stationary Phases*, In *Handbook of Chromatography*; Vol 78, J. Cazes, Marcel Dekker Inc, New York, New York 1998 p 300.
- [10] N.H.C. Cooke, K. Olsen, *J. Chromatogr. Sci.* 18 (1980) 512-524.
- [11] L.C. Sander, S.A. Wise, *Anal. Chem.* 59 (1987) 2309-2313.
- [12] J.J. Kirkland, F.A. Truszkowski, R.D. Ricker, *J. Chromatogr. A* 965 (2002) 25-34.
- [13] J.J. Pesek, M.T. Matyska, R.J. Yu, *J. Chromatogr. A* 947 (2002) 195-203.
- [14] J.J. Kirkland, M.A. van Straten, H.A. Claessens, *J. Chromatogr. A* 797 (1998) 111-120.
- [15] J. J. Kirkland, J. W. Henderson, J. J. DeStefano, M. A. van Straten, H. A. Claessens, *J. Chromatogr. A* 762 (1997) 97-112.
- [16] J.J. Kirkland, J.L. Glajch, R.D. Farlee, *Anal. Chem.* 61 (1989) 2-11.
- [17] S. Kobayashi, I. Tanaka, O. Shirota, T. Kanda, Y. Ohtsu, *J. Chromatogr. A* 828 (1998) 75-81.
- [18] L. Zhou, C. Welch, C. Lee, X. Gong, V. Antonucci, Z. Ge, *J. Pharm. Biomed. Anal.* 49 (2009) 964-969.

- [19] M.R. Euerby, P. Petersson, W. Campbell, W. Roe, *J. Chromatogr. A* 1154 (2007) 138-151.
- [20] S. Kayillo, G.R. Dennis, R.A. Shalliker, *J. Chromatogr. A* 1126 (2006) 283-297.
- [21] D.H. Merchand, K. Croes, J.W. Dolan, L.R. Snyder, *J. Chromatogr. A* 1062 (2005) 57-64.
- [22] J.E. O’Gara, B.A. Alden, C.A. Gendreau, P.C. Iraneta, T.H. Walter, *J. Chromatogr. A* 893 (2000) 245-251.
- [23] M. Przybyciel, *LC-GC* 23 (2005) 554-565.
- [24] W. Zhang, *J. Fluorine Chem.* 129 (2008) 910-919.
- [25] C. McNeff, L. Zigan, K. Johnson, P.W. Carr, A. Wang, A.M. Weber-Main, *LC-GC* 18 (2000) 514-529.
- [26] J. Nawrocki, C. Dunlap, A. McCormick, P.W. Carr, *J. Chromatogr. A* 1028 (2004) 1-30.
- [27] J. Nawrocki, C. Dunlap, J. Li, C.V. McNeff, A. McCormick, P.W. Carr, *J. Chromatogr. A* 1028 (2004) 31-62.
- [28] J. Ge, L. Zhao, Y. Shi, *J. Liq. Chromatogr. Related Technol.* 31 (2008) 151-160.
- [29] S. Coppi, G. Blo, A. Betti, *J. Chromatogr.* 388 (1987) 135-142.
- [30] M.R. Buchmeiser, *J. Chromatogr. A* 918 (2001) 233-266.
- [31] H.A. Claessens, M.A. van Straten, *J. Chromatogr. A* 1060 (2004) 23-41.
- [32] J. Nawrocki, *J. Chromatogr. A* 779 (1997) 29-71.
- [33] G.B. Cox, R.W. Stout, *J. Chromatogr.* 384 (1987) 315-336.
- [34] B. A. Bidlingmeyer, F. V. Warren Jr, *Anal. Chem.* 56 (1984) 1583A-1596A.
- [35] J.P. Foley, J.G. Dorsey, *Anal. Chem.* 55 (1983) 730-737.
- [36] A. Berthod, *J. Liq. Chromatogr.* 12 (1989) 1187-1201.
- [37] G.B. Cox, *J. Chromatogr. A* 656 (1993) 353-367.
- [38] B.A. Bidlingmeyer, J.K. Del Rios, J. Korpi, *Anal. Chem.* 54 (1982) 442-447.
- [39] J.D. Sunseri, W.T. Cooper, J.G. Dorsey, *J. Chromatogr. A* 1011 (2003) 23-29.

- [40] A. Berthod, *J. Chromatogr.* 549 (1991) 1-28.
- [41] M.J. Wirth, M.D. Ludes, D.J. Swinton, *Anal. Chem.* 71 (1999) 3911-3917.
- [42] A. Méndez, E. Bosch, M. Rosés, U.D. Neue, *J. Chromatogr. A* 986 (2003) 33-44.
- [43] H. Engelhardt, C. Blay, J. Saar, *Chromatographia* 62 (2005) S19-S29.
- [44] F. Gritti, G. Guiochon, *J. Chromatogr. A* 1099 (2005) 1-42.
- [45] G. Gotmar, T. Fornstedt, G. Guiochon, *J. Chromatogr. A* 831 (1999) 17-35.
- [46] D.V. McCalley, *J. Chromatogr. A* 902 (2000) 311-321.
- [47] S.M.C. Buckenmaier, D.V. McCalley, M.R. Euerby, *J. Chromatogr. A* 1060 (2004) 117-126.
- [48] F. Gritti, G. Guiochon, *J. Chromatogr. A* 1028 (2004) 75-88.
- [49] F. Gritti, G. Guiochon, *J. Chromatogr. A* 1098 (2005) 82-94.
- [50] F. Gritti, G. Guiochon, *J. Chromatogr. A* 1103 (2006) 69-82.
- [51] B.C. Trammell, C.A. Boissel, C. Carignan, D.J. O'Shea, C.J. Hudalla, U.D. Neue, P.C. Iraneta, *J. Chromatogr. A* 1060 (2004) 153-163.
- [52] J.J. Kirkland, M.A. van Straten, H.A. Claessens, *J. Chromatogr. A* 691 (1995) 3-19.
- [53] M.A. Stadalius, J.S. Berus, L.R. Snyder, *LC-GC* 6 (1988) 494-500.
- [54] A. Nahum, C. Horváth, *J. Chromatogr.* 203 (1981) 53-61.
- [55] R.J.M. Vervoort, F.A. Maris, H. Hindriks, *J. Chromatogr.* 623 (1992) 207-220.
- [56] E. Papp, G. Vigh, *J. Chromatogr.* 259 (1983) 49-53.
- [57] M. Reta, P.W. Carr, *J. Chromatogr. A* 855 (1999) 121-127.
- [58] F. Gritti, G. Guiochon, *J. Chromatogr. A* 1103 (2004) 57-69.
- [59] F. Gritti, G. Guiochon, *J. Chromatogr. A* 1047 (2004) 33-48.
- [60] L.C. Sander, S.A. Wise, *Anal. Chem.* 56 (1987) 504-510.
- [61] K.K. Unger, N. Becker, P. Roumeliotis, *J. Chromatogr.* 125 (1976) 115-127.

- [62] F. Großmann, V. Ehwald, C. du Fresne von Hohenesche, K.K. Unger, *J. Chromatogr. A* 910 (2001) 223-236.
- [63] J.D. Sunseri, T.E. Gedris, A.E. Stiegman, J.G. Dorsey, *Langmuir* 19 (2003) 8608-8610.
- [64] M. Przybyciel, R.E. Majors, *LC-GC* 20 (2002) 516-523.
- [65] U.D. Neue, Y.F. Cheng, Z. Lu, P.C. Iraneta, C.H. Phoebe, K. Van Tran, *Chromatographia* 54 (2001) 169-177.
- [66] T.H. Walter, P. Iraneta, M. Capparella, *J. Chromatogr. A* 1075 (2005) 177-183.
- [67] D.V. McCalley, *J. Chromatogr. A* 844 (1999) 23-38.
- [68] J.E. O'Gara, B.A. Alden, T.H. Walter, J.S. Petersen, C.L. Niederlaender, U.D. Neue, *Anal. Chem.* 67 (1995) 3809-3813.
- [69] M.R. Euerby, P. Petersson, *J. Chromatogr. A* 1088 (2005) 1-15.
- [70] L.R. Snyder, J.W. Dolan, P.W. Carr, *J. Chromatogr. A* 1060 (2004) 77-116.
- [71] J. Layne, *J. Chromatogr. A* 957 (2002) 149-164.
- [72] J. Köhler, D.B. Chase, R.D. Farlee, A.J. Vega, J.J. Kirkland, *J. Chromatogr.* 352 (1986) 275-305.
- [73] D.W. Sindorf, G.E. Maciel, *J. Am. Chem. Soc.* 102 (1980) 7606-7607.
- [74] B. Pfeleiderer, K. Albert, E. Bayer, *J. Chromatogr.* 506 (1990) 343-355.
- [75] D.W. Sindorf, G.E. Maciel, *J. Am. Chem. Soc.* 105 (1983) 1848-1851.
- [76] K. Jinno, T. Ibuki, N. Tanaka, M. Okamoto, J.C. Fetzer and, W.R. Biggs, P.R. Griffiths, J.M. Olinger, *J. Chromatogr.* 461 (1989) 200-227.
- [77] M. Pursch, L.C. Sander, K. Albert, *Anal. Chem.* 68 (1996) 4107-4113.
- [78] K.B. Sentell, *J. Chromatogr. A* 656 (1993) 231-263.
- [79] L.C. Sander, K.L. Lippa, S.A. Wise, *Anal. Bioanal. Chem.* 382 (2005) 646-668.
- [80] N. Sagliano Jr., R.A. Hartwick, R.E. Patterson, B.A. Woods, J.L. Bass and, N.T. Miller, *J. Chromatogr.* 458 (1988) 225-240.
- [81] L.C. Sander, J.B. Callis, L.R. Field, *Anal. Chem.* 55 (1983) 1068-1075.

- [82] C.A. Doyle, T.J. Vickers, C.K. Mann, J.G. Dorsey, *J. Chromatogr. A* 779 (1997) 91-112.
- [83] C.A. Doyle, T.J. Vickers, C.K. Mann, J.G. Dorsey, *J. Chromatogr. A* 877 (2000) 25-39.
- [84] Z. Liao, C.J. Orendorff, L.C. Sander, J.E. Pemberton, *Anal. Chem.* 78 (2006) 5813-5822.
- [85] Z. Liao, C.J. Orendorff, J.E. Pemberton, *Chromatographia* 64 (2006) 139-146.
- [86] C.H. Lochmüller, D.B. Marshall, D.R. Wilder, *Anal. Chim. Acta* 130 (1981) 31-43.
- [87] J. Ståhlberg, M. Almgren, *Anal. Chem.* 57 (1985) 817-821.
- [88] R.H. Hansen, J.M. Harris, *Anal. Chem.* 68 (1996) 2879-2884.
- [89] M.D. Ludes, M.J. Wirth, *Anal. Chem.* 70 (2002) 386-393.
- [90] Z. Zhong, M.L. Geng, *Anal. Chem.* 79 (2007) 6709-6717.
- [91] P. Jandera, Z. Pošvec, P. Vraspír, *J. Chromatogr. A* 734 (1996) 125-136.
- [92] C. Horváth, A. Nahum, J.H. Frenz, *J. Chromatogr.* 218 (1981) 365-393.
- [93] J. Jacobson, J. Frenz, C. Horváth, *J. Chromatogr.* 316 (1984) 53-68.
- [94] A. Seidel-Morgenstern, *J. Chromatogr. A* 1037 (2004) 255-272.
- [95] D.H. James, C.S.G. Phillips, *J. Chem. Soc.* (1954) 1066-1070.
- [96] S. Brunauer, P.H. Emmett, E. Teller, *J. Am. Chem. Soc.* 60 (1938) 309-319.
- [97] I. Hägglund, J. Ståhlberg, *J. Chromatogr. A* 761 (1997) 13-20.
- [98] J. Dai, P.W. Carr, D.V. McCalley, *J. Chromatogr. A* 1216 (2009) 2474-2482.
- [99] E.V. Dose, S. Jacobson, G. Guiochon, *Anal. Chem.* 63 (1991) 833-839.
- [100] F. Gritti, G. Guiochon, *J. Chromatogr. A* 1043 (2004) 159-170.
- [101] L. Rohrschneider, *Anal. Chem.* 45 (1973) 1241-1247.
- [102] L.R. Snyder, *J. Chromatogr.* 92 (1974) 223-230.
- [103] M.J. Kamlet, R.W. Taff, *J. Am. Chem. Soc.* 98 (1976) 377-383.
- [104] R.W. Taff, M.J. Kamlet, *J. Am. Chem. Soc.* 98 (1976) 2886-2894.



- [105] M.J. Kamlet, J.L. Abboud, R.W. Taft, *J. Am. Chem. Soc.* 99 (1977) 6027-6038.
- [106] C. Horváth, W. Melander, I. Molnár, *J. Chromatogr.* 125 (1976) 129-156.
- [107] L. Szepesy, *J. Chromatogr. A* 960 (2002) 69-83.
- [108] P.W. Carr, J. Li, A.J. Dallas, D.I. Eikens, L.C Tan, *J. Chromatogr. A* 656 (1993) 113-133.
- [109] L.C. Tan, P.W. Carr, *J. Chromatogr. A* 775 (1997) 1-12.
- [110] J.G. Dorsey, K.A. Dill, *Chem. Rev.* 89 (1989) 331-346.
- [111] T. L. Hafkenschied, E. Tomlinson, *J. Chromatogr.* 218 (1981) 409-425.
- [112] T. L. Hafkenschied, E. Tomlinson, *J. Chromatogr.* 292 (1984) 305-317.
- [113] R. Kaliszan, T. Bączek, A. Buciąński, B. Buszewski, M. Sztupecka, *J. Sep. Sci.* 26 (2003) 271-282.
- [114] K. Valkó, *J. Chromatogr. A* 1037 (2004) 299-310.
- [115] M. Hsieh, J.G. Dorsey, *J. Chromatogr.* 631 (1993) 63-78.
- [116] M. Vitha, P.W. Carr, *J. Chromatogr. A* 1126 (2006) 143-194.
- [117] K. Héberger, *J. Chromatogr. A* 1158 (2007) 273-305.
- [118] E. Lesellier, C. West, *J. Chromatogr. A* 1158 (2007) 329-360.
- [119] T. Németh, E. Haghedooren, B. Noszál, J. Hoogmartens, *J. Chemometrics* 22 (2008) 178-185.
- [120] P.C. Sadek, P.W. Carr, R.M. Doherty, M.J. Kamlet, R.W. Taft, M.H. Abraham, *Anal. Chem.* 57 (1985) 2971-2978.
- [121] Á. Sándi, M. Nagy and L. Szepesy, *J. Chromatogr. A* 893 (2000) 215-234.
- [122] M.H. Abraham, A. Ibrahim, A.M. Zissimos, *J. Chromatogr. A* 1037 (2004) 29-47.
- [123] C.F. Poole, S.K. Poole, *J. Chromatogr. A* 965 (2002) 263-299.
- [124] Á. Sándi, L. Szepesy, *J. Chromatogr. A* 818 (1998) 1-17.
- [125] Á. Sándi, L. Szepesy, *J. Chromatogr. A* 818 (1998) 19-30.

- [126] L.A. Lopez, S.C. Rutan, J. Chromatogr. A 965 (2002) 301-314.
- [127] R. J. M. Vervoort, M. W. J. Derksen, F. A. Maris, J. Chromatogr. A 678 (1994) 1-15.
- [128] K. Croes, A. Steffens, D.H Marchand, L.R. Snyder, J. Chromatogr. A 1098 (2005) 123-130.
- [129] M. Yang, S. Fazio, D. Munch, P. Drumm, J. Chromatogr. A 1097 (2005) 124-129.
- [130] L. C. Sander, S. A. Wise, J. Chromatogr. A 656 (1993) 335-351.
- [131] L.C. Sander, M. Pursch, S.A. Wise, Anal. Chem. 71 (1999) 4821-4830.
- [132] L.C. Sander, Certificate of Analysis, SRM 869a, Standard Reference Material Program, NIST, Gaithersburg, MD 2007.
- [133] H. Engelhardt, M. Aranglo, T. Lobert, LC-GC 15 (1997) 856-866.
- [134] H.A. Claessens, M.A. van Straten, C.A. Cramers, M. Jezierska, B. Buszewski, J. Chromatogr. A 826 (1998) 135-156.
- [135] K. Kimata, K. Iwaguchi, O.S. Jinno, R. Eksteen, K. Hosoya, M. Araki, N. Tanaka, J. Chromatogr. Sci. 27 (1989) 721-728.
- [136] U.D. Neue, E. Serowik, P. Iraneta, B.A. Alden, T.H. Walter, J. Chromatogr. A 849 (1999) 87-100.
- [137] U.D. Neue, B.A. Alden, T.H. Walter, J. Chromatogr. A 849 (1999) 101-116.
- [138] E. Cruz, M.R. Euerby, C.M. Johnson, C.A. Hackett, Chromatographia 44 (1997) 151-161.
- [139] M.R. Euerby, P. Petersson, W. Campbell, W. Roe, J. Chromatogr. A 1154 (2007) 138-151.
- [140] S.D. Rogers, J.G. Dorsey, J. Chromatogr. A 892 (2000) 57-65.
- [140] M. Verzele, C. Dewaele, Chromatographia 18 (1984) 84-86.
- [141] D.V. McCalley, J. Sep. Sci. 26 (2003) 187-200.
- [142] R.J.M Vervoort, E. Ruyter, A.J.J. Debets, H.A. Claessens, C.A. Cramers, G.J., de Jong, J. Chromatogr. A 931 (2001) 67-79.
- [143] N.S. Wilson, M.D. Nelson, J.W. Dolan, L.R. Snyder, R.G. Wolcott, P.W. Carr, J. Chromatogr. A 961 (2002) 171-193.

- [144] N.S. Wilson, M.D. Nelson, J.W. Dolan, L.R. Snyder, R.G. Wolcott, P.W. Carr, *J Chromatogr. A* 961 (2002) 195-215.
- [145] J.H. Knox, G. Vasvari, *J. Chromatogr.* 83 (1973) 181-194.
- [146] D. Haidacher, A. Vailaya, C. Horváth, *Proc. Natl. Acad. Sci.* 93 (1996) 2290-2295.
- [147] L.A. Cole, J.G. Dorsey, *Anal. Chem.* 64 (1992) 1317-1323.
- [148] E. Grushka, H. Colin, G. Guiochon, *J. Chromatogr.* 248 (1982) 325-339.
- [149] R.J.M. Vervoort, E. Ruyter, A.J.J. Debets, H.A. Claessens, C.A. Cramers, G.J. de Jong, *J. Chromatogr. A* 964 (2002) 67-76.
- [150] H.J.A. Philipsen, H.A. Claessens, H. Lind, B. Klumperman, A.L. German, J., *Chromatogr. A* 790 (1997) 101-116.
- [151] M. Kazusaki, T. Shoda, H. Kawabata, H. Matsukura, *J. Liq. Chromatogr. Related Technol.* 24 (2001) 141-151.
- [152] A.W. Purcell, M.I. Aguilar, M.T.W. Hearn, *J. Chromatogr.* 593 (1992) 103-117.
- [153] R.J. Smith, C.S. Nieass, M.S. Wainwright, *J. Liq. Chromatogr.* 9 (1986) 1387-1430.
- [154] A. Alhedai, D.E. Martire, R.P.W. Scott, *Analyst* 114 (1989) 869-875.
- [155] J.H. Knox, R. Kaliszan, *J. Chromatogr.* 349 (1985) 211-234.
- [156] R.M. McCormick, B.L. Karger, *Anal. Chem.* 52 (1980) 2249-2257.
- [157] F. Gritti, Y. Kazakevich, G. Guiochon, *J. Chromatogr. A* 1161 (2007) 157-169.
- [158] C.A. Rimmer, C.R. Simmons, J.G. Dorsey, *J. Chromatogr. A* 965 (2002) 219-232.
- [159] D.P. Nowotnik, R.K. Narra, *J. Liq. Chromatogr.* 16 (1993) 3919-3932.
- [160] B.A. Bidlingmeyer, F.V. Warren, A. Weston, C. Nugent, *J. Chromatogr. Sci.* 29 (1991) 275-279.
- [161] Y.V. Kazakevich, H.M. Nair, *J. Chromatogr. Sci.* 33 (1995) 321-327.
- [162] H. Engelhardt, H. Müller, B. Dryer, *Chromatographia* 19 (1984) 240-245.
- [163] F.Z. Oumada, M Rosás, E. Bosch, *Talanta* 53 (2000) 667-677.

- [164] G.E. Berendsen, P.J. Schoenmakers, L. de Galan, J. Liq. Chromatogr. 3 (1980) 1669-1686.
- [165] S. Pous-Torres, J.R. Torres-Lapasio, M.C Garcia-Alvarez-Coque, J. Liq. Chromatogr. Related Technol. 32 (2009) 1065-1083.
- [166] A. Tchaplal, H. Colin, G. Guiochon, Anal. Chem. 56 (1984) 621-625.
- [167] P. Jandera, H. Colin, G. Guiochon, Anal. Chem. 54 (1982) 435-441.
- [168] K.B. Sentell, J.G. Dorsey, J. Liq. Chromatogr. 11 (1988) 1875-1885.
- [169] W. Cheng, Anal. Chem. 57 (1985) 2409-2412.
- [170] F. Chan, L.S. Yeung, R. LoBrutto, Y.V. Kazakevich, J. Chromatogr. A 1082 (2005) 158-165.
- [171] L.A. Cole, J.G. Dorsey, K.A. Dill, Anal. Chem. 64 (1992) 1324-1327.
- [172] R.I. Boysen, Y. Wang, H.H. Keah, M.T.W. Hearn, Biophys. Chem 77 (1999) 79-97.
- [173] D. Morel, J. Serpinet, J.M. Letoffe, P. Claudy, Chromatographia 22 (1986) 103-108.
- [174] T.L. Chester, J.W. Coym, 1003 (2003) 101-111.
- [175] K.M. Biswas, D.R. DeVido, J.G. Dorsey, J. Chromatogr. A 1000 (2003) 637-655.
- [176] S.J. Gill, N.F. Nicols, I. Wadsö, J. Chem. Thermodynamics 8 (1976) 445-452.
- [177] T. Tanford, *The Hydrophobic Effect: Formation of Micelles and Biological Membranes*, Wiley, New York, 1980.
- [178] R.P.J. Ranatunga, P.W. Carr, Anal. Chem. 72 (2000) 5679-5692.
- [179] K.B. Sentell, A. N. Henderson, Anal. Chim. Acta 246 (1991) 139-149.
- [180] Y. Liu, N. Grinberg, K.C. Thompson, R.M. Wenslow, U.D. Neue, D. Morrison, T.H. Walter, J.E. O’Gara, K.D. Wyndham, Anal. Chim. Acta 554 (2005) 144-151.
- [181] B.A. Bidlingmeyer, J. Henderson, J. Chromatogr. A 1060 (2004) 187-193.
- [182] N.S. Wilson, J. Gilroy, J.W. Dolan, L.R. Snyder, J. Chromatogr. A 1026 (2004) 91-100.
- [183] J.E. O’Gara, D.P. Walsh, C.H. Phoebe Jr., B.A. Alden, E.S.P. Bouvier, P.C. Iraneta, M. Capparella, T.H. Walter, LC-GC 19 (2001) 632-642.

- [184] J.E. O’Gara, B.A. Alden, T.H. Walter, J.S. Petersen, C.L. Niederländer, U.D. Neue, *Anal. Chem.* 67 (1995) 3809-3813.
- [185] H.A. Claessens, M.A. van Straten, J.J. Kirkland, *J. Chromatogr. A* 728 (1996) 259-270.
- [186] D.V. McCalley, *J. Chromatogr. A* 738 (1996) 169-179.
- [187] D.V. McCalley, *J. Chromatogr. A* 769 (1997) 169-178.
- [188] S. Pous-Torres, J.R. Torres-Lapasió, J.J. Baeza-Baeza, M.C. García-Álvarez-Coque, *J. Chromatogr. A* 1163 (2007) 49-62/
- [189] L.G. Garliardi, C.B. Castells, C. Ràfols, M. Rosés, E. Bosch, *Anal. Chem.* 78 (2006) 5858-5867.
- [190] S. Heinisch, G. Puy, M. Barrioulet, J. Rocca, *J. Chromatogr. A* 1118 (2006) 234-243.
- [191] M.H. Chen, C. Horváth, *J. Chromatogr. A* 788 (1997) 51-61.
- [192] J.W. Coym, *J. Sep. Sci.* 31 (2008) 1712-1718.
- [193] K.B. Sentell, N.I. Ryan, A.N. Henderson, *Anal. Chim. Acta* 307 (1995) 203-215.
- [194] E.H. Slaats, W. Markovski, J. Fekete, H. Poopé, *J. Chromatogr.* 207 (1980) 299-323.
- [195] C.R. Yonker, T.A. Zwier, M.F. Burke, *J. Chromatogr.* 241 (1982) 269-280.
- [196] I. Poplewska, W. Piątkowski, D. Antos, *J. Chromatogr. A* 1103 (2006) 284-295.
- [197] K.S. Yun, C. Zhu, J.F. Parcher, *Anal. Chem.* 67 (1995) 613-619.
- [198] L.A. Cole, J.G. Dorsey, *Anal. Chem.* 62 (1990) 16-21.

## **BIOGRAPHICAL SKETCH**

Van Quach was born in Vietnam on December 19, 1977. He moved to Florida in 1980 and was raised in Orlando, FL. He graduated from Colonial High School in May 1996. Shortly after, he began his undergraduate studies at the University of Florida in Gainesville, FL where he received his Bachelors of Science degree in chemistry in August 1999. After taking some time off, he started graduate school at Florida State University in June 2002. The following spring, he joined the Dorsey Research Group. He also spent the summer of 2005 as an intern in Indianapolis, IN with Eli Lilly and Company. Van will receive his Ph.D. in Analytical Chemistry in Fall 2009.